iPSC-derived cortical neurons from patients with schizophrenia exhibit changes in early neuronal development

Dissertation

der Mathematisch-Naturwissenschaftlichen Fakultät
der Eberhard Karls Universität Tübingen
zur Erlangung des Grades eines
Doktors der Naturwissenschaften
(Dr. rer. nat.)

vorgelegt von
Lena-Marie Grunwald
aus Berlin

Tübingen
2018

Gedruckt mit Genehmigung der Mathematisch-Naturwissenschaftlichen Fakultät der Eberhard Karls Universität Tübingen.

Tag der mündlichen Qualifikation: 23.03.2018

Dekan:	Prof. Dr. Wolfgang Rosenstiel
1. Berichterstatter:	Prof. Hans-Georg Rammensee
2. Berichterstatter:	Prof. Hansjürgen Volkmer

TABLE OF CONTENTS

ABBREVIATIONS

µ	micro
°C	degree celsius
AC	adenyl cyclase
ASD	autism
ASD 1	patient with autism number 1
ASD 2	patient with autism number 2
ASD 3	patient with autism number 3
BDNF	brain derived neuronal factor
bFGF	fibroblast growth factor-basic
bp	base pairs
cAMP	cyclic adenosine monophosphate
cm	centimeter
CO_2	carbon dioxide
CRISPR	clustered regularly interspaced short palindromic repeats
cTIP2	COUP-TF-interaction protein 2
CTNT	cardiac troponin T
CTR	control
CTR 1	healthy individual number 1
CTR 2	healthy individual number 2
CTR 3	healthy individual number 3
DISC 1	disrupted in schizophrenia 1
dNTP	desoxynucleosidtriphosphat
DMEM	Dulbecco´s modified eagle´s medium
DMSO	dimethylsulfoxide
DNA	desoxyribonucleic acid
DSM	Diagnostic and Statistical Manual of Mental Disorders
EDTA	ethylenediaminetetraacetic acid
FBS	fetal bovine serum
FDA	Food and Drug Administration
FGA	first generation antipsychotics
FGF1	fibroblast growth factor receptor 1
g	gram
g	gravitation constant
GABA	glutamate or ɣ-aminobutyric acid
GDNF	glial cell line-derived neurotrophic factor

GFP	green fluorescent protein
GFAP	glial fibrillary acidic protein
GPCR	G-protein coupled receptor
GWAS	genome-wide association studies
h	hour
HLA	human leukocyte antigen
H_2O	water
hES	human embryonal stem cells
iN	induced neuron
iPSC	induced pluripotent stem cells
m	milli
l	litre
mm	millimeter
MAP2	microtubule-associated protein 2
MEA	multielectrode array
MEF	mouse embryonic fibroblasts
MHC	major histocompatibility complex
min	minute
mRNA	messenger RNA
NEAA	non-essential amino acids
NGS	normal Goat Serum
NMDA	N-methyl-D-aspartic acid
NOTCH4	neurogenic locus notch homolog 4
NP55	neuroplastin 55
NPC	neural progenitor cells
PAX 6	paired box protein 6
PBS	Dulbecco´s Phospate Buffered Saline
PCP	phencyclidine
PCR	polymerase chain reaction
PFA	paraformaldehyde
PKA	protein kinase A
RNA	ribonucleic acid
ROI	region of interest
PSD95	post synaptic density protein 95
s	second
SGA	second generation antipsychotics

sgRNA	single guide RNA
SHP	synaptophysin
SSEA 4	stage-specific embryonic antigen 4
SOX17	SRY-related HMG-box 17
SZ	schizophrenia
SZ 1	patient with schizophrenia number 1
SZ 2	patient with schizophrenia number 2
SZ 3	patient with schizophrenia number 3
Tra 1-81	tumor related antigen 1-81
U	units
UV	ultra violet
VGaT	vesicular GABA transporter
VGluT	vesicular glutamate transporter
ZO 1	zona occludens 1

SUMMARY

One percent of the world population suffers from the neurodevelopmental disorder schizophrenia. During the last years, above hundreds of risk genes and functional changes in glutamatergic, GABAergic and dopaminergic signalling have been identified. Furthermore, prenatal complications increase the risk to develop schizophrenia. First symptoms occur between puberty and early adolescence and are divided into positive, negative and cognitive symptoms. Until today no suitable cellular test system has been developed to study the disease background and treatment opportunities. The development of iPSC technology enables the investigation of schizophrenia related changes based on patient-derived cells.

In this thesis, fibroblast derived from healthy and disease individuals were reprogrammed into iPSC and further differentiated into cortical neurons. Each developmental step starting as iPSC and resulting as neurons showed the same morphological properties independent from the donor. Despite these similarities changes in early neurodevelopmental processes were observed in iPSC-derived neurons from patients with schizophrenia. The neurite outgrowth, the PSD95 cluster density and the calcium flux were reduced in case of schizophrenia. Transcriptome analysis revealed changes in gene expression related to gene of neuronal development, synapse, calcium signalling and immune response. In increased expression of MHCII related genes was measured via transcriptome analysis and immunocytochemical staining in cells from patients witch schizophrenia. Additionally, the effect of the antipsychotics clozapine, haloperidol and olanzapine as well as the mimetic peptides narpin, neurexide and FN4-NF3 on neurite outgrowth were investigated. A significantly reduced neurite outgrowth was observed in iPSC-derived neurons from CTR 1 after treatment with haloperidol or olanzapine. Above mentioned characteristics of cortical neurons cells exhibited similarities to previously described primary cells from patients with schizophrenia. Based on these findings iPSC-derived neurons could be used as test system for basic research and for the development of new therapeutical approaches for neurodevelopmental diseases like schizophrenia.

ZUSAMMENFASSUNG

Ca. 1% der Weltbevölkerung ist an der neuronalen Entwicklungsstörung Schizophrenie erkrankt. In den letzten Jahrzehnten wurden über hundert potentielle Risikogene und zahlreiche Veränderungen in glutamatergen, GABAergen und dopaminergen Signalwegen identifiziert. Auch pränatale Vorkommnisse wie Infektionen der Mutter oder Komplikationen bei der Geburt erhöhen das Risiko an Schizophrenie zu erkranken. Erste Symptome treten zwischen der Pubertät und dem frühen Erwachsensein auf. Die Patienten leiden an positiven, negativen und kognitiven Symptomen sowie an Anomalien ihrer Gehirnmorphologie. Bis heute gibt es kein geeignetes zelluläres Modellsystem, um die Ursachen der Krankheit sowie mögliche Behandlungsansätze zu erforschen. Die Entwicklung der iPSC Technologie ermöglicht die Erforschung des Krankheitsbildes Schizophrenie an Patienten-abgeleiteten Zellen.

In dieser Arbeit wurden Fibroblasten aus gesunden und erkrankten Individuen zu induzierten pluripotenten Stammzellen (iPSC) reprogrammiert und in neuronale, kortikale Zellen differenziert. Die iPSC, die neuronalen Vorläuferzellen und die Neurone zeigten gleiche morphologische Merkmale unabhängig vom Spender. Unterschied in frühen neuronalen Entwicklungsschritten wurden in Neuronen von Patienten mit Schizophrenie im Vergleich zu iPSC-abgeleitet Neuronen von gesunden Individuen nachgewiesen. Das Neuritenauswachsen, die Anzahl an PSD95 Clustern und die Calciummobilisierung waren reduziert in Neuronen von Patienten. Transkriptomanalysen zeigten eine veränderte Genexpression von Genen wichtig für die Ausbildung von synaptischen Strukturen, neuronaler Entwicklung, den Calciumtransport und die Immunantwort. Eine erhöhte Expression von MHCII Genen wurde in Transkriptomanalysen und in neuronalen Vorläuferzellen mittels immunocytochemischer Färbung nachgewiesen. Zusätzlich wurde der Einfluss von den bekannten Antipsychotika Clozapin, Haloperidol und Olanzapin sowie den mimetischen Peptiden Narpin, Neurexide und FN4-NF3 auf das Neuritenauswachsen untersucht. Eine signifikante Reduktion des Neuritenauswachsens wurde nach Applikation von Haloperidol und Olanzapin in iPSC-abgeleiteten Neuronen von CTR 1 nachgewiesen. Die hier beschriebenen Eigenschaften der kortikalen neuronalen Zellen zeigen Übereinstimmungen mit bisherigen Forschungsergebnissen von humanen Zellen aus Schizophreniepatienten. Daraus resultiert eine mögliche Anwendung als neuronales Testsystem mit patienten-abgeleiteten Zellen für die Erforschung des Krankheitsbildes Schizophrenie und die Entwicklung neuer Therapiekonzepte.

1. INTRODUCTION

1.1 Mental disorder schizophrenia

Approximately one percent of the world's population is affected by some form of schizophrenia [1]. This complex and symptomatically heterogeneous disorder is characterised by a strong genetic predisposition and a variety of morphological changes in the brain. Additionally, environmental factors have an impact on the occurrence and the course of the disease [2]. In case of schizophrenia, quality of life for the patients and their families is diminished and personal as well as societal costs are immensely increased [3, 4]. The suicide rate of patients with schizophrenia is increased as well [5]. First symptoms are diagnosed between the age of 15-35 years. The occurrence of schizophrenia is equal between men and women [6], but the onset is delayed in women [7].

For classification and detection of psychiatric disorders, the 'Diagnostic and Statistical Manual of Mental Disorders' (DSM) was developed to help clinicians. Treatment of the disease mostly starts after presenting first symptoms, even if a treatment would be more efficient in an early disease stage. More effective early stage treatments are still needed.

1.1.1 Symptoms of schizophrenia

Three different categories of symptoms are common in the course of schizophrenia: positive, negative and cognitive symptoms [8], which continuously reappear in episodes. This chronic and relapsing aetiopathology differs among patients. Positive symptoms comprise hallucinations and delusions, psychomotor anomalies, bizarre and disorganized thoughts, speech and behaviour. They are diagnosed in the first episode of psychosis, and are mostly treated with antipsychotics. Patients with negative symptoms are characterized by an affective and social dysfunction. They show a decreased expression of speech and diminished social interactions. Diagnosis and treatment of negative symptoms are difficult. Finally, cognitive symptoms include limited attention to the environment and deficits in working memory and language. Additionally, executive functions like planning and decision making are impaired [9]. The prefrontal cortex represents the most affected brain region in patients with schizophrenia exhibiting cognitive symptoms [10].

1.1.2 Hypotheses of schizophrenia

In the early twentieth century, Paul Eugen Bleuler introduced the term schizophrenia, which described a fundamental disorder of thoughts and feelings. At that time, the disease was characterised by the four 'A's: disturbances of associations, affect, ambivalence and autistic isolation [11]. The American psychiatrist Silvano Arieti was convinced that schizophrenia has

a psychological etiology. He suggested the main cause was a wrong family situation and an ambivalent mother which inhibited the building of a stable ego [12].

In the second half of the twentieth century researchers focused on biochemical mechanisms to explain the pathology. The pathophysiology is characterised by aberrations in multiple neurotransmitter systems, like dopamine, glutamate or γ-aminobutyric acid (GABA). The effective treatment with dopamine receptor antagonists such as chlorpromazine and haloperidol helped to develop the first hypothesis of schizophrenia: the dopamine hypothesis [13]. The neurotransmitter dopamine is important for neuronal signaling in many brain regions, like the prefrontal cortex [14]. In case of schizophrenia a hyperactive dopamine transmission is suggested to trigger the disease. Positive, negative and cognitive symptoms may result from aberrant dopamine transmission [15] or an imbalance of dopamine receptors [16, 17]. In 2006, Coyle et al. developed an alternative hypothesis of schizophrenia based upon changes of glutamatergic signaling [18]. Phencyclidine (PCP) and other compounds blocking the N-methyl-D-aspartic acid (NMDA)-type glutamatergic receptors induced typical behavior effects such as psychotic symptoms [19, 20]. These findings led to the concept that a dysfunction or dysregulation of NMDA receptor-mediated neurotransmission may evoke symptoms of schizophrenia. Another explanation was put forth by diminished GABAergic inhibition. GABA is the primary inhibitory neurotransmitter, important for the inhibitory-excitatory balance in the human brain [21]. A reduced neuronal GABA concentration and neurotransmission [22] or disruption of GABAergic interneurons [23] may underlie many symptoms of schizophrenia.

Neurodevelopmental hypothesis

These theories try to explain symptoms which occur in late adolescence or in early adulthood. The neurodevelopmental hypothesis describes schizophrenia as a neurodevelopmental disorder with psychosis as final stage of the disease [24]. Here, suitable environmental risk factors which affect *in utero* development, birth, childhood and early adolescence are encompassed (Fig. 1). The risk increased during periods of maternal malnutrition [25, 26], infections during pregnancy [27] and obstetric complications [28]. The risk for later development of schizophrenia was highest, when stress factors impinged during the second trimester of pregnancy. Adverse maternal life events like death or illness of a close relative increased the risk during this vulnerable time [29]. Prenatal infections of the mother like influenza, Toxoplasma gondii or Herpes Simplex Virus Type 2 enhance the risk for the child [27]. The incidence of schizophrenia was highest during an influenza epidemic [30]. Cytokines which are released in case of an infection may influence the disease risk. They are important mediators of an immune response. Excessive amounts of Interleukin-8 or tumor necrosis factor-α are linked with the occurrence of schizophrenia [27, 31]. Fetal brain and early neural

development are disturbed by an immense cytokine release as well [32, 33]. Other complications during validity like hypoxia increase the risk, too [34]. During childhood and early adolescence severe trauma, infections [27] and consumption of cannabis [35, 36] increase the chance of developing schizophrenia. Patients exhibit an impaired early brain development and a delayed maturation [37]. Abnormalities in social and intellectual properties during childhood are observed as well [38]. Developmental milestones were reached slower and the frequency of speech and educational problems was higher [38]. The place and season of birth are the most significant risk factor compared to genetics [39]. People living in an urban environment [40] or in a minority status had a higher risk for developing schizophrenia [41].

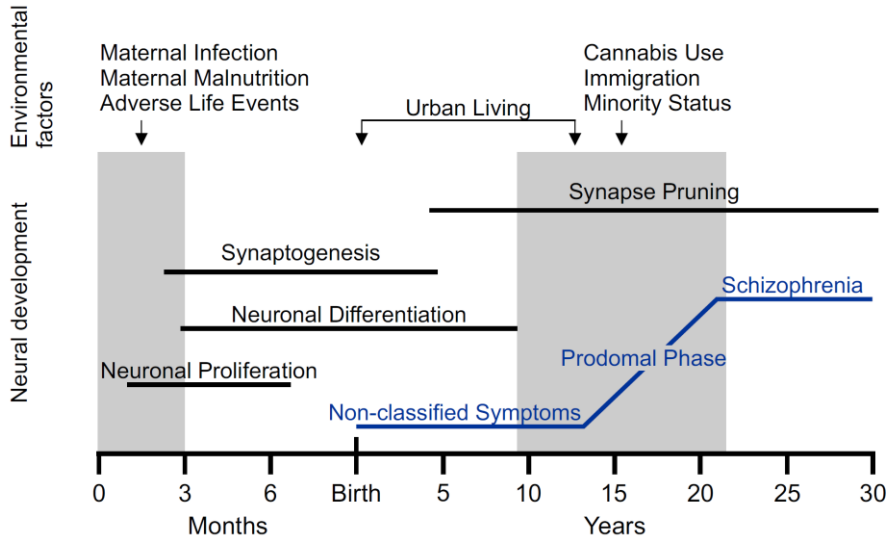

Fig. 1: Overview of environmental factors and neural development influencing the course of schizophrenia. Major developmental processes are indicated by horizontal lines. First prenatal development (in months), followed by postnatal development (in years). Shaded boxes indicate time frames of the first trimester of gestation and adolescence. In the upper part environmental factors that may impact neural development. Blue lines show the course of schizophrenia, starting with an asymptomatic state in childhood followed by full expression of the disease in late adolescence. (adapted from [42])

1.2 Neuropathology of schizophrenia

The neuropathology of schizophrenia is complex and multifaceted. It changes over time and depends on age and length of the illness. Post-mortem tissue and induced pluripotent stem cells (iPSC) from patients can be used to study the neuropathology.

As early as 1976, Johnstone et al. observed enlarged ventricles in patients with schizophrenia using computerized axial tomography techniques [43]. Later, meta-analyses confirmed this finding [44, 45] and investigated decreased gray matter, brain volume and brain weight [46]. Further morphological changes were observed in the prefrontal cortex, temporal loops and the hippocampus. Supporting the neurodevelopmental hypothesis, the prefrontal cortex exhibited excessive loss of gray matter and cortical thinning during childhood of patients with

schizophrenia [47]. In later periods of the disease a reduced size of the hippocampus [48], decreased asymmetry of the brain hemispheres [49] and an altered gyrification [50] were observed. Disruptions of cortical cytoarchitecture may be related to abnormal neuronal migration, embryonal neuronal development and neuronal connectivity [51]. Dislocated neurons are found in cortical layer 2 and 3 [52] as well as in the subcortical white matter [53]. During early gestation cell proliferation is essential for normal cortical development. Diminished cell proliferation led to smaller cortical surface area and aberrant cortical organization [54].

Neural progenitor cells from patients with schizophrenia exhibited a reduced migration relative to control cells in a neurosphere migration assay [55] and changes in the apical polarity of neural rosettes [56]. Maternal infections or stress cause stimulated cytokine pathways which negatively impact mechanisms of symmetric neural progenitor cells division in the developing embryo. Further aberrations in early neuronal development were obvious during the differentiation process. The loss of pluripotency markers was found to be delayed in iPSC-derived neurons from patients with schizophrenia [57]. Efficiency to differentiate into glutamatergic or dopaminergic neurons was impaired in case of schizophrenia [58].

In adolescent, the size of neurons is reduced leading to diminished dendritic and axonal arborizations [59-61]. Selemon and Goldman-Rakic supposed a reduced neuropil hypothesis for schizophrenia [62]. The neuropil is defined as space between cells in the brain including axons, dendrites and synapses. Over time the neuropil decreased because of aberrations in dendrites and axons. Studies investigating the dendritic arbors in cortical areas found a 14-29 % reduction of dendritic length or dendritic number in the prefrontal cortex [63-66]. In cortical layer V Black et al. measured a 40 % reduced basilar dendritic field size [63]. Loss of dendrites and axons resulting in an increase of neuronal density, which can provoke a selective reduction of large pyramidal neurons [67]. A reduction in the number and length of neurites was observed in iPSC-derived neurons from patients with schizophrenia as well [58, 68]. A possible cause of neuropil shrinkage can be an excessive synaptic pruning during brain development and maturation [69]. Synapses are essential for functionality and connectivity in the brain. Schizophrenia is known as a disease with synaptic dysfunction [70]. The main finding in the synaptic morphology was a reduction of dendritic spines in post-mortem studies [63, 66] and iPSC-derived neurons [71]. The postsynaptic density (PSD) is a multiprotein complex and plays a central role in the dendritic spines architecture and the regulation of synaptic plasticity. Post synaptic density protein 95 (PSD95) is a major structural component of the PSD and interacts with many membrane-spanning molecules. PSD95 was reduced in iPSC-derived neurons from patients with schizophrenia [55]. Beside a reduction of important synaptic proteins, the number of glutamatergic synapses were reduced, too [59, 60]. As a result,

imbalance of the excitatory-inhibitory neuronal signaling may impact neuronal synaptic transmission and connectivity [72]. Decreased neuronal connectivity in iPSC-derived neurons from patients with schizophrenia was observed by Brennand et al. [55].

Furthermore, an increased microglial cell density is present in the prefrontal cortex and other parts of the brain from patients with schizophrenia [73, 74]. Microglia are important for the immune response in the brain and are the base for the pro-inflammatory cytokines. An increase in pro-inflammatory cytokines has been also found [75]. Activated microglia and enriched pro-inflammatory cytokines impact fundamentally neurogenesis and may impact the course of schizophrenia.

1.3 Genetics of schizophrenia

Schizophrenia is known as a polygenetic disease characterised by a variety of genetic aberrations. Human brain material and iPSC-derived neurons are used for genetical analysis. Patient-derived material contain the whole genetic repertoire of the donor, allowing a most relevant study of genetic aberrations. Family and twin studies demonstrated a high heritability [76, 77] but the concordance in monozygotic twins was only 50% [78]. The risk increases in case of a family history of psychosis indicating the importance of the genetic origin.

Genome-wide association studies (GWAS), next-generation sequencing and transcriptome analysis identified risk genes and genetic changes in coding and non-coding regions of patients with schizophrenia [79]. The genetics of schizophrenia is highly divergent. Today, the cause is unclear because of the complicated interaction of genetic, epigenetic, developmental and environmental factors which collectively impact normal brain development and maturation [24]. A variety of genes related to dopaminergic, glutamatergic, neurodevelopmental processes, synapse, calcium channels and immune system activation are important parts of the genetic mechanism of schizophrenia.

In 2014, a large collaboration of researchers from the Psychiatric Genomics Consortium identified 108 conservatively defined loci that meet genome-wide significance in schizophrenia. 75% percent of the loci include protein-coding genes for dopaminergic signaling (DRD2) and glutamatergic neurotransmission [80, 81]. Combining environmental factors and genetic predisposition the ‘two hit hypothesis’ of schizophrenia has developed. The first hit is the genetic background which is influenced by the second hit of all environmental factors [82]. Deregulated genes belong to gene families involved in cell migration, proliferation, axonal outgrowth, myelination and synaptogenesis supporting the neurodevelopmental theory [83]. The expression of an important synaptic protein PSD95 is changed and depends on the age

of disease onset. Young patients exhibited a reduced PSD95 thalamic level [84] and elderly patients an increased PSD95 protein expression [85]. Kristiansen et al. reported a decreased PSD95 protein expression in sub regions of the prefrontal cortex of post-mortem brains [86].

Changes in gene expression responsible for synaptic plasticity [80] are important for synapse formation and stabilization [87, 88] and can lead to a disturbed synaptic phenotype observed in patients with schizophrenia. Aberrations in genes related to voltage-gated calcium channels are found in genetical analyses [89]. Voltage-gated calcium channels are regulators of neuronal excitability, activity and synaptic plasticity. Changes in neurobiological and functional key processes may explain disease mechanisms of aberrant brain development and disturbed pathophysiology [90].

The major histocompatibility complex (MHC) is the most powerful region of association for schizophrenia [91]. Patients with schizophrenia exhibited a reduced expression of MHC related genes [92, 93] which could be a link between the immune system and schizophrenia [80]. Eaton et al. showed an increased prevalence to autoimmune disorders [94]. In the genetic analysis of schizophrenia one gene has been most associated with the disease and is handled as one potential risk gene. This gene is named *Disrupted in schizophrenia 1* (DISC1). DISC1 is an important regulator of embryonic and adult neurogenesis [95], brain development [96] and signalling pathways [97]. These findings suggest that mutation in DISC1 impair morphology and functionality of the human brain and is one of the key players. Wen et al. generated iPSC from four members of the family with known DISC1 mutation. In their analysis DISC1 mutation causes dysregulation of genes related to nervous system development, dendritic spine formation and synaptic transmission [98].

1.4 Development of drugs for schizophrenia

The development of first generation antipsychotics (FGA) for schizophrenia started in the 1950s. The length of hospitalization and the risk of a relapse could be reduced by these drugs [99]. All FGA are characterised by a high affinity for dopamine D2 receptors (see Tab. 1). FGA, such as haloperidol have an effective binding to the dopamine D2 receptor and dissociate slowly [100]. Positive symptoms are treated well with this type of antipsychotic. Almost 30 % of drugs are ineffective and produce intolerable side effects [101, 102]. These drugs are no treatment option and their benefit is low compared to the side effects. Second generation antipsychotics (SGA) were developed to improve the treatment options for schizophrenia. SGA are characterized by a higher affinity to serotonin 5-HT receptors than to dopamine D2 receptors. No effective antipsychotic is known without some degree of D2 receptor binding [103].

The SGA clozapine and olanzapine are characterized by a binding affinity for serotonin, adrenergic, dopamine, histamine and muscarinic receptors (see Tab. 1). Clozapine is known to reduce negative and cognitive symptoms and is used for patients who are non-responder to FGAs or show neurological side effects. Its binding affinity to dopamine D2 receptors is reduced in comparison to classical FGA.

Tab. 1: Relative neurotransmitter receptor affinities for first and second generation antipsychotics at therapeutic doses. (adapted from [104] and modified)

Receptor	Clozapine	Olanzapine	Haloperidol
D_1	+	++	+
D_2	+	++	++++
D_3	+	+	+++
D_4	++	++	+++
5-HT_{1A}	-	-	-
5-HT_{1D}	-	-	-
5-HT_{2A}	+++	+++	+
5-HT_{2C}	++	++	-
5-HT_6	++	++	-
5-HT_7	++	-	+++
DA transporter	++	++	
Na transporter	+	++	
Legend: - minimal to none; + low; ++ moderate; +++ high; ++++ very high			

Beside dopamine, NMDA receptor signaling has been targeted to find a treatment for negative symptoms in schizophrenia [105]. Potential effects of SGAs may be associated with the inhibition of the hypofunction of NMDA receptor [106]. Drugs targeting the glutamatergic system and rescue the hypofunction of NMDA receptor, give an opportunity for patients with schizophrenia who failed to respond to dopaminergic agents [107].

Zhao et al. established a large-scale high-throughput screening assay using human iPSC-derived neural progenitor cells [108]. They used an integrated stable, luciferase-based receptor system to screen known bioactive compounds as well as (Food and Drug Administration) FDA-approved drugs according to their effect on an important signaling pathway for schizophrenia. Cultivation in 384-well plates allows parallel approaches and individual changes of culture conditions. iPSC-derived neural cell types are a promising

approach to identify new disease mechanisms and unprecedented drug targets and allow the development of new drugs and therapy options for schizophrenia.

1.5 Autism

Schizophrenia and autism are both neuronal disorders with a complex genetic etiology and overlapping behavioral phenotypes. Comparable to schizophrenia 1 % of the world population [109] is affected by autism. In the past, autism was mentioned as “schizophrenia syndrome of childhood” [110, 111]. Symptoms of autism occur early between the 6th and the 12th months of life. Autism is mostly diagnosed up to the 4th year of life [112]. Deficits in social interaction, cognitive and executive functions and problems in emotional processing are commonly observed in both disorders [113]. A subset of patients with autism have auditory and visual hallucinations in acute phases like patients with schizophrenia [114].

Beside psychotic problems, a variety of morphological changes of the brain and the synapses are described for patients with autism. During the childhood, patients show aberrations in early brain morphology [115] and functionality [116]. Postmortem studies of brains derived from patients with autism found aberrations in synapse number, spine morphology [117, 118] and an impaired synapse maturation [117]. Synaptic dysfunction during early brain development belongs to the autism phenotype too [119].

Comparable to schizophrenia, autism has a strong genetic background with a heritability at 50 % [120]. Genetical analyses described changes in gene expression encoding proteins for the formation of the PSD as well as synaptic development and functionality [121]. Interestingly 17 out of 107 genes were mentioned before in sequencing studies for schizophrenia including genes related to glutamatergic synaptic transmission [122]. Overlapping symptoms, morphological and genetical changes in autism and schizophrenia may base on shared disease relevant molecular, cellular and signaling processes.

1.6 Induced pluripotent stem cells as a model for neuropsychiatric disorders

In 2007, Yamanaka et al. described the successful reprogramming of human fibroblasts into iPSC [123]. Reprogramming was enabled by the introduction of four specific transcription factors Oct3/4, Sox2, c-Myc, Klf4 via retroviral transduction. Currently different somatic cell types can be used for the generation of iPSCs: fibroblasts [123, 124], keratinocytes [125], hair follicles [126], dental pulp cells [127] as well as blood cells [128, 129]. After reprogramming, iPSC can be differentiated into cell types of all three germ layers, *in vitro*. A differentiation into

neuronal cells was preferred to study disease's neuropathology of autism [130, 131] and schizophrenia [68]. Schizophrenia was one of the first neurodevelopmental diseases, modeled using patient specific iPSC-derived neurons [68, 132]. iPSC-derived neuronal cells carry patient's genetic repertoire and can be used to investigate morphological, developmental and functional changes in disease relevant cell types as described above. iPSC represent an unlimited source for patient-derived neurons, which are otherwise difficultly accessible from patient brains. The generation of iPSC-derived neurons is well described and does not raise ethical concerns. Until today iPSC technology is the only method to study mechanisms of human neurodevelopment. During the differentiation of iPSC into neuronal cells like cortical neurons, each step of the early neuronal development and relevant signaling processes can be followed and analysed.

1.7 Aims and objectives of the thesis

Aim of the thesis is to investigate the early cortical neuronal development of patients with schizophrenia and to identify disease relevant mechanisms for new therapeutic approaches. Human fibroblasts from three patients with schizophrenia, three patients with autism and three healthy individuals will serve as cellular starting material. After reprogramming, iPSC will be differentiated into cortical neuronal cells *in vitro* and characterised. Neuronal and disease relevant morphological and functional characteristics will be proofed via immunocytochemical staining and live cell imaging. Early neurodevelopmental processes like brain layer marker expression, neurite outgrowth, synapse formation and calcium influx and efflux will be focussed, to identify potential disease relevant changes based on the schizophrenic genetic background. Disease relevant changes in gene expression will be investigated by transcriptome analysis of iPSC-derived neurons. The effects of first and second-generation antipsychotics on early neuronal development will be analysed using the neurite outgrowth experiment. Findings will evaluate the explanatory power and the potential application of patient-specific iPSC-derived neurons as cellular model system for schizophrenia.

2. MATERIAL AND METHODS

2.1 Material

2.1.1 General material, chemicals and equipment

Tab. 2: General material

general material	manufacture, city
24, 12 and 6 well-plate	Constar®, Corning Incorporated, New York, USA
24 well µ-plate	ibidi GmbH, Martinsried, Germany
37 µm Reversible Strainers	Stemcell Technologies, Vancouver, Canada
AggreWell 800	Stemcell Technologies, Vancouver, Canada
Cell culture flasks (75, 25 cm^2)	Corning Incorporated, New York, USA
Cell scraper	Constar®, Corning Incorporated, New York, USA
Cryo tubes™	Greiner Bio-One, Frickenhausen, Germany
Eppendorf Tubes® (1,5 and 2 ml)	Eppendorf AG, Hamburg, Germany
Falcon Tubes (15 and 50 ml)	Corning Incorporated, New York, USA
Parafilm	Pechiney Plastic Packaging, Chicago, USA
Pauster Pipette	Carl Roth GmbH & Co.KG, Karlsruhe, Germany
Petridish (10 cm^2)	Constar®, Corning Incorporated, New York, USA
Plastic pipets	Greiner Bio-One, Frickenhausen, Germany
Syringes (5 ml and 20 ml)	Corning Incorporated, New York, USA
Syringes filter (0.45 µm)	Corning Incorporated, New York, USA

Tab. 3: Chemicals and reagents

chemical and reagent	manufacture, city
1 kb DNA marker	New England Biolabs, Frankfurt am Main, Germany
Acetic acid	Carl Roth GmbH & Co.KG, Karlsruhe, Germany
Agarose	Carl Roth GmbH & Co.KG, Karlsruhe, Germany
AggreWell™ Rinsing Solution	Stemcell Technologies, Vancouver, Canada
Ascorbic acid	Sigma-Aldrich Inc., Munich, Germany
B27 supplement	Thermo Fisher Scientific, Waltham, USA
β-mercaptoethanol	Sigma-Aldrich Inc., Munich, Germany
Bacto™ Agar	BD, Biosciences, Heidelberg Germany
BDNF (brain derived neuronal factor)	New England Biolabs, Frankfurt am Main, Germany
BrainPhys™ Neuronal Medium	Stemcell Technologies, Vancouver, Canada
Cal520® AM	AAT Bioquest®, CA, USA
Clozapine	Sigma-Aldrich Inc., Munich, Germany
Dibutyryl-cAMP	Enzo Life Sciences GmbH, Lörrach, Germany
Dimethylsulfoxid (DMSO)	Sigma-Aldrich Inc., Munich, Germany
Dorsomorphin dihydrochloride	Tocris, Bristol, UK
Dulbecco´s modified eagle´s medium (DMEM/F-12), glucose	Life Technologies™ Gibco®, Darmstadt, Germany
Dulbecco´s Phospate Buffered Saline (DPBS)	Life Technologies™ Gibco®, Darmstadt, Germany
Effectene Transfection Reagent	Qiagen GmbH, Hilden, Germany

Ethanol (96%)	Carl Roth GmbH & Co.KG, Karlsruhe, Germany
Ethylenediaminetetraacetic acid (EDTA)	Carl Roth GmbH & Co.KG, Karlsruhe, Germany
UltraPure™ Ethidium Bromide	Thermo Fisher Scientific, Waltham, USA
Fetal Bovine Serum (FBS)	Life Technologies™ Gibco®, Darmstadt, Germany
Fibroblast growth factor-Basic (bFGF)	Sigma-Aldrich Inc., Munich, Germany
Fibroblast Growth Medium 2	PromoCell, Heidelberg, Germany
Fungizone	Thermo Fisher Scientific, Waltham, USA
GDNF (glia derived neuronal factor)	Tocris, Bristol, United Kingdom
Gelantin	Sigma-Aldrich Inc., Munich, Germany
Gentamicin	Sigma-Aldrich Inc., Munich, Germany
Haloperidol	Sigma-Aldrich Inc., Munich, Germany
Insulin	Sigma-Aldrich Inc., Munich, Germany
Isopropanol	Carl Roth GmbH & Co.KG, Karlsruhe, Germany
KnockOut™ serum	Thermo Fisher Scientific, Waltham, USA
Laminin	Sigma-Aldrich Inc., Munich, Germany
L-glutamine	PAA Laboratories GmbH, Pasching, Austria
Matrigel	Corning Incorporated, New York, USA
M-MulV Reverse Transcriptase	New England Biolabs, Frankfurt am Main, Germany
mTeSR™1 medium	Stemcell Technologies, Vancouver, Canada
N2 Supplement	Thermo Fisher Scientific, Waltham, USA
Natriumacetat	Carl Roth GmbH & Co.KG, Karlsruhe, Germany
Natriumchlorid (NaCl)	Carl Roth GmbH & Co.KG, Karlsruhe, Germany
Neurobasal™ Medium	Thermo Fisher Scientific, Waltham, USA
NeuroCult SM1 Neuronal Supplement	Stemcell Technologies, Vancouver, Canada
Non-essential amino acids	PAA Laboratories GmbH, Pasching, Austria
Normal Goat Serum (NGS)	Jackson ImmunoResearch Laboratories Inc., West Grove, PA, USA
Olanzapine	Sigma-Aldrich Inc., Munich, Germany
Paraformaldehyd (PFA)	Carl Roth GmbH & Co.KG, Karlsruhe, Germany
Penicillin/Streptomycin (100x)	Life Technologies™ Gibco®, Darmstadt, Germany
Phusion® High-Fidelity DNA Polymerase	New England Biolabs, Frankfurt am Main, Germany
PluriSTEM™ human ES/iPS medium	Merck KGaA, Darmstadt, Germany
Poly-l-ornithine (PLO)	Sigma-Aldrich Inc., Munich, Germany
Puromycin	PAA Laboratories GmbH, Pasching, Austria
Recombinant Human Noggin Fc Chimera Protein	Bio-Techne GmbH, Wiesbaden-Nordenstadt, Germany
RLT Buffer	Qiagen GmbH, Hilden, Germany
RQ1 Rnase-Free Dnase	Promega, Fitchburg, USA
SB 431542	Tocris, Bristol, UK
Sodium Azid	Sigma-Aldrich Inc., Munich, Germany
Sodium bicarbonate	Carl Roth GmbH & Co.KG, Karlsruhe, Germany
Sodium pyruvate	Carl Roth GmbH & Co.KG, Karlsruhe, Germany
STEMdiff™ Neural Induction Medium	Stemcell Technologies, Vancouver, Canada
STEMdiff™ Neural Progenitor Freezing Medium	Stemcell Technologies, Vancouver, Canada
STEMdiff™ Neural Progenitor Medium	Stemcell Technologies, Vancouver, Canada
STEMdiff™ Neural Rosette Selection Reagent	Stemcell Technologies, Vancouver, Canada

StemPro™ Accutase Cell Dissociation Reagent	Life Technologies™ Gibco®, Darmstadt, Germany
Tris-base	Carl Roth GmbH & Co.KG, Karlsruhe, Germany
Triton-X-100	Sigma-Aldrich Inc., Munich, Germany
Trypsin	Life Technologies™ Gibco®, Darmstadt, Germany
Y-27632 dihydrochloride (ROCK inhibitor)	Tocris, Bristol, UK

Tab. 4: Instruments and equipment

instrument	**manufacture, city**
Amaxa 4D Nucleofector® system	Lonza, Cologne, Germany
C25 Incubator shaker	New Bunswick Scientific, New Jersey, USA
Cell Observer SD	Zeiss, Oberkochen, Germany
Centrifuge (5424 and 5810 R)	Eppendorf AG, Hamburg, Germany
Centrifuge	Andreas Hettich GmbH & Co KG, Tuttlingen, Germany
Centrifuge 5424 & 5415R & MiniSpin	Eppendorf AG, Hamburg, Germany
CO2 incubator CB 150	WTC Binder, Tuttlingen, Germany
DNA-agarose-gel fluorescence-system	IntasScience Imaging Instruments GmbH, Göttingen, Germany
Gelelektrophorese-Kammer HU13	Thermo Fisher Scientific, Waltham, USA
ImageXpress micro XL	Molecular Devices, CA, USA
Mr. Frosty™ Freezing Container	Thermo Fisher Scientific, Waltham, USA
Nanodrop, Specthrophotometer ND-100	Thermo Fisher Scientific, Waltham, USA
Neubauer Counting chamber	Marienfeld GmbH & Co. KG, Lauda-Königshofen, Germany
PCR-Gerät Primus 96 plus MWG	Biotech AG, Ebersberg, Germany
PH-Meter (Seven easy)	Mettler Toledo, Gießen, Germany
Pipetboy	INTEGRA Biosciences GmbH, Femwald, Germany
Pipette (0.5-10 µl; 10-100 µl; 100-1000 µl)	Eppendorf AG, Hamburg, Germany
Scale BP 3100S	Sartorius AG, Göttingen, Germany
Scale XS205 & AE160	Mettler-Toledo GmbH, Giessen, Germany
T3000 Thermocycler	Biometra GmbH, Göttingen, Germany
Thermomixer (comfort)	Eppendorf AG, Hamburg, Germany
Vortex Genie 2	Scientific Industries Inc., Biochemia, USA
Water bath	GFL®, Burgwedel, Germany

2.1.2 Antibodies

Tab. 5: Primary Antibodies

antibody against	host species	working concentration	manufacture, city
SSEA 4	mouse	1:500	Cell Signaling Technology, Frankfurt am Main, Germany
Tra 1-81	mouse	1:500	Cell Signaling Technology, Frankfurt am Main, Germany
Hoechst 33258		1:1000	Sigma-Aldrich Inc., Munich, Germany
CTNT	mouse	1:200	Thermo Fisher Scientific, Waltham, USA
SOX17	goat	1:250	R&D Systems GmbH, Wiesbaden-Nordenstadt, Germany
ZO 1	mouse	1:150	Thermo Fisher Scientific, Waltham, USA
PAX 6	rabbit	1:300	BioLegend, CA, USA
Nestin	mouse	1:1000	Synaptic Systems GmbH, Göttingen, Germany
SOX 1	rabbit	1:500	Abcam, Cambridge, UK
β-III-tubulin	rabbit	1:1000	Abcam, Cambridge, UK
β-III-tubulin	mouse IgG2	1:250	Stemcell Technologies, Vancouver, Canada
SHP (Synaptophysin)	rabbit	1:500	Synaptic Systems GmbH, Göttingen, Germany
NeuN	mouse	1:500	Merck KGaA, Darmstadt, Germany
PSD95	mouse	1:200	New England Biolabs, Frankfurt am Main, Germany
VGluT	mouse	1:300	Synaptic Systems GmbH, Göttingen, Germany
Gephyrin	mouse	1:100	Synaptic Systems GmbH, Göttingen, Germany
VGaT	rabbit	1:1000	Synaptic Systems GmbH, Göttingen, Germany
MAP2	mouse	1:1000	Sigma-Aldrich Inc., Munich, Germany
GFAP	rabbit	1:500	NeuroMab, Davis CA, USA
cTIP2	rat	1:600	Abcam, Cambridge, UK
Tü39	mouse	1:200	BioLegend, CA, USA

Tab. 6: Secondary Antibodies

fluorescence dye and target	species	working concentration	manufacture, city
AlexaFluor 647-anti-mouse IgG1	goat	1:800	Invitrogen GmbH, Darmstadt, Germany
AlexaFluor 488-anti-mouse IgG2	goat	1:800	Invitrogen GmbH, Darmstadt, Germany
Alexa Fluor 488-pure anti-mouse	goat	1:600	Dianova GmbH, Hamburg, Germany
Cy3-pure anti-rabbit	goat	1:600	Dianova GmbH, Hamburg, Germany
Cy3-anti-rabbit	goat	1:600	Dianova GmbH, Hamburg, Germany
Cy5-anti-rabbit	goat	1:600	Dianova GmbH, Hamburg, Germany
Alexa Fluor 488-anti-mouse	goat	1:600	Dianova GmbH, Hamburg, Germany
Cy3-anti-mouse	goat	1:600	Dianova GmbH, Hamburg, Germany
Cy5-anti-mouse	goat	1:600	Dianova GmbH, Hamburg, Germany
Cy5-anti-goat	donkey	1:600	Dianova GmbH, Hamburg, Germany

2.1.3 Buffer and Solutions

Tab. 7: Buffer and Solutions

buffer and solution	ingredients
4 % (w/v) PFA/PBS	40 g PFA +1 l PBS; pH 7.4
20 % (v/v) Triton X-100	20 ml Triton X-100 + 1 l water
0,02 % EDTA/PBS	500 µl 0.5 M EDTA, 0.9 g NaCl in 500 ml DPBS
Blocking solution	0.5 % NGS + PBS
Permeabilisation solution	0.2 % Triton X-100 + 0.5 % NGS in PBS
Poly-L-ornithine coating	20 % PLO + PBS
Laminin coating	10 % laminin + DMEM/F-12
Matrigel coating	10 % matrigel + DMEM/F-12
TAE-Puffer (50x)	2 M Tris + 250 mM Natriumacetat + 50 mM EDTA, pH 7.8 with 96 % (v/v) acetic acid

2.1.4 Cell lines

Tab. 8: Cell lines

cell line	manufacture, city
EmbryoMax - Primary Mouse Embryo Fibroblasts (MEF)	Merck KGaA, Darmstadt, Germany
Phoenix-AMPHO (ATCC® CRL-3213™)	ATCC, Teddington, UK

2.1.5 Media

Tab. 9: List of cell culture media

F12-10 Carrier Medium	10 % FKS + 50 µg/ml gentamicin, 50 units/ml fungizone in DMEM/F12
Dissociation medium	0.2 % Trypsin in DMEM/F12
3N medium	1:1 Mix of N2- and B27-medium N2-medium: 1x N2 supplement, 5 µg/ml insulin, 1 mM L-glutamine, 100 µM non-essential amino acids, 100 µM 2-mercaptoethanol, 50 U/ml penicillin, 50 mg/ml streptomycin in DMEM/F12 B27-medium: 1x B27 supplement, 2 mM L-glutamine, 50 U/ml penicillin, 50 mg/ml streptomycin in Neurobasal Media
STEMdiff™ Neural Induction Medium + supplements	STEMdiff™ Neural Induction Medium plus Dorsomorphin dihydrochloride (1 µM), SB 431542 (10 µM) and recombinant Human Noggin Fc Chimera Protein (500 ng/ml)
BrainPhys™ Neuronal medium + supplements	For 10 ml BrainPhys™ Neuronal Medium: 200 µl NeuroCult™ SM1 Neuronal Supplement, 100 µl N2 supplement, 2 µl of 100 µ/ml BDNF, 2 µl of 100 µg/ml GDNF, 50 µl of 100 mg/ml dibutyryl cAMP, 7 µl of 50 mg/ml ascorbic acid
iPSC-Freeze medium	1:1 Mix of Medium A and B Medium A: 50 % DMEM/F-12 + 50 % Knockout serum Medium B: 80 % DMEM/F-12 + 20 % DMSO
Fibroblast Freeze medium	80 % FBS + 20 % DMSO
MEF medium	10 % FKS, 1 % Penicillin/Streptomycin, 1 % L-glutamine (200 mM) in DMEM/F12
hES medium	10 % Knockout serum, 2 mM L-glutamine, 1 % Penicillin/Streptomycin, 0.1 mM non-essential amino acids, 0.1 mM 2-Mercaptoethanol, 10 ng/ml bFGF in DMEM/F12
Phoenix medium	2 mM L-glutamine, 1.5 g/l sodium bicarbonate, 0.1 mM non-essential amino acids, 1 mM sodium pyruvate, 10 % FBS in DMEM/F12

2.1.6 Human material

Skin Biopsies from three healthy individuals, three patients with schizophrenia and three patients with autism were obtained by the psychiatry in Tübingen.

Tab. 10: Signature for samples

explanation	**signature**
healthy individual number 1	CTR 1
healthy individual number 2	CTR 2
healthy individual number 3	CTR 3
patient with schizophrenia number 1	SZ 1
patient with schizophrenia number 2	SZ 2
patient with schizophrenia number 3	SZ 3
patient with autism number 1	ASD 1
patient with autism number 2	ASD 2
patient with autism number 3	ASD 3

2.1.7 Commercially available Kits

Tab. 11: Kits

Kit	manufacture, city
MinElute PCR Purification Kit (50)	Qiagen GmbH, Hilden, Germany
NEBuilder® HiFi DNA Assembly Master Mix	New England Biolabs, Frankfurt am Main, Germany
P3 Primary Cell 4D-Nucleofector® X Kit S (32 RCT)	Lonza Ltd, Basel, Switzerland
PSC Cardiomyocyte Differentiation Kit	Thermo Fisher Scientific, Waltham, USA
PureLink® Quick Plasmid Miniprep Kit	Life Technologies GmbH, Darmstadt, Germany
QIAamp DNA Mini Kit (50)	Qiagen GmbH, Hilden, Germany
QIAGEN Plasmid Plus Midi Kit (100)	Qiagen GmbH, Hilden, Germany
Qiagen QuiaQuick® Gel Extraction Kit	Qiagen GmbH, Hilden, Germany
RNAeasy Mini Kit	Qiagen GmbH, Hilden, Germany
STEMdiff™ Definitive Endoderm Kit	Stemcell Technologies, Vancouver, Canada

2.1.8 Mimetic peptides, plasmids and vectors

Tab. 12: Mimetic peptides

mimetic peptide	delivered quantity (mg)	molecular weight (g/mol)	concentrations (µM)
Narpin	51	6467.5	3, 9, 12
scrambled Narpin	51	6467.5	3, 9, 12
Neurexide	56	4801.4	9, 27, 50
scrambled Neurexide	58	4801.4	9, 27, 50
FN4-NF3	64	5454.1	3, 9, 18
scrambled FN4-NF3	70	5454.1	3, 9, 18

Tab. 13: Plasmids for reprogramming

plasmid	source	concentration (µg/ml)
gRNA_Cloning-Vector	Addgene #41824	1
pCAS9_GFP	Addgene #44719	1
pMXs-Oct3/4	Addgene #13366	1000
pMXs-Sox2	Addgene #13367	1100
pMXs-c-Myc	Addgene #13375	1200
pMXs-Klf4	Addgene #13370	1280
pRev CMV-EGFP	NMI, control GFP plasmid	115
VSV-G	NMI, empty cloning vector	1736

2.1.9 Software

Fiji, version 2017 – open source, https://fiji.sc/
Imaris8 x64, version 8.1.2 - Bitplane AG, Zurich, Switzerland
MetaXpress, 64 bit, version 5.1.0.41 - Molecular Devices, CA, USA
Origin 2015 - OriginLab Corporation, MA, USA
StatView, version 5.0 - SAS Institute Inc., NC, USA
GraphPad Instat, version 3.10 – GraphPad Software, Inc., CA, USA

2.2 Methods

2.2.1 Cell culture

2.2.1.1 Skin Biopsy and Fibroblast cultivation

Skin biopsies were collected at the University Department of Psychiatry and Psychotherapy of Tübingen and transported in 50 ml falcons containing F12-10 Carrier Medium. After mechanical dissection with a sterile scalpel, skin pieces were incubated in a 50 ml tube containing dissociation medium for two to four days. Samples were washed three times with F12-10 Carrier medium and transferred to 10 cm petridishes. After an incubation time of 15 minutes for cell adhesion, dishes were filled with 10 ml of Fibroblast Growth Medium 2. Samples were incubated at 37 °C, 5 % CO_2 and medium was changed every two to three days. Outgrowth of fibroblasts was observed with a phase-contrast microscope, using a 10x objective. Skin pieces exhibited an outgrowth of approximately 20 mm were transferred to a new 10 cm petri dish and further cultivated. When 100 % confluence of fibroblasts was reached, cells were separated using trypsin for five minutes and transferred to 75 cm^2 dish. Fibroblasts were passaged until passage 5. For each passage cells were cryopreserved using Fibroblast Cryo Medium.

2.2.1.2 Transfection of Phoenix-AMPHO cells and retroviral transduction of fibroblasts

7-8x10^5 Phoenix-AMPHO (ATCC, Teddington, UK) cells per well were cultivated in a 6-well plate. For each well 4 ml of Phoenix medium were used. In total 8 wells were covered with Phoenix-AMPHO cells. For the transfection of two wells 1.1 µg DNA+VSV-G, 270 µl EC-Puffer and 17.1 µl Enhancer were mixed and incubated for 5 minutes at room temperature. 100 µl plasmid and 20 µl effectene were added and incubated for 10 minutes at room temperature. In total, 5 different plasmids were used: pMXs-Oct4 (Addgene #13366), pMXs-c-Myc (Addgene #13375), pMXs-Sox2 (Addgene #13367), pMXs-KLF4 (Addgene #13370) and pRev CMV-EGFP. 120 µl of the transfection mix were seeped on Phoenix-AMPHO cells and incubated for 6 hours at 37 C, 10 % CO_2, with additional full medium change. Next day, patient-derived

fibroblasts were seeded in 6-well plates at a density of $2x10^5$ cells per well using Fibroblast Growth Medium 2 (PromoCell, Heidelberg, Germany). The following three days fibroblasts were retroviral infected with the supernatant of Phoenix-AMPHO cells in the morning and evening. For transduction, wells with fibroblasts were filled with 2 ml Fibroblast Growth Medium 2 without antibiotics. The Supernatant of all GFP-producing Phoenix-AMPHO cells was collected in a 50 ml tube and sterilised with a 0.45 µm filter. 2 ml per well of this supernatant was pipetted on fibroblasts as transduction control. A minimum of one well was infected per donor. During the night cells were incubated in a 34 C incubator. During the day cells were cultured in a 37 °C incubator. To check the transduction efficiency, GFP expression on day three was analysed via fluorescence microscopy. Transduction medium of infected fibroblasts was changed every second day. Six days after transduction, fibroblasts were detached and seeded on mouse embryonic fibroblasts (MEF)-coated plates and fed with hES medium. For MEF cultivation, 6-well plates were coated with gelantin (0.1% in H_2O) for four hours at 4 °C and washed twice with H_2O. $2x10^4$ MEFs per cm were seeded on top of the gelantin and fed with MEF medium. After one day, MEF coated plates were used for cultivation of infected fibroblasts. Fibroblasts were grown on MEF-coated plates until a clonal morphology occured. Medium was changed every second day and iPSC clones were manually passaged weekly.

2.2.1.3 Cultivation of iPSCs on MEFs

For cultivation of iPSCs on MEFs well plates were coated with MEFs. Therefore, $1x10^6$ MEFs were plated in 6-well plates and cultured at 37 °C with hES medium. After two days of cultivation, iPSCs were plated on top of the MEFs. iPSCs were cultivated until the typical clone shape was visible and manually passaged. For young passages (1-3) iPSC clones were cultivated again on MEFs. Afterwards cultivation was carried out on Matrigel-coated plates.

2.2.1.4 Cultivation of iPSC on Matrigel

For storing single cells or clone pieces, cells were resuspended in iPSC freezing medium and frozen at -80 °C for 48 h with “Mr. Frosty”. For long-term storage cells were placed in liquid oxygen. For long-term cultivation iPSCs were cultured on Matrigel (Corning Incorporated, New York, USA). A Matrigel stock solution was stored at -80 C and diluted according to the manufacturers recommendation (ca. 1:100) in cold DMEM/F-12, tips and medium were cooled to 4 C, for covering with Matrigel well plates. Wells were filled with a minimum amount of diluted Matrigel solution in order to cover the plate bottom. Plates were incubated for at least 2 hours at room temperature. Plates were stored at 4°C for up to two weeks. For cultivation of iPSCs, clone fragments or single cells were thawed, suspended in warm DMEM/F-12 and centrifuged at 300 g for 5 min. Subsequently, DMEM was discarded and cells resuspended in cultivation medium. iPSC clones were cultivated in mTeSR1 (Stemcell Technologies, Vancouver,

Canada) or Pluristem medium (Merck KGaA, Darmstadt, Germany). mTeSR1 medium was changed daily, Pluristem medium three times a week. iPSC clones were passaged when clones showed a dense fragmentation or clones started to overgrow, normally once a week. Clones were passaged using EDTA/PBS or mechanical scratching with pipette tips. In case of detachment by EDTA/PBS treatment, cells were washed twice with PBS and further incubated for maximum 7 minutes. In the presence of larger amounts of differentiated cells, clones were treated only for 2 minutes with EDTA/PBS. Afterwards cells were washed with cultivation medium and transferred to a new Matrigel-coated well plate. For mechanical passaging clones were scraped with a 100 µl pipette and transferred to a new Matrigel-coated well. Up and down pipetting was omitted to keep the clone fragments stable. For both passaging methods, cells were equally distributed by shaking the well plate horizontal and vertical in the incubator. To enable efficient cell adhesion, medium was changed only after 48h.

2.2.1.5 Endodermal differentiation

For endodermal differentiation, cells were incubated with mTeSR1 medium and 10 µM Y-27632 dihydrochloride (ROCK inhibitor) for two hours. StemPro™ Accutase Cell Dissociation Reagent (Life Technologies™ Gibco®, Darmstadt, Germany) was used for dissociation of iPSC cells. $3x10^5$ cells were seeded in a 24-well plate, covered with glass cover slips and filled with mTeSR1/ 10 µM ROCK inhibitor. Next day, medium was changed according to the instuctions given by the STEMdiff™ Definitive Endoderm Kit protocol (Stemcell Technologies, Vancouver, Canada). After 5 days of differentiation cells were fixed with 4 % PFA and stained with human anti-SOX17 antibody.

2.2.1.6 Mesodermal differentiation

PSC Cardiomyocyte Differentiation Kit supplied by Thermo Fisher Scientific was used for mesodermal differentiation. According to the manufacturers protocol, cells were dissociated into single cells. $0,8x10^5$ cells were plated in a 12 well plate covered with glass cover slips and filled with mTeSR1 medium (Stemcell Technologies, Vancouver, Canada). For the next three days, mTeSR1 medium was changed daily. On day four, medium was changed to differentiation medium A. On day six, medium was changed to differentiation medium B. Media were changed every second day. After 8 days, cells were further incubated in cardiomyocyte maintenance medium with a change every second day. When rhythmic contraction of cells occurred, cells were fixed using 4 % PFA and stained against cardiomyocyte marker genes like cardiac troponin T (mouse anti-CTNT, Thermo Fisher Scientific).

2.2.1.7 Neural Progenitor Cell (NPC) generation and cultivation

The success of NPC generation depends on the quality and purity of the iPSC culture. If necessary, differentiated cells were mechanically removed one day before further processing. For detachment, iPSC were washed twice with PBS and incubated for 7 minutes in StemPro™ Accutase Cell Dissociation Reagent (Life Technologies™ Gibco®, Darmstadt, Germany) at 37 °C, 5 % CO_2. The cells were detached via slowly up and down pipetting with a 1 ml pipette, collected in 5 ml DMEM/F-12, centrifuged, resuspended in STEMdiff™ Neural Induction Medium (Stemcell Technologies, Vancouver, Canada) plus ROCK inhibitor and counted. 2 to $3x10^6$ iPSCs were plated in one well of an AggreWell™ plate (Stemcell Technologies, Vancouver, Canada). AggreWell™ plates were coated with AggreWell™ Rinsing Solution for 5 minutes. Subsequently, plates were centrifuged at 2000 x g for 5 minutes to discard all air bubbles in the plate. After washing with PBS and DMEM, each well was filled with 500 µl STEMdiff™ Neural Induction Medium plus ROCK inhibitor (final concentration 10 µM). Calculated volume of iPSC suspension was transferred into the AggreWell™ plate and slowly and evenly distributed via up and down pipetting. Afterwards the AggreWell™ plate was centrifuged at 100 x g for 3 minutes. The plate was incubated at 37 °C, 5 % CO_2 for 5 days with daily medium change. After 5 days, the 37 µm Reversible Strainers (Stemcell Technologies, Vancouver, Canada) cells was used to harvest cells. All cells of one AggreWell™ well were plated into one well of a poly-L-ornithine/ laminin-coated 6-well plate and cultivated for 7 days in STEMdiff™ Neural Induction Medium. For poly-L-ornithine/ laminin coating, plates were first coated with 20 % poly-L-ornithine in PBS for minimum two hours at room temperature, followed by two times washing with PBS and once with DMEM/F-12. Afterwards 10 % laminin in cold DMEM/F-12 were filled in the wells for further incubation of a minimum of two hours at 37 °C.

After cultivation with daily medium change for 7 days, neural rosettes were selected using the STEMdiff™ Neural Rosette Selection Reagent (Stemcell Technologies, Vancouver, Canada). To this end, medium was discarded and cells were incubated with 1 ml STEMdiff™ Neural Rosette Selection Reagent for one hour at 37 °C. Afterwards medium was discarded and each well was washed with warm DMEM/F-12 for several times. Total medium was collected in a 15 ml tube and centrifuged at 300 x g for 5 minutes. The cell pellet was resuspended in STEMdiff™ Neural Induction Medium and plated on a poly-L-ornithine/ laminin-coated 6-well plate. Cells were cultivated using STEMdiff™ Neural Induction Medium plus Dorsomorphin dihydrochloride (1 µM), SB 431542 (10 µM) and recombinant Human Noggin Fc Chimera Protein (500 ng/ml) up to 80-90% confluence. After the first passage, cultivation medium was changed to STEMdiff™ Neural Progenitor Medium (Stemcell Technologies, Vancouver, Canada). Cells were passaged a maximum of 10 passages.

2.2.1.8 Freezing and thawing of NPC

$3x10^6$ dissociated NPCs were frozen in 1 ml STEMdiff™ Neural Progenitor Freezing Medium (Stemcell Technologies, Vancouver, Canada). For the first two days, cells were cooled down with “Mr. Frosty”. Subsequently, tubes were stored in liquid oxygen. For thawing, tubes were thawed using a 37 °C water bath and immediately resuspended in 15 ml prewarmed DMEM/F-12. Tubes were centrifugated at 300 x g for 10 minutes, medium was discarded and cells were resuspended in 2 ml STEMdiff™ Neural Progenitor Medium.

2.2.1.9 Neuronal differentiation and cultivation

For neuronal differentiation, NPCs were detached from plates using StemPro™ Accutase Cell Dissociation Reagent, dissociated and $1x10^6$ cells were transferred to 6-well plates and incubated in 3N medium plus 10 % bFGF. After two days of predifferentiation cells were dissociated again using StemPro™ Accutase Cell Dissociation Reagent and counted with the help of the Neubauer counting chamber. Glass coverslips with a diameter of 12 mm or 15 mm were coated first with 20 % poly-L-ornithine in PBS for minimum two hours at room temperature, followed by minimum of two 2 hours coating with 10 % laminin in DMEM/F-12. Each well of a 24-well plate or a 12-well plate were filled with one glass coverslips placed on the bottom. $1x10^5$ cells were plated in a well of a 24-well or 12-well plate with glass coverslips. 3N medium and BrainPhys™ Neuronal Medium (Stemcell Technologies, Vancouver, Canada) were used for cultivation and changed twice a week.

2.2.1.10 High-content analysis of neurite outgrowth

For neurite outgrowth experiments neurons were differentiated in poly-l-ornithine/ laminin-coated 24-well µ-plates (ibidi, Munich, Germany) using 3N medium. Per well, $1x10^5$ cells were seeded and cultured for four days. After differentiation, cells were fixed with 4 % PFA solution and stained with surface marker β-III-tubulin and nuclei marker Hoechst 33258. For the detection of β-III-tubulin primary antibodies, anti-mouse Alexa-488 conjugated secondary antibody was used. Because of similar fluorescence excitation and emission spectra, FITC and DAPI channel of the microscope were used for recording the antibody staining. Images were automatically retrieved via ImageXpress micro XL and analysed using the “MetaXpress High-content Image Acquisition and Analysis” software (64 bit, 5.1.0.41). Automated segmentation of nuclei and neurite outgrowth was carried out with an adjusted “Neurite Outgrowth” tool. FITC and DAPI channels were imaged for each image. As an example, a screenshot of the software surface is shown in Fig.2. DAPI channel was used for the staining and detection of nuclei. To this end, a nucleus was defined as a segment with a minimal width of 8 µm and a maximal width of 16 µm. A threshold of 3000 gray levels above local background was set for defined segments. For the detection of cell bodies, segments were processed by applying a pixel

fluorescence intensity above local background of 2000 gray levels in the β-III-tubulin staining (FITC channel). Subsequently, identified objects with a maximal width of 25 µm and minimal area of 150 μm^2 were defines as cell bodies. For the detection of neurites, segments were processed by applying a pixel fluorescence intensity above local background of 2500 gray levels in the β-III-tubulin staining (FITC channel). An outgrowth was defined as a segment with a maximal width of 8 µm and minimal cell growth of 20 µm. This length was calculated from the center of the nuclei. Normally, a nuclei had a radius of 10 µm. Outgrowth shorter than 10 µm from the border of the nucleus were excluded from the final readout. The number of total cells was determined automatically based on the Hoechst signal (DAPI channel). Number of cells with neurites longer than 10 µm were counted manually during analysis. To calculate the percentage of neurons with neurites, number of cells with neurites >10 µm was divided by total number of cells. In each experiment, the percentage of neurons with neurites was calculated for a single donor. Relative neurite induction was calculated with the control CTR 1 set 100 %. Likewise, mean neurite length was calculated for each experiment and each donor. To this end, the sum of the total neurite outgrowth was divided by the number of cells with neurites >10 µm in length or by the number of total cells. In each experiment, more than 150 cells were analysed. Six independent experiments were performed applying the same parameters. Kruskal-Wallis test and Dunn's post hoc test were used for statistical evaluation. Statistics were performed on groups: healthy, SZ and ASD. Parameters set were kept constant for all images.

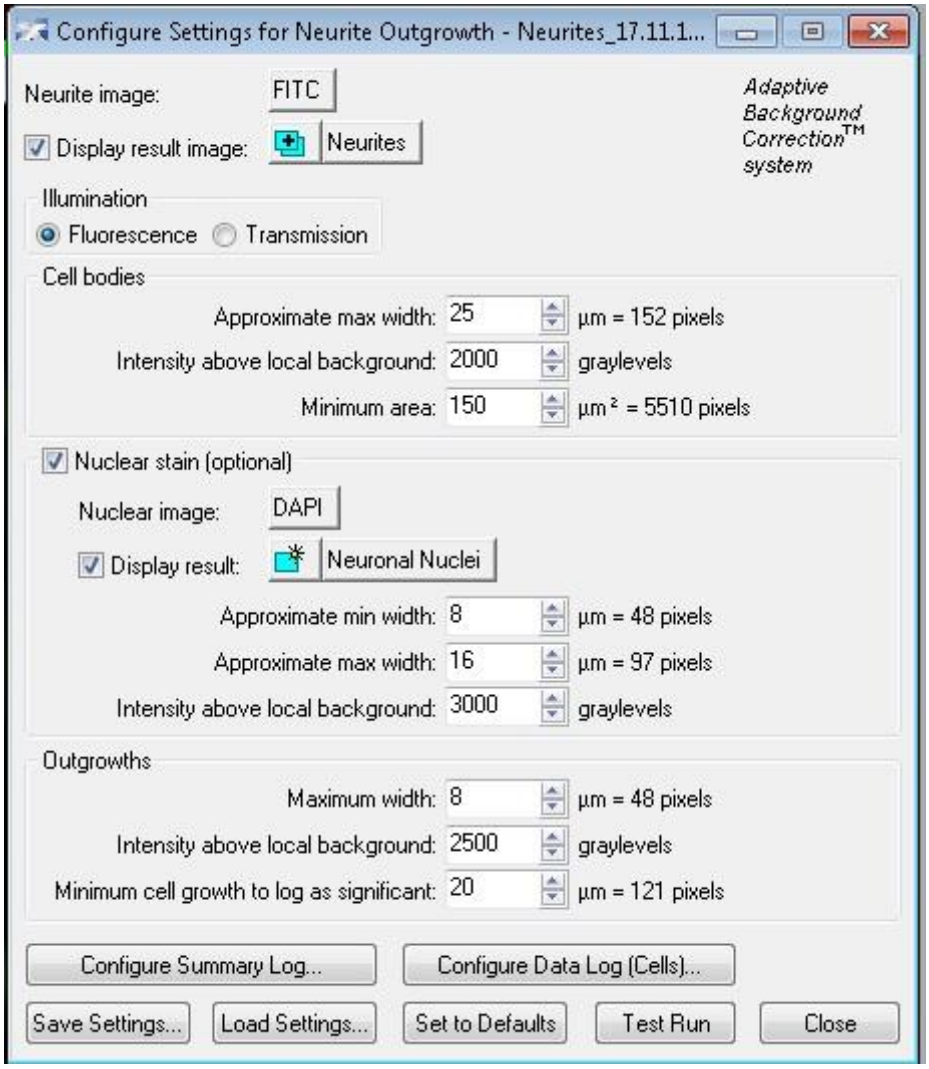

Fig. 2: Parameters set for neurite outgrowth. Screenshot of parameters for the neurite outgrowth experiment using the MetaXpress software.

2.2.1.11 Treatment of neurons with drugs and peptides

To test the effects of drug or peptide treatment, $1x10^5$ cells were seeded in one well of a 24-well µ-plate (ibidi GmbH, Martinsried, Germany) and treated once after 24 hours as depicted in Tab. 14 and 15. Subsequently, cells were cultivated for 48 hours, fixed with 4 % PFA solution, stained using β-III-tubulin antibody and Hoechst and automatically analysed as described above.

For antipsychotic treatment, drugs clozapine, haloperidol and olanzapine were diluted in DMSO. Percentage of neurons with neurites and mean neurite length were calculated for each treatment condition. Data were normalised to value of solvent control in each experiment. Kruskal-Wallis test and Dunn's post hoc test were used for statistic.

Tab. 14: Range of drug concentrations

drug	solvent	concentrations in µM
clozapine	DMSO	0.15, 0.62, 1, 1.5, 2, 4
haloperidol	DMSO	0.005, 0.027, 0.067, 0.133, 1.3, 4
olanzapine	DMSO	0.15, 0.25, 0.5, 1, 2, 4

Three different types of mimetic peptides (Tab. 14) were applied in neurite outgrowth experiment. As control a scrambled version of the peptides was added at identical concentrations. H_2O served as solvent control. Percentage of neurons with neurites and mean neurite length were calculated for each treatment condition as described above. Data were normalised to value of solvent control in each experiment. Kruskal-Wallis test and Dunn's post hoc test were used for statistic.

Tab. 15: Range of peptide concentrations

mimetic peptide	solvent	concentrations in µM
Narpin	H_2O	3, 9, 12
Neurexide	H_2O	9, 27, 50
FN4-NF3	H_2O	3, 9, 18

2.2.1.12 Analysis of PSD95 cluster density

For the analysis of PSD95 cluster density, iPSC-derived neurons were differentiated for eight weeks according to differentiation protocol described above (see section: Neuronal differentiation and cultivation). Cells were fixed with 4 % PFA solution and stained for synaptic markers PSD95 and VGluT as well as for the surface marker β-III-tubulin. Nuclei were stained with Hoechst. Confocal fluorescence z-stacks of neuronal cultures were acquired with Cell Observer SD equipped with a 63 x Plan-Apochromat oil immersion objective. Within each experiment, all settings for exposure times, contrast, brightness, resolution and threshold values were kept constant. For each donor 40 neurons were imaged per experiment. Acquired z-stacks were further processed and analysed with Imaris8 software without knowing the group classification. A surface mask was built for the β-III-tubulin channel (parameters: surface area detail level: 0.3 µm, Background subtraction: 1.00 µm). Along neurites, a region of interest of 20 µm in length was selected to build a mask. This mask was used to generate a new channel for the PSD95 and VGluT staining. According to the size (parameter: XY diameter 0.5 µm, Z diameter 1.00 µm), synaptic puncta of PSD95 and VGluT staining were marked as spots. For colocalization, a new channel mask was generated for PSD95 spots. Again, synaptic spots were analysed with VGluT channel. As requirement for colocalization, the intensity for the new masked channel of PSD95 spots had to be more than 1. Imaris8 software was applied to

calculate the number of synaptic spots in the areas of interest. The percentage of synaptic spots in each neuritic segment was normalised to CTR1 in each experiment. Density of PSD95 spots was defined as the percentage of synaptic PSD95 spots in a 20 µm neuritic segment. For calculating of the density of PSD95/ VGluT colocalization, only double positive spots for PSD95 and VGluT were included. Three independent experiments were performed. Statistics was performed in groups: healthy, SZ and ASD. Kruskal-Wallis test and Dunn's post hoc test were used for statistics.

2.2.1.13 Functional assay for calcium mobilization

For calcium imaging, iPSC-derived neurons were cultivated for eight weeks in 24-well plates covered with glass cover slips. In the first six weeks neurons were fed with 3N medium followed by a two weeks feeding with BrainPhys™ Neuronal Medium (Stemcell Technologies, Vancouver, Canada) plus supplements. For calcium imaging, neurons were stained with 1 µM Cal520® AM (AAT Bioquest) dissolved in BrainPhys™ Neuronal Medium for 30 minutes. Cal520® AM medium was discarded and cells were incubated in BrainPhys™ Neuronal Medium for further 10 minutes. The cover slips were inserted in the Patch Clamp rack. BrainPhys™ Neuronal Medium covered cells. Calcium waves were measured for 120 seconds with the Cell Observer SD microscope. 20 images were retrieved per second. Images were analysed with open source software Fiji. To this end, the nuclei of a spontaneously active neuronal cell was selected as region of interest (ROI). Fluorescence intensity of each ROI and each image was determined. Fluorescence intensity of one ROI over 120 seconds was visualised using the diagram tool of the Origin software. The number of peaks per 120 seconds was determined manually. As a measure for peak dynamics, the time from the inflection point until the peak maximum was calculated in seconds. This time is named peak length for the following analysis. Each peak was analysed manually and normalised to values of CTR 1 in each experiment. Three independent experiments were performed for one donor per group. Kruskal-Wallis test and Dunn's post hoc test were used for statistic.

2.2.2 Molecular Biology

2.2.2.1 Immunocytochemistry

For immunocytochemistry, cells were fixed using 4 % PFA solution for 10 minutes. Fixed cells were stored in well plates with DPBS. For staining, cells were permeabilised and blocked using the permeabilization and blocking solution including 0.2 % Triton-X-100 and NGS for 30 minutes. Afterwards the indicated concentration of primary antibody (see Tab. 5) were incubated over night at 4 °C or for minimum of two hours at room temperature. Primary and secondary antibodies were diluted in blocking solution. During the incubation time cells were slowly moved on a swinging compensator. After incubation, cells were washed three times for

5 minutes using DPBS. Afterwards secondary antibody was incubated for two hours at room temperature in the dark. Cells were washed again three times using DPBS. Nuclear staining was performed using Hoechst for 30 minutes at room temperature in the dark. Again cells were washed three times using DPBS and once using H_2O. For long-term storage cover slips were fixed with Mounting medium overnight and stored at 4°C. For live cell staining, cells were exposed to primary antibodies for 10 min. After a further washing step, cells were fixed for 10 min in 4 % PFA solution, and finally stained

2.2.2.2 RNA isolation

Cells were harvested, and centrifuged at 2000 g for five minutes. Having discarded the supernatants, the pellets were resuspended in 350 µl of RLT buffer. For long-term storage pellets were frozen at -20 °C. RNAeasy Mini Kit (Qiagen GmbH, Hilden, Germany) was used for RNA isolation. According to manufacturer's protocol, RNA dissolvent in 350 µl of RLT buffer was thawed and mixed with 350 µl of 70 % ethanol. Total suspension was added to the silica-membrane RNeasy spin columns and centrifuged for 30 seconds at 10000 rpm. After discarding the flow-through, spin column was washed with 700 µl of RW1 buffer and centrifuged for 30 seconds at 10000 rpm. Again, flow-through was discarded and 500 µl of RPE buffer were added to the spin column and centrifuged for 30 seconds at 10000 rpm. This step was repeated once. RNA eluates were collected and diluted with RNase free water (50 µl) and centrifuged for 1 minute at 10000 rpm. RNA can be stored at -20 C.

2.2.2.3 DNase digestion

RQ1 RNase-Free DNase was used for DNase digestion. For each sample 8 µl of RNA were mixed with 1 µl 10x buffer and 1 µl RQ1 RNase-Free DNase and incubated for 30 minutes at 37°C. 1 µl of stop solution was added and incubated for 10 minutes at 65 C. The RNA was used as a substrate for cDNA preparation after DNase digestion.

2.2.2.4 cDNA synthesis

Primers were diluted 1:50 in water. To a sample of 6 µl of RNA, 2 µl Oligo DT Primer, 0.4 µl dNTP and 7,6 µl H2O were added in one PCR tube. After incubation for 5 minutes at 70 °C, 2 µl RT Buffer, 1 µl Murine RNAse Inhibitor and 1 µl M-MuLV were added and incubated for one further hour at 42 °C followed by five minutes incubation at 80 °C. cDNA was stored at - 20°C.

2.2.2.5 Polymerase chain reaction

Polymerase chain reaction (PCR) was used for the mRNA detection of embryonic stem cell marker genes in iPSCs. cDNA prepared from iPSC clones served as starting material. Components for a standard PCR approach are listed in Tab. 16. The respective PCR program is shown in Tab. 17. A PCR amplification of genomic DNA was performed to validate the mutation in the DISC1 locus in iPSC and NPCs of CTR 1. QIAamp DNA Mini Kit (Qiagen GmbH, Hilden, Germany) was used for extraction of genomic DNA. Substances for one experiment (Tab. 18) and PCR program (Tab. 19) are mentioned below.

Tab. 16: Components for standard PCR

component	**volumen for 20 µL approach (µl)**
10x buffer	2.5
10 mM dNTP	0.2
RedTaq	1.25
H_2O	19.05
cDNA	1
Primer forward und reverse (10 µM)	0.5

Tab. 17: Standard PCR program

step	**PCR program**	**time/temperature**
1	initialization	2 min/94 °C
2	denaturation	1 min/94 °C
3	annealing	45 s/58 °C
4	elongation	45 s/72 °C
5	final elongation	10 min/72 °C
6	final hold	∞ /4 °C

The steps 2-4 were repeated for 32 cycles.

Tab. 18: Components for genomic PCR

component	**volumes for a 20 µL sample (µl)**
5x Phusion GC buffer	4
10 mM dNTP	0.4
DMSO	1
Phusion DNA Polymerase	0.2
H_2O	10
genomic DNA (200 ng/µL)	0.4
Primer forward und reverse (10 µM)	1

Tab. 19: Genomic PCR program

step	PCR program	time/temperature
1	initialization	1 min 30 s/98 °C
2	denaturation	10 s/98 °C
3	annealing	60 s/63 °C
4	elongation	15 s/72 °C
5	final elongation	10 min/72 °C
6	final hold	∞ /4 °C

The steps 2-4 were repeated for 35 cycles.

2.2.2.6 Agarose gel electrophoresis

DNA fragments were separated with agarose gel electrophoresis according to their size. Here DNA samples were mixed with 6x DNA loading buffer and loaded on a 1-2 % agarose gel in TAE buffer. To visualise all separated DNA bands with UV light, 10 µl ethidium bromide (10 mg/ml) was added to the gel. Gel electrophoresis was run at a voltage of 120 Volt for 45 minutes. The fragment size was identified using a DNA ladder.

2.2.2.7 Design of sgRNA

The online tool “ChopChop“ (http://chopchop.cbu.uib.no/) was used for designing of suitable sgRNA sequences. Human DISC1 gene (Ensembl-ID ENSG00000162946) was selected as a target sequence. Two sgRNAs in the beginning and in the end of exon 2 were selected as useful targets. Suitable PCR primers were chosen as recommended by the online tool. 851 base pairs of exon 2 were deleted to achieve a complete inactivation of the gene and a disturbed protein production. Homology sequences had to be added to insert both gRNA sequences into the gRNA cloning vector using the HiFi DNA Assembly Master Mix. Below, additional bases attached to the gRNAs are shown. Plasmid sequencing was performed for sequence control. Production of gRNA plasmids was done by Kathrina Haag in her master thesis.

forward strand 5’ to 3’:
-TCTTGGCTTTATATATCTTGTGGAAAGGACGAAACACCGNNNNNNNNNNNNNNNNNNN-
reverse strand 5’ to 3’:
-ACTAGCCTTATTTTAACTTGCTATTTCTAGCTCTAAAACNNNNNNNNNNNNNNNNNNNC-

gRNA1

gRNA2

Fig. 3: Sequencing of gRNA plasmids. Part of the gRNA sequencing of gRNA1 and gRNA2 which were used for knockout in DISC1 gene. green=100 bp insertion, red=gRNA sequences

GATGCTGTGTTGATTTCTACATGTTCCAGGCAAATACTTCCTGAGGATTGTCAGGATTTACATAATGGATTGGCCCTGGGAC
CACTGAGCCAGCATCTATCTTTGACAGGTGTACTGAGAGATGACCTTTAAACCTAGGGATGTTCTCCAGATGCAGTTCCAGC
TGGGCCAGTAAGATCTGCATGTTTATGGTGCTGTTTTTTCTTTTCTTCCCAGGCAGCCGGGATTGCTTACCACCTGCAGCGT
GCTTTCGGAGGCGGCGGCTGGCACGGAGGCCGGGCTACATGAGAAGCTCGACAGGGCCTGGGATCGGGTTCCTTTCCCC
AGCAGTGGGCACACTGTTCCGGTTCCCAGGAGGGGTGTCTGGCGAGGAGTCCCACCACTCGGAGTCCAGGGCCAGACAG
TGTGGCCTTGACTCGAGAGGCCTCTTGGTCCGGAGCCCTGTTTCCAAGAGTGCAGCAGCCCCTACTGTGACCTCTGTGAG
AGGAACCTCGGCGCACTTTGGGATTCAGCTCAGAGGTGGCACCAGATTGCCTGACAGGCTTAGCTGGCCGTGTGGCCCTG
GGAGTGCTGGGTGGCAGCAAGAGTTTGCAGCCATGGATAGTTCTGAGACCCTGGACGCCAGCTGGGAGGCAGCCTGCAG
CGATGGAGCAAGGCGTGTCCGGGCAGCAGGCTCTCTGCCATCAGCAGAGTTGAGTAGCAACAGCTGCAGCCCTGGCTGT
GGCCCTGAGGTCCCCCCAACCCCTCCTGGCTCTCACAGTGCCTTTACCTCAAGCTTTAGCTTTATTCGGCTCTCGCTTGGC
TCTGCCGGGGAACGTGGAGAAGCAGAAGGCTGCCCACCATCCAGAGAGGCTGAGTCCCATTGCCAGAGCCCCCAGGAGA
TGGGAGCCAAAGCTGCCAGCTTGGACGGGCCTCACGAGGACCCGCGATGTCTCTCTCGGCCCTTCAGTCTCTTGGCTACA
CGGGTCTCTGCAGACTTGGCCCAGGCCGCAAGGAACAGCTCCAGGCCAGAGCGTGACATGCATTCTTTACCAGACATGGA
CCCTGGCTCCTCCAGTTCTCTGGATCCCTCACTGGCTGGCTGTGGTGGTGATGGGAGCAGCGGCTCAGGGGATGCCCACT
CTTGGGACACCCTGCTCAGGAAATGGGAGCCAGTGCTGCGGGACTGCCTGCTGAGAAACCGGAGGCAGATGGAGGTCAG
TGTCTCTTCCACCTCTGTGGCCCGAGATTGTCGTGAGCTCAGATTAGCACTGGGCAGACGGCAGGAAACGAGGGGTTCTG
GGCTCAACTGACTTCCTCCTGGAAGCTGCAGCAGCTCCTTTTGGAGCCGGCTGCACAGGATGTTGCTGCACTTCTGTCTCT
TTGAATTGGACACAGATCTACTCTCCTTTTTGTCTTCTCTGTCACTTAGGTGCTCAGATTTGCTCTCCATTGGGCCGCAGGC
TCCTCTGCAGGCCCCGGCTTAGGTGAGACGTGGTTCATGCAGCCCAGCTCTGCTTTGAGACAGGAAACTGGGGGCAGGG
GAGATTGAGCTGGGTGATGTTTGGAAGGACTTGAGAGATACAAAAATGGGGATGCCCTCTATCAGGGCGATCCTGCTCTTC
ATCCGCTTCACTCATTCCCTTCCATCCTGCTGCAGTGGCTGCTGCCTTCCACAGGGTCGGGAGACTTCGCTTCTGGTCATT
GAACCTCTTTGGCTCTCAGTTTCCGTATTTAGAGATAACACCAACTCATAGGATTGTTCTAAGGCTCAAATGAGAATGTAGCT
GCTTTGGAAATAAGTACAAACTGGAGACATCTAAGGCCCAGCCTTATGATGATGCTGTCCATCCAGTTATCTGAGAGGTGG

GTATAGCCGGAAGTAGGTAGGGTTCCTCTACCCACAAAAGTTCCCAGAGAAGCCCAGGTAGAGATGCTCTGTGGCTCATCT
GTTGCCAGACTGTATTTTAATCCTGGTGTGTGTGTGCATATGTGTTTGTGTGTGTATGTGTGTGCATGTAGGTGTGCCTGTG
TGTGCGTGTGTGT

Fig. 4: Part of the sequence of DISC1 gene. For visualisation, part of the DISC1 gene is shown. Binding position of primers for genomic DNA PCR are highlighted in yellow, binding positions of gRNAs are marked in red. After successful CRISPR event 851 base pairs had been deleted.

2.2.2.8 Electroporation

gRNA plasmids were introduced into iPSCs of donor CTR 1 via nucleofection. Stem cells were cultivated in mTeSR1 without antibiotics for minimum of one passage. Medium mTeSR1 with 4 ng/µl bFGF and 10 µM ROCK inhibitor was changed two hours before nucleofection. Cells were washed with DPBS and detached with StemPro™ Accutase Dissocation Reagent. The number of cells was calculated with the Neubauer Counting Chamber. Amaxa 4D-Nucleofector™ system was used for transfection of stem cells in 16-well nucleocuvettes stripes of the P3 primary cell 4D-Nuclofector® X Kit S produced by Lonza. 200.000 cells were resuspended in 10 µl of P3 solution per well for transfection. Plasmids were diluted in P3 solution. Thereby, different amounts of DNA (0.5, 0.75 and 1 µg) and Cas9:gRNA ratios (1:1, 1:3 and 1:2) were tested. 10 µl of cell suspension and 10 µl of plasmid solution were combined in one well and electroporated with the program CB-150. Prewarmed medium was added to the cells immediately. Cells were cultivated on Matrigel coated 6-well plates in mTeSR1 medium supplemented with 10 µl/ml bFGF and 10 µg/ml ROCK inhibitor. Medium was changed one day after electroporation. Successfully transfected cells were selected by G418 selection for 72 hours. G418 resistance is encoded by the Cas9 plasmid, which is part of the transfection cocktail. Medium supplemented with bFGF was changed daily until clones of typical clonal iPSC morphology occurred. First developed clones were dissociated into single cells using StemPro™ Accutase Dissociation Reagent and further cultivated at low density until discriminable clones of iPSC morphology occurred. Larger clones were cultivated separately in a 6-well plate for several passages. Cell pellets of iPSC clones were used for PCR analysis to proof the CRISPR event.

2.2.2.9 Transcriptome analysis

Transcriptome analysis was performed by CeGaT located in Tübingen. For transcriptome analysis iPSC-derived neurons were differentiated for four weeks using 3N medium as described above. After four weeks of neuronal differentiation on cover slips in 12-well plates, $4x10^4$ neuronal cells were harvested. Therefore, cells were washed twice with PBS, scrapped, diluted in 350 µl RLT buffer and collected in 1.5 ml tubes. Tubes were frozen, stored and transported at -80°C. RNA extraction and transcriptome analysis were performed by CeGaT GmbH Tübingen. Lists of deregulated genes and significant deregulated genes (p=<0.05) from iPSC-derived neurons from patient with schizophrenia (SZ 1-3) or autism (ASD 1-3) in

comparison to healthy individuals (CTR 1-3) were provided. Lists of deregulated genes were used to analyse changes in gene expression with the PANTHER classification tool (http://pantherdb.org/). Statistical overrepresentation test was used to identify significant overrepresented gene groups of deregulated genes. Changes in gene expression have been classified according to their gene ontology group, molecular function, biological process and signaling pathway.

2.2.3 Statistics

All graphics were designed using Excel 2007, Origin2015 or Statview 5.0 (SAS Institute Inc., NC, USA). Statistical analyses were performed using Statview 5.0 or GraphPad InStat (Version 3.10, GraphPad Software, CA, USA). No data were distributed normally. Mann-Whitney U-test was performed for pairwise comparisons. Kruskal-Wallis test and Dunn's post hoc test were performed for comparisons in groups. P-values were assigned as follows: *: $p<0.05$; **: $p<0.01$; ***: $p<0.001$. Error bars represent s.e.m.

3. RESULTS

Aims of the thesis is to investigate the early cortical neuronal development of patients with schizophrenia and to identify disease relevant mechanisms for new therapeutic approaches. Therefore, iPSC from three patients with schizophrenia, three patients with autism and three healthy individuals were generated. Fibroblasts of each donor were used as cellular starting material and reprogrammed into iPSC. Generated iPSC were characterized concerning the expression of stem cell specific markers.

3.1 Generation and characterization of human iPSCs

The Psychiatry of Tübingen selected three patients with schizophrenia (SZ 1, SZ 2, SZ 3), three patients with autism (ASD 1, ASD 2, ASD 3), and three healthy individuals (CTR 1, CTR 2, CTR 3). Only patients with a family history, for example father, mother or a sibling is affected, were selected. Gender and age of patients with schizophrenia and autism were not matched to healthy individuals. In total five men (SZ 1, SZ 3, ASD 1, ASD 2, CTR 3) and four women (SZ 2, ASD 3, CTR 1, CTR 2) were selected as donors. All patients were in medical treatment at the Department of Psychiatry and Psychotherapy, University hospital, Tübingen. Diagnose for patients with schizophrenia differs between donors. SZ 1 and SZ 3 were diagnosed with a schizoaffective disorder (DSM IV: 295.70). This kind of schizophrenia is characterized by a major depressive or manic episode. During this time patients have also delusions or hallucinations [133]. Patient SZ 2 was diagnosed with a schizoaffective residuum (DSM IV: 295.60). This type of schizophrenia is characterized by an absent of delusions and hallucination and prominent negative symptoms [133]. All patients with autism were diagnosed for Asperger syndrome (DSM IV: F84.5). Patients exhibit missing interaction with other individuals and the environment [133]. Focus of the work was to characterize patients with schizophrenia. Patients with autism served as disease control group because of shared symptoms and healthy individuals as healthy control group.

For the generation of iPSC, skin biopsies were obtained from each donor as cellular starting material. Under sterile conditions, skin biopsies were mechanically sheared, enzymatically digested and cultivated. Outgrowing fibroblasts were cultivated until a confluent monolayer. Donor specific fibroblasts were used for the reprogramming process into iPSC. As reprogramming plasmids, the four Yamanaka factors (OCT3/4, SOX 2, KLF4, c-Myc) were transduced via retrovirus as described before [123]. Reprogrammed fibroblasts changed morphology and gene expression into stem cell specific characteristics. Growing abilities changed from a monolayer into a clonal growing. Fig. 5 shows typical stem cell morphology of newly generated iPSC colonies. Cells exhibit large nuclei and scant cytoplasm, comparable to

embryonic stem cell morphology Generated iPSC expressed stem cell specific marker genes, like the cell membrane markers stages-specific embryonic antigen (SSEA) 4 and tumor related antigen (Tra)1-81.

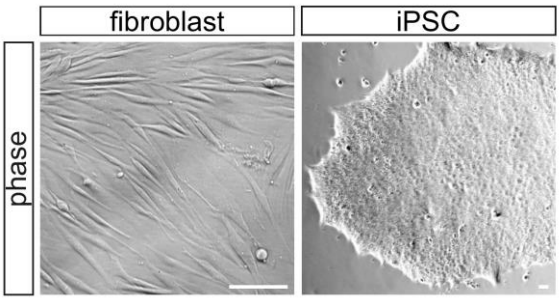

Fig. 5: Phase-contrast images of fibroblasts and an iPSC clone. Exemplarily part of a fibroblast culture derived from a healthy individual is shown on the left side. Right side iPSC clone with typical stem cell morphology from the same donor is shown. Scale bars: 10 µm.

After 10 passages, iPSC clones of all donors were tested for human embryonic stem cell marker expression [134] by immunocytochemical staining. Exemplary images of representative iPSC clones derived from each group are shown in Fig. 6. Based on the morphological analysis new generated iPSC showed clonal growing. All iPSC clones exhibited stem cell specific marker expression of stem cell markers SSEA 4 and Tra 1-81 (Supplement Fig. 1).

In addition to immunocytochemical stainings, the expression of induced exogenous genes and typical endogenous embryonic stem cell marker genes were analysed in all iPSC clones by PCR (Fig. 7). An overexpression of induced exogenous genes (OCT3/4, SOX2, KLF4 and c-Myc) is only necessary during the reprogramming process. A silent expression of induced exogenous genes after 10 passages is essential for a further usage of the iPSC clone. Specific primers for retroviral transcripts were used to differ between exogenous and endogenous expressed genes. The pluripotent human embryonal carcinoma cell line (NTERA) served as positive control for all stem cell markers. DNA of human derived fibroblast (HDF) served as a negative control for all stem cell markers. The expression of GAPDH was analysed as a loading control.

The silencing of the four exogenous induced genes after passage 10 was shown for all iPSC clones. 21 typical stem cell markers including OCT3/4, NANOG and FGF4 were mostly expressed in all iPSCs. On basis of PCR analysis all new reprogrammed iPSCs from patient with schizophrenia and autism as well as the healthy control group showed a silenced expression of exogenous induced genes and exhibited stem cell specific gene expression.

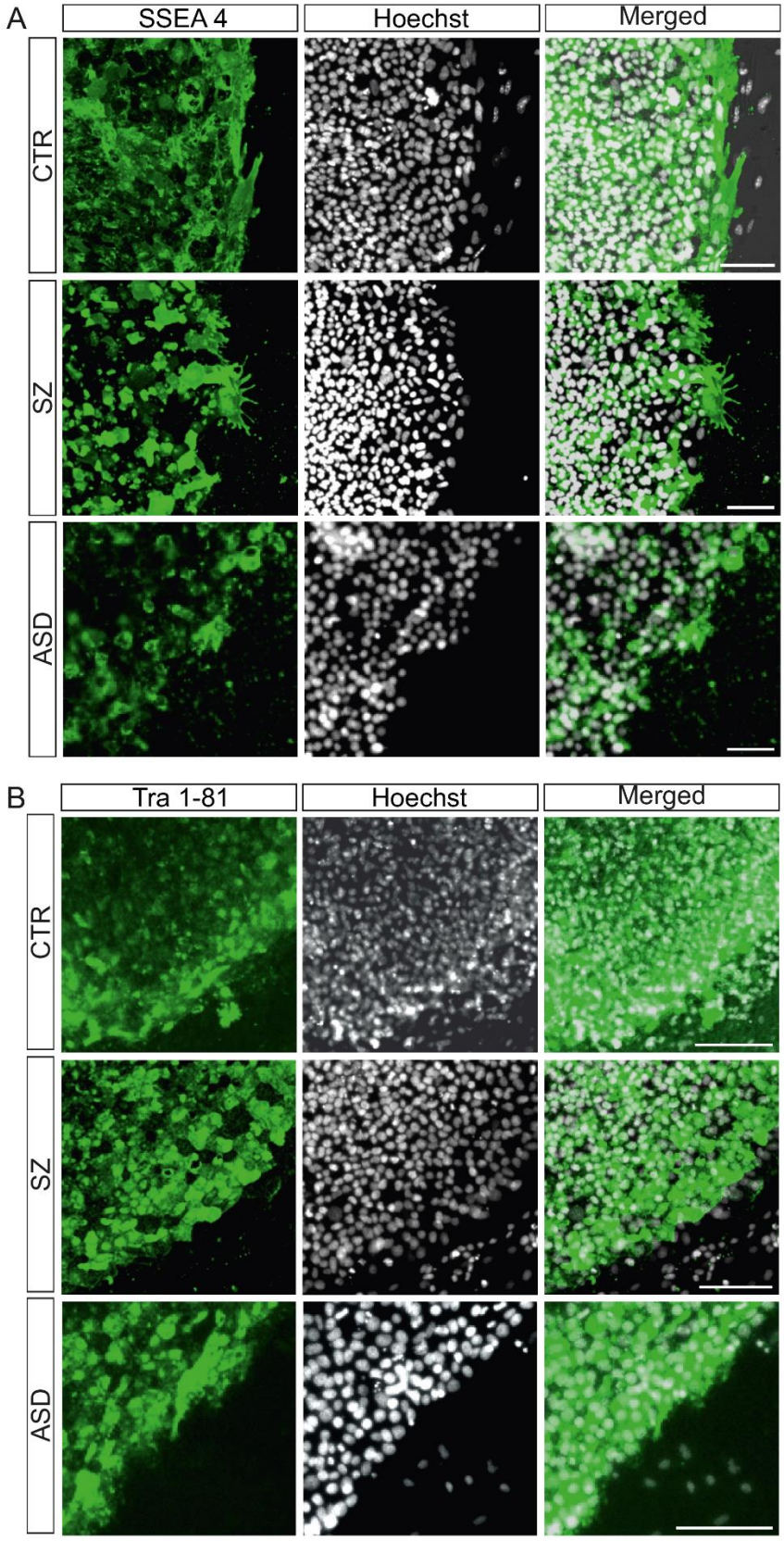

Fig. 6: Immunocytochemical staining of iPSCs against stem cell marker genes SSEA 4 and Tra 1-81. Exemplarily iPSC clones of one donor per group are shown. Via immunocytochemical staining the expression of stem cell marker genes SSEA 4 (A) and Tra 1-81 (B) is validated. Scale bars: 100 µm.

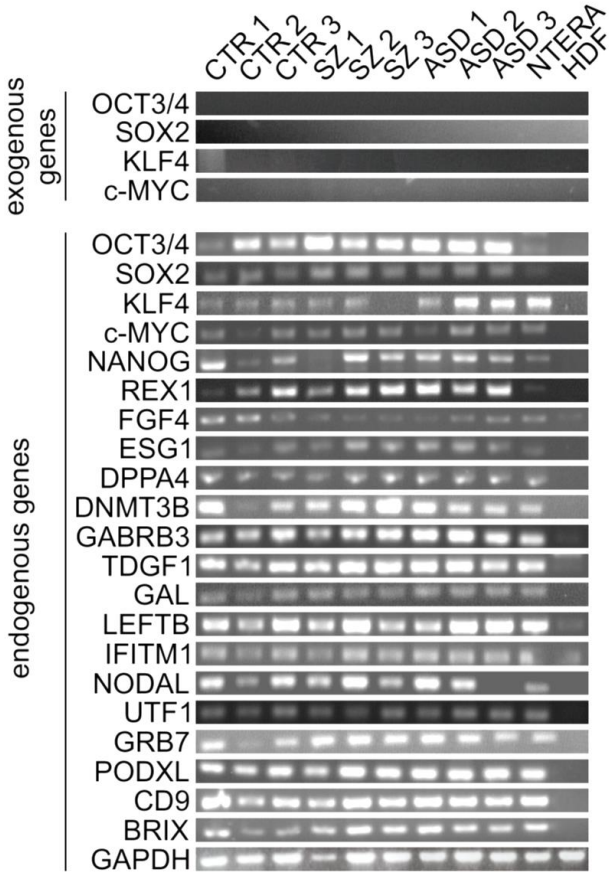

Fig. 7: RT-PCR analysis of embryonic stem cell marker genes in iPSCs. All iPSCs (CTR 1-3, SZ 1-3, ASD 1-3) were analysed with regard to the expression of 21 typical stem cell markers (endogenous genes). The silenced expression of exogenous genes was confirmed (exogenous genes). NTERA served as positive, HDF as negative control for stem cell markers. Housekeeping gene GAPDH was used as loading control. NTERA=human embryonal carcinoma cell line, HDF=human derived fibroblast

One test for pluripotency of iPSC is the differentiation into all three germ layers. Newly generated iPSCs were differentiated into ectoderm, early endoderm and cardiomyocytes as proof of pluripotency. Differentiation into endoderm and cardiomyocytes as cell type of the mesoderm, was done by Kathrina Haag during her master thesis.

Exemplarily differentiation of iPSC from the healthy donor CTR 1 into cardiomyocytes and early endoderm is shown in Fig. 8. Germ layer specific markers were stained using immunocytochemistry. Cardiac troponin T (CTNT) served as cardiomyocytes marker, SOX 17 as early endoderm marker.

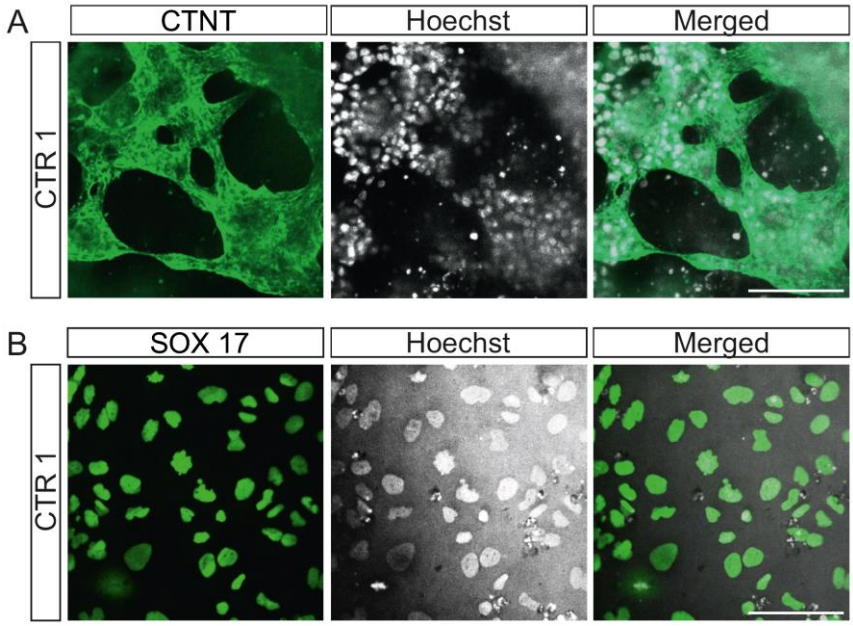

Fig. 8: Immunocytochemical staining of differentiated iPSCs against mesodermal marker CTNT and endodermal marker gene SOX 17. (A) Staining of CTR 1-derived cells against a cardiomyocyte marker cTNT (cardiac Troponin T) after mesodermal differentiation. (B) Early endodermal transcription factor SOX17 was stained in CTR 1-derived cells as marker for endoderm germ layer. (A, B) Scale bars: 100 µm.

During cardiomyocyte differentiation cells changed morphology and structure. Shown in Fig. 8A cells got clustered and built three-dimensional strands. After 14 days of differentiation, single cell cluster started rhythmical contraction like a heart muscle. After differentiation cells were fixed and stained against cardiac Troponin T (CTNT) a typical marker for cardiomyocytes [135]. Successful differentiation into cardiomyocytes was also shown for CTR 2, CTR 3, ASD 1 and ASD 2.

For endodermal differentiation cells were differentiated into early endodermal cells. Single cell iPSCs were cultivated in differentiation medium for five days, fixed and stained. One typical marker for endodermal germ layer is the transcription factor SOX 17 [136]. Fig. 8B shows a positive immunocytochemical staining for SOX17 of CTR 1-derived cells. In contrast to cardiomyocytes, early endoderm cells grew in a monolayer. Differentiation into early endoderm was shown for CTR 2, CTR 3, ASD 1, ASD 2 and SZ 2. Missing differentiations are still in progress.

As proof of pluripotency iPSC clones from donor CTR 1, CTR 2, CTR 3, ASD 1 and ASD 2 were successfully differentiated into cardiomyocytes and early endoderm cells. The differentiation into the third germ layer, the ectoderm will be shown in the next chapter.
In addition to stem cell specific gene expression and pluripotency, iPSC clones should not exhibit major genomic aberrations after the reprogramming and differentiation process. A

comparative genomic hybridization array was performed by the industrial partner CeGaT GmbH, located in Tübingen, to analyse genomic aberrations. For CTR 1, CTR 2, CTR 3, ASD 1, ASD 2, ASD 3, SZ 1 and SZ 2 big chromosomal changes could be excluded.

3.2 Neuronal differentiation of iPSC-derived cells

3.2.1 Generation of Neuronal Progenitor Cells

For investigation of diseases relevant molecular and cellular mechanisms, the generation of neuronal cell types is essential. iPSC from each donor were differentiated first into neural progenitor cells (NPC) and afterwards into cortical neurons. Subtype of cortical neurons were chosen to focus prefrontal mechanisms more in detail.

First part of the differentiation focussed on the generation of NPC. NPC can divide a limited number of times and have the capacity to differentiate into a subset of neuronal and glial cell types. Only a high-quality iPSC culture with dense and compact colonies and less undifferentiated cells, was used for generating NPC. iPSC were submitted to embryoid body formation, plated for neural rosette formation and selected for NPC. NPC were characterized according to their morphology and NPC marker gene expression (Supplement Fig. 2 and 3) As example NPC from one donor of each group are shown in Fig. 9.

Growing characteristics differed between individual donors. NPCs derived from donor CTR grew like a rosette like structure in comparison to the wide spread single cells of the other donors. In comparison to iPSCs, NPCs of all donors grew as monolayer and had a bigger proportion of cytoplasm. Immunocytochemical staining against ZO 1, PAX 6, Nestin and SOX 1 were used to show expression of NPC specific marker genes [137-139] (Fig. 9). NPC of all donors showed a concentrated expression of ZO 1 at the border of the cells. PAX 6 and Nestin were spread all over the cell with the highest concentration in the cell nucleus in all donors. The expression of the transcription factor SOX 1 was concentrated in the cell nucleus for all NPC lines.

iPSC of each donor were differentiated into NPC. The rosette formation during the differentiation process differed between single donors. Changes in differentiation did not influence characteristics of final NPC. NPC of all donors grew in a monolayer and exhibited NPC specific gene expression. All generated NPC lines were used as cellular starting material for each differentiation into cortical neurons.

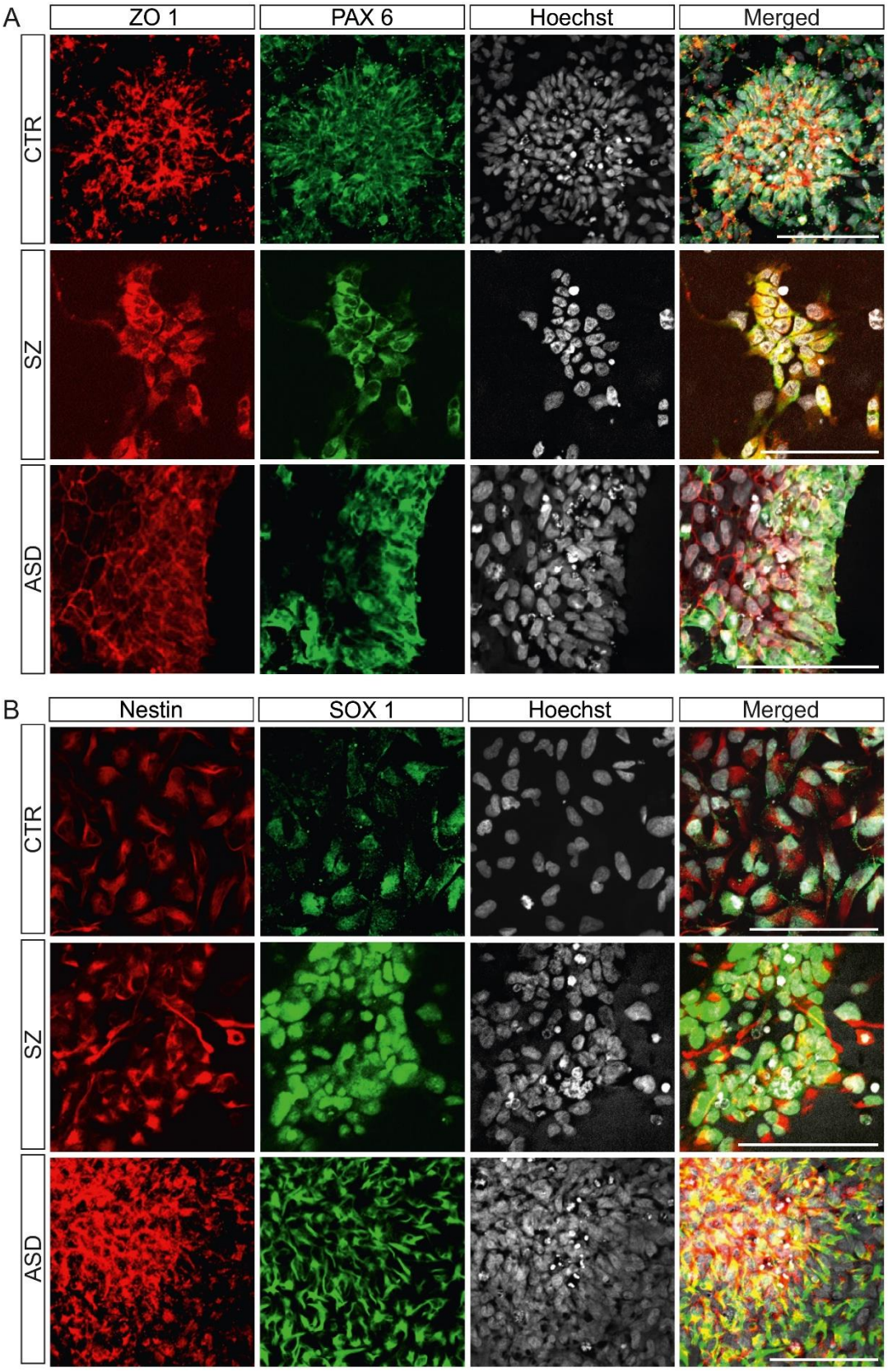

Fig. 9: Immunocytochemical staining of NPCs against marker genes ZO 1, PAX 6, Nestin and SOX 1. Expression of NPC marker genes like cell surface marker ZO 1 and transcription factor PAX 6 (A) as well as Nestin and transcription factor SOX 1 (B) was validated via immunocytochemical staining in NPCs derived from one donor per group. ZO 1=Zona Occludens 1, PAX 6=Paired box gene 6, SOX 1=SRY box 1, Scale bars: 100 µm.

3.2.2 Differentiation into cortical neurons

According to Shi et al. [140] NPCs were differentiated for eight weeks into a mixture of cortical neuronal cells and stained against typical neuronal markers. This protocol allows a defined and controlled differentiation and the investigation of early neurodevelopmental events of human cortical development. First of all, NPCs were detached and pre-differentiated using 3N medium plus fibroblast growth factor (FGF) which stimulates proliferation. After two days cells were detached again and disseminated on poly-l-ornithine/laminin-coated plates in 3N medium without FGF for the induction of cortical neurogenesis.

Already during the first week, cells changed morphology and showed a typical neuronal morphology forming a dense neuronal network. Marker expression of iPSC-derived neurons from donor CTR 1 is shown in Fig. 10. Fig. 10A shows the expression of the major synaptic vesicle protein synaptophysin and the neuron-specific β-III-tubulin, which served as whole cell surface marker in most of the images. The expression of the neuronal nuclear antigen NeuN analysed the maturation of the neuronal culture (Fig. 10B). The expression of synapse-specific markers is shown in Fig. 10C and 10D. Postsynaptic marker PSD95, enriched at the postsynaptic density of excitatory, glutamatergic neurons is co-stained with the vesicular glutamate transporter 1 (VGluT), important for uptake and storage of glutamate into synaptic vesicles at the presynaptic part (Fig. 10C). Colocalization of postsynaptic PSD95 and presynaptic VGluT was taken as an indication for a potential synapse. In analogy, colocalization of gephyrin and VGAT was examined (Fig. 10D). Gephyrin is localised at postsynaptic parts of inhibitory, GABAergic neurons while the vesicular GABA transporter (VGAT) transports GABA into synaptic vesicles. The differentiation protocol produced a mixture of neural cells including astrocytes expressing the marker gene GFAP (Fig. 10E).

In conclusion, a mixture of neural cells was successfully derived using this differentiation protocol. Exemplarily the positive expression of neuronal, synaptic and astrocytic markers is shown for donor CTR 1. A generation of neural cells enable to study disease relevant mechanisms in neural development.

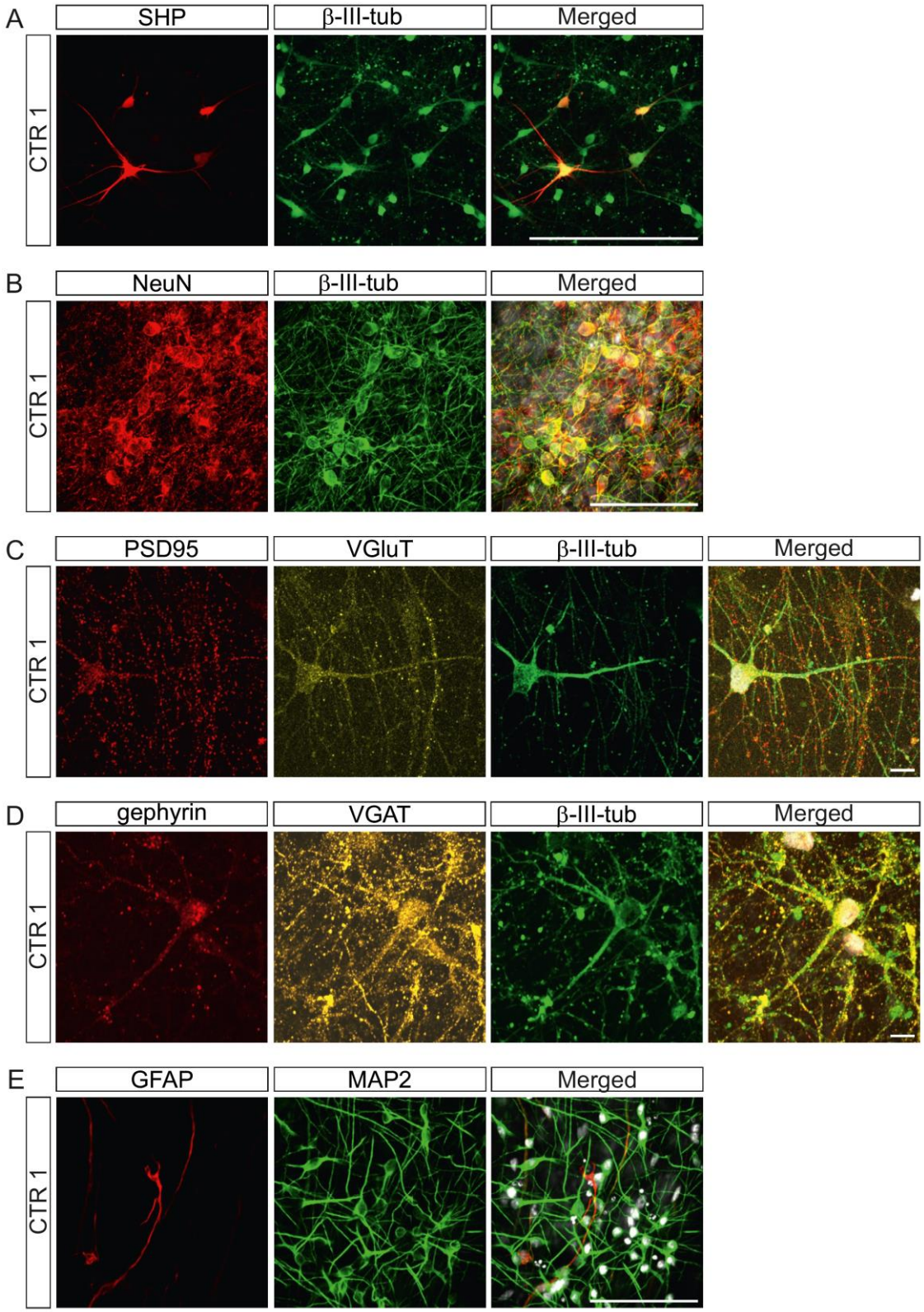

Fig. 10: Immunocytochemical staining of iPSC-derived neurons against neuronal marker genes. iPSC-derived neurons from CTR 1 were stained against neuronal markers: (A) Synaptophysin, (B) NeuN, (C) PSD95 and VGluT and (D) gephyrin and VGAT. (E) Astrocytes were stained using GFAP marker gene. β-III-tubulin and MAP2 were used as neuronal surface marker genes. SHP=Synaptophysin, PSD95=Post synaptic density protein 95, VGluT=vesicular glutamate transporter 1, VGAT=vesicular GABA transporter, GFAP=glial fibrillary acidic protein, β-III-tub=β-III-tubulin, MAP2=microtubule associated protein 2, (A, B, E) Scale bars: 100 µm, (C, D) Scale bars: 10 µm.

3.3 Significant less Ctip2 expressing neurons in patients with schizophrenia

Starting with NPCs and differentiate into neuronal cells mimic a very early embryonic neuronal development. Deep brain layer neurons are produced first followed by upper layer neurons. Ctip2 is a marker for subcortical projection neurons [141], neurons of brain layer V. To follow the dynamic development of human layer V neurons in culture, NPC were differentiated into cortical neurons and Ctip2 expression was analysed at different time points in culture. To analyse potential differences of Ctip2 expression related to a disease background, iPSC-derived neurons of one donor per group were selected.

Fig. 11A shows CTIP2 expression by immunocytochemistry in iPSC-derived neuronal cultures after 28 days of differentiation. As expected Ctip2 expression was confined to the nuclei [142]. Fig. 11B and 11C quantify the percentage of Ctip2 expressing cells for different time points and different donors. iPSC-derived neurons were differentiated, fixed and stained against Ctip2 and Hoechst. Minimal six images were taken for each time point and each donor. According to fluorescence intensity number of Ctip2 and Hoechst positive cells were obtained and percentage of Ctip2 positive cells was calculated. In Fig. 11C values of SZ 2 and ASD 1 were normalized to CTR 1 for each experiment. iPSC-derived neurons were cultivated for 56 days in four independent experiments and Ctip2 expression was analysed in a minimum of 10 images afterwards. The percentage of Ctip2 expressing cells from patient with schizophrenia SZ 2 (55 %) and autism ASD 1 (21 %) was much lower than in CTR 1 (100 %) derived cells. Differences in Ctip2 expression were observed in the analysis of different time points, too. In Fig. 11B all values were minimized by the six day data of each donor as starting value. The Graph shows the percentages of Ctip2 expression from donor CTR 1, SZ 2 and ASD 1 of one neuronal differentiation. After 40 days, the percentage of Ctip2 positive neurons differs significantly among CTR 1, SZ 2 and ASD 1. SZ 2 (10 %) and ASD 1 (23 %) expressed significantly less Ctip2 positive cells in comparison to CTR 1. In contrast to the result of 56 days differentiation of four independent experiments, iPSC-derived neurons from SZ 2 exhibited less Ctip2 expressing cells than ASD 1. Until day 20, SZ 2 exhibited the most limited percentage of Ctip2 expressing cells. At time points 27 and 31 days, the percentage of Ctip2 expressing cells is nearly similar to ASD 1. At 37 days, level of Ctip2 cells is in between CTR 1 and ASD 1.

Percentage of iPSC-derived Ctip2 positive neurons was highest for ASD 1 (29 %) after 15 days neuronal differentiation and kept that level until day 27. At day 31, percentage is nearly similar to SZ 2 and still higher than CTR 1. Order changed at day 37 and level of Ctip2 expressing

cells was lower than in CTR 1. Until day 20, iPSC-derived neurons from CTR 1 expressed less Ctip2 than ASD1 and more than SZ 2. For time point 27 and 31 days CTR 1 exhibited less Ctip2 positive neurons than the two other donors. After day 37 order changed and percentages of Ctip2 expressing iPSC-derived neurons was the highest in donor CTR 1. Differences in Ctip2 expressing cells did not belong to cell death or a reduced number of cells (Fig. 11D). In case of schizophrenia (166 %) significant more cells were analysed per images than in CTR 1. Differences in layer specific marker expression of one of the first developed brain layer gave hints for differences in the early neuronal development in iPSC-derived neurons from patients with schizophrenia.

3.4 Significant reduction of neurite outgrowth in iPSC-derived neurons from patients with schizophrenia

The changed expression of Ctip2 in iPSC-derived neurons from patients with schizophrenia suggest defects in early neuronal development. Neurite outgrowth is a characteristic of early neuronal development, too. Potential differences in neurite outgrowth during early neuronal development of iPSC-derived neurons from patients with schizophrenia was investigated.

iPSC-derived neurons were differentiated for four days on 24-well µ-plates, fixed and stained against cell surface marker β-III-tubulin. Images of Hoechst and β-III-tubulin stained neuronal cultures were retrieved using the ImageXpress micro XL microscope. The neurite outgrowth of iPSC-derived neurons was analysed using the MetaXpress software. The procedure of calculating neurite outgrowth is shown in Fig. 12A. For each image, Hoechst staining was used for staining and counting of cell nuclei. β-III-tubulin staining was used for the analysis of neurite outgrowth and neurite length. Data of CTR 1 served as normalization control in each experiment to minimize differences caused by variable neuronal differentiation among independent experiments.

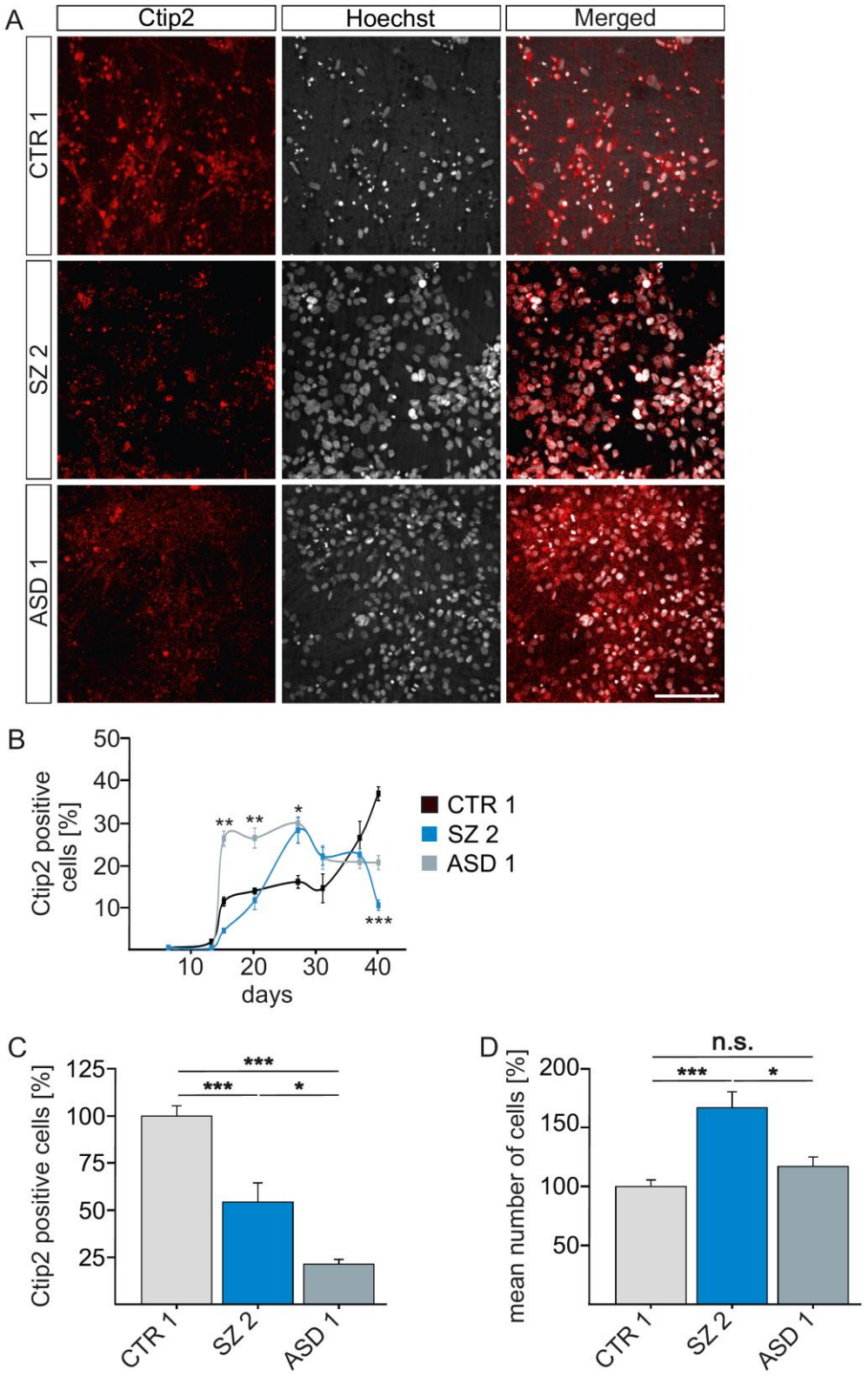

Fig. 11: Ctip2 expression analysis of iPSC-derived neurons. (A) Immunocytochemical staining against Ctip2 in CTR 1, SZ 2 and ASD 1. (B) Percentage of Ctip2 expressing cells during the first 40 days of differentiation in iPSC-derived neurons from CTR 1, SZ 2 and ASD 1. n>6, for clarity reasons only significant points are marked, non-marked dots are not significant, day 6 $H(2)=7.6$, day 13 $H(2)=11.6$, day 15 $H(2)=15.3$, day 20 $H(2)=13.1$, day 27 $H(2)=6.8$, day 31 $H(2)=1$, day 37 $H(2)=0.3$, day 40 $H(2)=21.9$, (C) Percentage of Ctip2 positive cells of iPSC-derived neurons from CTR 1, SZ 2 and ASD 1 after eight weeks neuronal differentiation, $H(2)=7.6$, n>35. (D) Mean number of counted cells after eight weeks neuronal differentiation, $H(2)=25.7$, n>35. (B, C, D) Kruskal-Wallis Test and Dunn's post hoc test, $p<0.05$*, $p<0.01$**, $p<0.001$***, Error bars are s.e.m.

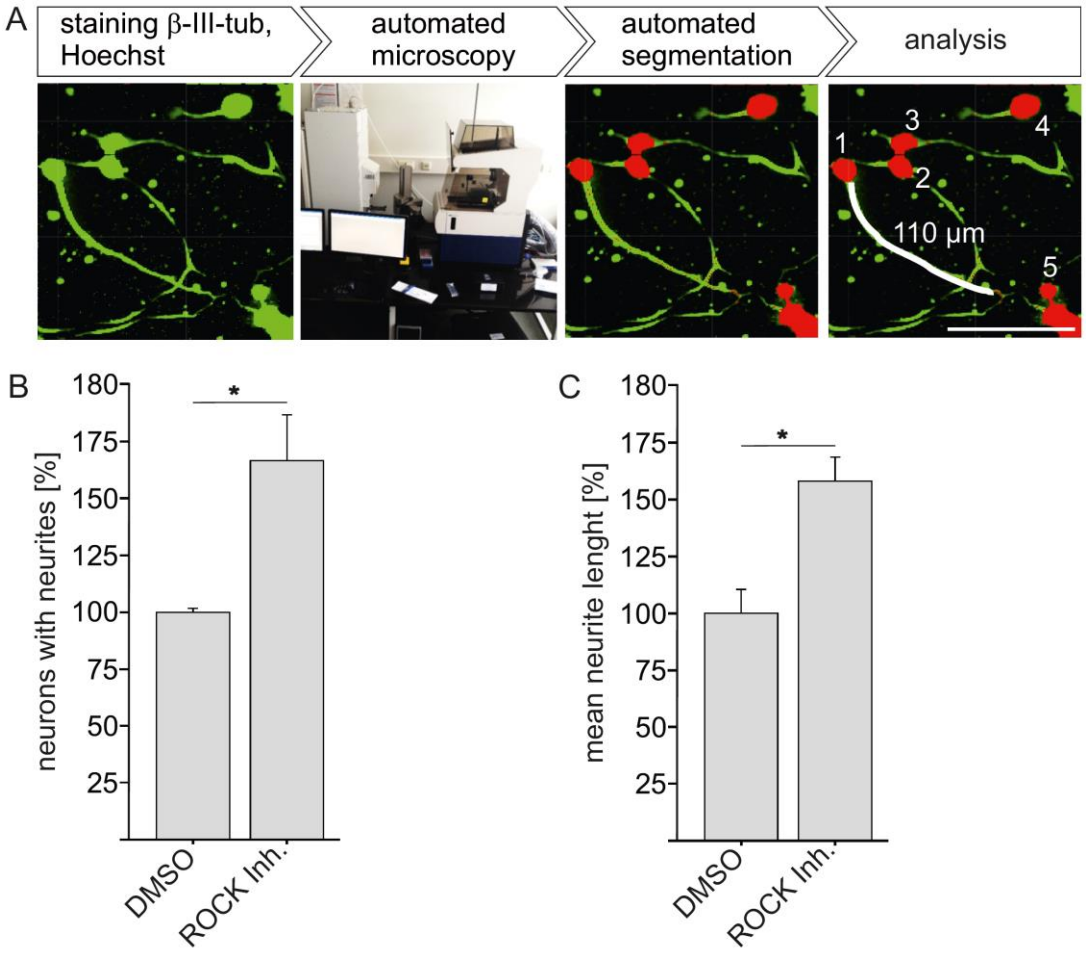

Fig. 12: Test of high content analysis of neurite outgrowth in iPSC-derived neurons. (A) Procedure of neurite outgrowth experiments: staining using β-III-tubulin antibody and Hoechst, automated imaging via ImageXpress micro XL and segmentation with the MetaXpress Software. Scale bar: 100 µm (B) Percentage of neurons with outgrowing neurites >10 µm of iPSC-derived neurons from donor CTR 1 after treatment with DMSO or ROCK inhibitor. DMSO served as solvent control. (C) Percentage of mean neurite length of iPSC-derived neurons from donor CTR 1 after treatment with DMSO or ROCK inhibitor. (B,C) Data normalised to DMSO, Mann-Whitney U-Test, $p<0.05$*, n=3.

After four days of neuronal differentiation, neurite length and percentage of neurons with neurites were calculated to analyse the ability of neurite development. Processes longer than 10 µm were defined as neurites. Suitable measurable differences between iPSC-derived neurons from patients and healthy individuals have to be identified. Y-27632 (ROCK inhibitor) was used as test substance to calibrate the system. A stimulating effect on neurite outgrowth is already known from literature [143-145]. Treatment with ROCK inhibitor allows the measurement of neurite outgrowth under controlled conditions. Pure DMSO served as dilution control. Two parameters were calculated, which reproduce the stimulating effect of neurite outgrowth after ROCK inhibitor treatment: percentage of neurons with neurites and mean neurite length. Hoechst staining was used to determine the number of total cells. Number of cells with a neurite outgrowth >10 µm was calculated via β-III-tubulin channel. Percentage of neuron with neurites >10 µm was generated for each donor and each experiment.

Fig. 12B shows a significant higher number of neurons with neurites after ROCK inhibitor treatment (167 %) in comparison to DMSO. The stimulating effect of ROCK inhibitor on neurite outgrowing can be positively measured. As additional parameter the mean neurite length of outgrowing neurites was analysed. The lengths of all measured neurites >10 µm were summed up and divided by the number of analysed cells with neurites >10 µm. Mean neurite length was calculated per donor and individual experiment. Fig. 12C shows a significant higher mean neurite length (158 %) for four days old neurons after ROCK inihibitor treatment in comparison to DMSO. To sum up an automated analysis using ImageXpress micro XL microscope for imaging and MetaXpress software for automated analysis positively measured the known stimulating effect of ROCK inhibitor on neurite formation and neurite length. These findings indicate the validity of this method and was used as tool to compare potential differences of neurite formation and the mean neurite length between healthy individuals and patients with schizophrenia or autism. According to the previous described procedure iPSC-derived neurons from patients with schizophrenia, autism and healthy individuals were differentiated for four days, fixed, stained and analysed with regard to neurite induction and length. Potential differences in early neuronal development have to be tested.

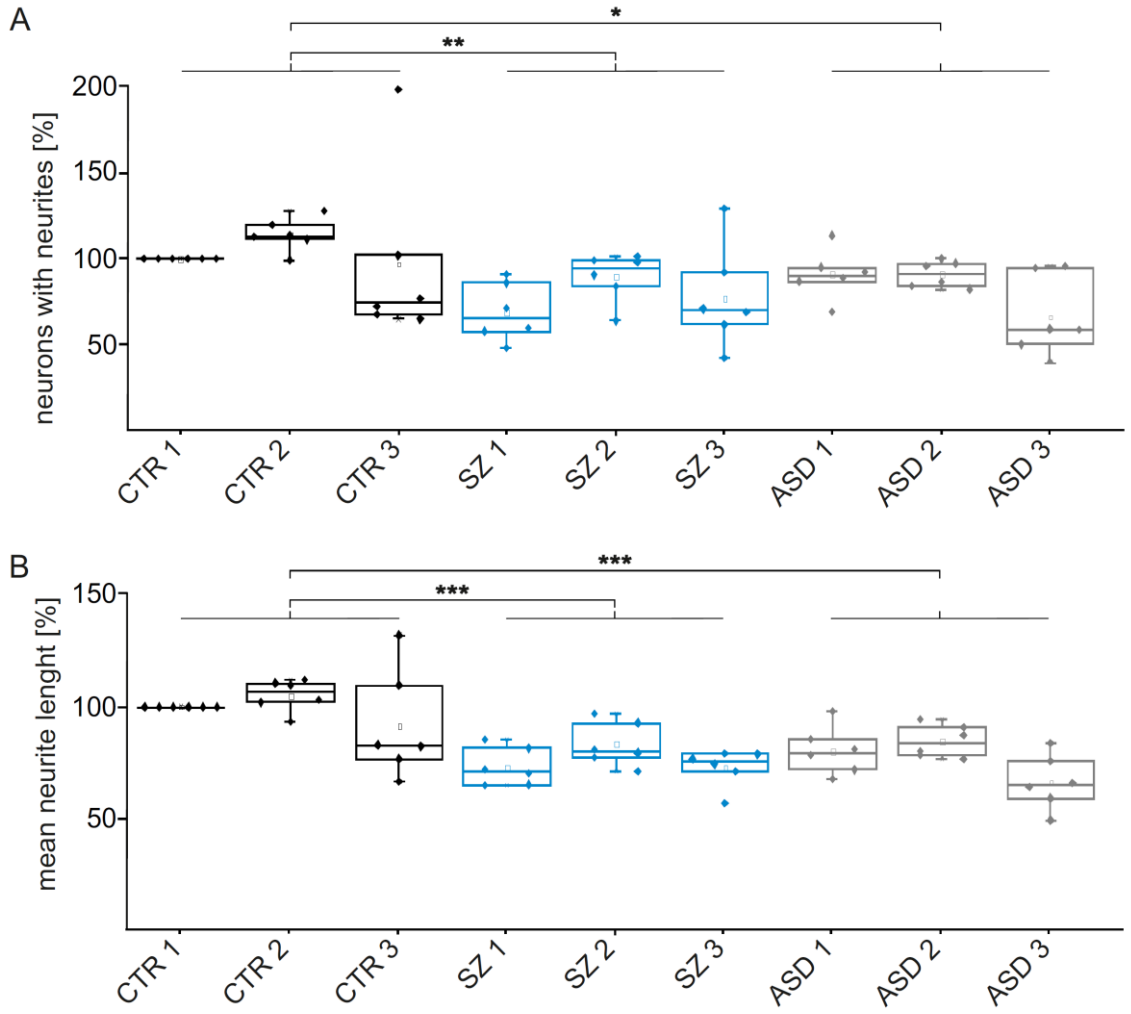

Fig. 13: High content analysis of neurite outgrowth in iPSC-derived neurons. (A) Percentage of neurons with neurites > 10 µm of iPSC-derived neurons from healthy donors (CTR 1-3), patients with schizophrenia (SZ 1-3) and patients with autism (ASD 1-3), H(2)=11.3. (B) Mean neurite length of iPSC-derived neurons from healthy donors (CTR 1-3), patients with schizophrenia (SZ 1-3) and patients with autism (ASD 1-3), H(2)=21.6 (A,B) CTR 1 served as normalization control for each experiment, six independent experiments are shown in box-and-whisker plots: filled dots = data points, dot unfilled = mean, line in the box = median, lower end of the box = 25 % of all values are smaller, upper end of the box = 75 % of values are smaller, range of the whiskers = 95 %, dot outside box and whisker = spike, Statistic was performed group wise, n=18, Kruskal-Wallis Test and Dunn's post hoc test, $p<0.05$*, $p<0.01$**, $p<0.001$***, Error bars are s.e.m.

Fig. 13 shows the results of experiments measuring neurite induction and mean neurite length of donors with schizophrenia or autism compared to healthy individuals. In total six independent experiments were performed for each donor. Exemplarily, immunocytochemical staining of iPSC-derived neurons from donor CTR 1-3, SZ 1-3 and ASD 1-3 against β-III-tubulin is shown in Supplement Fig. 4. All values were normalized to CTR 1 in each experiment which was set 100%. Each single experiment is shown as dot in the diagram. For statistical analysis, data obtained from each donor were combined in one group and subsequently evaluated statistically.

The percentage of neurons extending neurites for all donors is shown in Fig. 13A. Neurons derived from patients with schizophrenia extended significant less neurites compared to the group of healthy individuals. The percentage of neurons with neurites was reduced by 39 %. In case of the patients with schizophrenia, only donor SZ 1 (51 %) and SZ 3 (65 %) showed a higher reduction of the percentage of neurons with neurites than the mean of all donors (67 %). In SZ 2 average 85 % of neurons elaborate neurites. This percentage is lower than the lowest value of donors from the healthy control group. iPSC-derived neurons from patients with autism extend significant less neurons with neurites >10 µm in comparison to healthy individuals, too. The percentage in case of autism was reduced by 33 %. Lowest level of neurons with neurites was measured for ASD 3 (46 %). 87 % of iPSC-derived neurons from donor ASD 1 and ASD 2 extend neurites. Highest variability between experiments was observed for donor CTR 3. Percentage of neurons with neurites from each healthy individual (CTR 1:100 %, CTR 2: 105 %, CTR 3: 98 %) was bigger than in patient-derived cells.

As second parameter, the mean neurite length was calculated for all donors in the same six independent neuronal differentiations as described above (Fig. 13B). Mean neurite length of iPSC-derived neurons from patients with schizophrenia and autism was significantly reduced by 23 % in comparison to neurons derived from healthy individuals. Again, donor SZ 1 (74 %) and SZ 3 (73 %) showed a more reduced mean neurite length in comparison to SZ 2 (84 %). But mean neurite length of SZ 2 was shorter than every mean neurite length of a healthy individuals. Mean neurite length of donor ASD 3 (66 %) exhibited the highest reduction in comparison to ASD 1 (80 %) and ASD 2 (84 %). Highest experimental variability was measured for donor CTR 3 again. Mean neurite length of iPSC-derived neurons from healthy individuals (CTR 1: 100 %, CTR 2:123 %, CTR 3: 96%) was longer than in patient-derived cells.

Percentages of neurons with neurites >10 µm as well as the mean neurite lengths were significantly reduced in iPSC-derived neurons from patients with schizophrenia. Both parameters indicate an impaired neurite outgrowth in case of schizophrenia.

3.5 Significant reduced PSD95 clusters density in iPSC-derived neurons from patients with schizophrenia

iPSC-derived neurons from patients with schizophrenia exhibited significant reduced mean neurite length. Decreased capacity for neurite outgrowth may result in delayed neuronal development or reduced morphological plasticity which may impair proper formation of neuronal network. Formation of synapses is a prominent process of early neuronal development and is important for synaptic functionality. Potential changes in synapse formation have to be investigated. iPSC-derived neurons from all donors were differentiated for eight weeks, fixed and stained against postsynaptic marker PSD95 and presynaptic marker VGluT (Fig. 14A). Hoechst solution was used for nuclei staining. Whole cell surface was marked using β-III-tubulin staining. The cluster densities of PSD95 and PSD95/VGluT co-localization were analysed for dendritic fragments of each donor (Fig. 14B).

First step was the segmentation of a 20 µm neuritic region of interest using the β-III-tubulin staining. This ROI was used to generate new channels for PSD95 and VGluT staining. According to size and fluorescence intensity, number of synaptic spots was automatically determined via Imaris software. Double positive spots were marked as PSD95-VGluT co-localization. In total, 40 segments per donor and experiment were analysed without knowing the classification of the donor. To find a differentiation time with significant measurable differences, iPSC-derived neurons were differentiated up to 12 weeks. First time point with significant measurable differences in PSD95 cluster density between single donors should be selected. PSD95 cluster density was analysed for one donor per group after four, eight and 12 weeks of neuronal differentiation (Fig. 14C).

Data were normalised to the PSD95 cluster density after one week of differentiation for each donor, individually. Donor CTR 1, SZ 1 and ASD 1 exhibited the highest PSD95 cluster density after 12 weeks of differentiation. At this time point, iPSC-derived neurons from SZ 1 (152 %) and ASD 1 (166 %) exhibited significant less PSD95 cluster than CTR 1 (230 %). The percentage of PSD95 cluster density continuously increased for donor CTR 1 and ASD 1 over time. Rise of PSD95 cluster density from donor SZ 1 stagnated at time point eight weeks of differentiation. First differences of PSD95 cluster density were measured at time point four weeks of differentiation. Patient with autism (125 %) showed a significant higher PSD95 cluster density in comparison to the healthy control group (113 %). PSD95 cluster density of SZ 1 (125 %) was higher than at time point 1 week but did not increased significantly. The time point eight weeks of neuronal differentiation was the first time point with significant differences in

both disease groups in comparison to CTR 1. CTR 1 exhibited the highest level of PSD95 cluster density (176 %) in comparison to SZ 1 (121 %) and ASD 1 (152 %).

For further analyses, neurons were differentiated for eight weeks because both donors showed significant differences in PSD95 cluster density. Additionally, the quality of neuronal culture and following analyses were better than after twelve weeks differentiation. PSD95 cluster density of three different iPSC clones derived from donor CTR 1 was compared to test clonal variability. After differentiation for eight weeks and analysis of PSD95 cluster density, iPSC clone a, b, and c showed no significant differences (Fig. 14D). For following experiments only one clone per donor was selected, differentiated for eight weeks and analysed concerning cluster density of PSD95 and PSD95/VGluT co-localization.

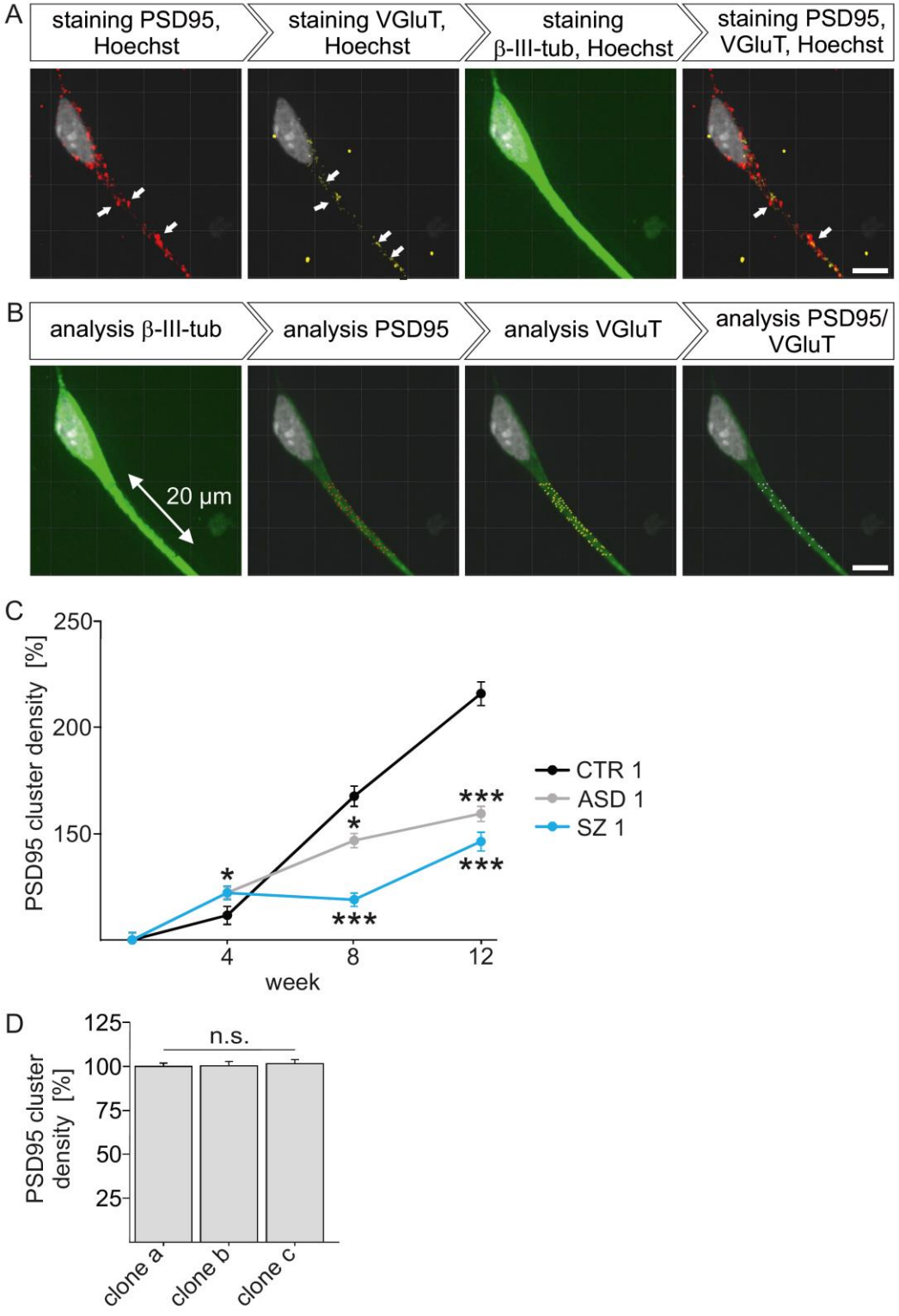

Fig. 14: Validation of PSD95 cluster density analysis. (A) Immunocytochemical staining against synaptic marker PSD95, VGluT and neuronal marker β-III-tubulin. Hoechst was used for nuclei staining. Scale bars: 10 µm. (B) Analysis of synaptic and neuronal marker expressions using Imaris software. Scale bars: 10 µm. (C) PSD95 cluster density of iPSC-derived neuron from CTR 1, SZ 1 and ASD 1 during twelve weeks differentiation. Data is normalised to one week value per donor. 4W: H(2)=9.6, 8W:H(2)= 54.7, 12W:H(2)=70.1, n=40. (D) PSD95 cluster density of iPSC-derived neurons from three different iPSC clones from donor CTR 1 after eight weeks differentiation. Data normalised to clone a, H(2)=8.8, n=50. (C,D) Kruskal-Wallis Test and Dunn's post hoc test, $p<0.05$*, $p<0.001$***, n.s.= not significant, error bars are s.e.m.

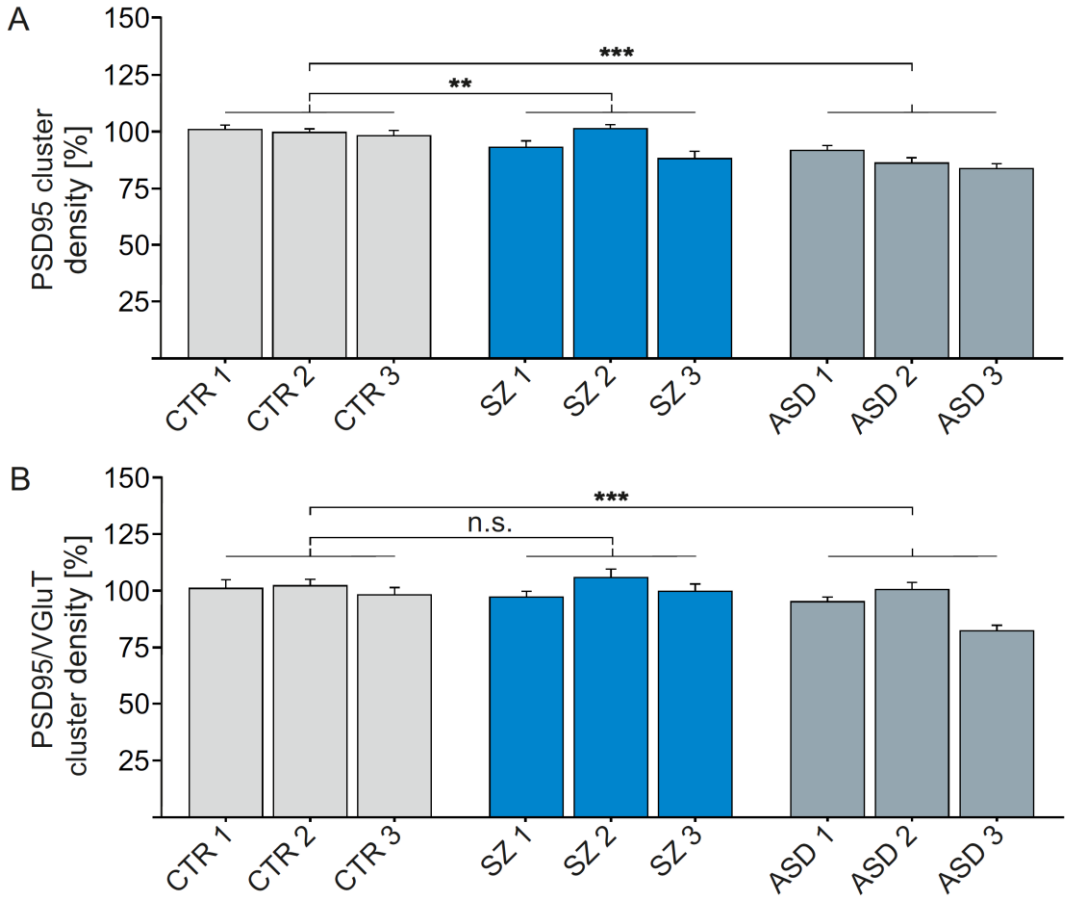

Fig. 15: PSD95 and PSD95/VGluT cluster density analysis in iPSC-derived neurons. (A) PSD95 cluster density of iPSC-derived neurons from donors CTR 1-3, SZ 1-3 and ASD 1-3 after eight weeks of differentiation, H(2)=62.4. (B) PSD95/VGluT cluster density of iPSC-derived neurons from donors CTR 1-3, SZ 1-3 and ASD 1-3 after eight weeks differentiation, H(2)=24.4. (A,B) Statistic is performed group wise. Data is normalised to CTR 1 in each experiment, three independent experiments are performed, Kruskal-Wallis Test and Dunn's post hoc test, $p<0.05$*, $p<0.01$**, $p<0.001$***, n.s.= not significant, n=360, error bars are s.e.m.

Potential changes in early neurodevelopmental processes like synapse formation of iPSC-derived neurons from patients with schizophrenia have to be tested. According to previous results, iPSC-derived neurons of one clone per donor were differentiated for eight weeks, fixed and stained against β-III-tubulin, PSD95 and VGlut. Imaris software helped to analyse PSD95 as well as PSD95/VGluT cluster density. Statistics of cluster densities were performed in groups related to disease group or non-disease group. Fig. 15 shows the PSD95 and PSD95/VGluT cluster density in iPSC-derived neurons from CTR 1-3, SZ 1-3 and ASD 1-3 after eight weeks of differentiation. PSD95 cluster densities of patients with schizophrenia and autism were significantly reduced in comparison to healthy individuals (Fig. 15A). The mean PSD95 cluster density of patients with schizophrenia was reduced by 5 %. Even if the reduction was significant, amounts of reduction measured in the neurite outgrowth experiment were not reached, based on the high variability of reduction between donors of one group. For example, donor SZ 2 (100 %) showed no reduction. PSD95 cluster density from SZ 1 (93 %) and SZ 3

(88 %) were more reduced than SZ 2. The mean PSD95 cluster density of patients with autism was reduced by 12 %. Variability is less and all donor exhibited a reduced PSD95 cluster density: ASD 1=91 %, ASD 2=86 % and ASD 3=83 %. PSD95 cluster density of each healthy donor (CTR 1=100 %, CTR 2=98 %, CTR 3=98 %) was higher and more consistent than levels of patients.

A synapse is characterised by closely co-located post- and presynaptic parts. An overlap of synaptic markers of the post- and presynaptic side was used, to identify potential synapses in iPSC-derived neurons. In addition to previous experiments, PSD95/VGluT co-localization was analysed in the same differentiation experiments. To analyse cluster density, PSD95/VGluT double positive spots were counted per 20 µm neuritic segment. Fig. 15B shows the PSD95/VGluT cluster densities for iPSC-derived neurons from CTR 1-3, SZ 1-3 and ASD 1-3 after eight weeks of neuronal differentiation. PSD95/VGluT density of patients with schizophrenia was not significantly changed in comparison to healthy individuals in contrast to a significant reduction of 9 % in iPSC-derived neurons from patients with autism. Values of the healthy control group exhibited highest similarity: CTR 1=100 %, CTR 2=102 % and CTR 3=98 %. PSD95/VGluT cluster densities of patients with schizophrenia differed a lot. Donor SZ 2 exhibited the highest cluster density of 106 % in comparison to SZ 1 (97 %) and SZ 3 (99 %). PSD95/VGluT cluster density of ASD 2 was highest (99 %) in comparison to ASD 1 (94 %) and ASD 3 (81%).

In addition to the percentage of neurons with neurites and the mean neurite length, mean PSD95 cluster density was significantly reduced in iPSC-derived neurons from patients with schizophrenia. PSD95/VGluT co-localization showed no significant differences. Based on these findings both experimental procedures showed an impaired early neuronal development in iPSC-derived neurons from patients with schizophrenia.

3.6 Transcriptome analysis of iPSC-derived neurons

Analysis of mRNA expression profiles of iPSC-derived neurons was performed to supplement the phenotypic assays. Experimental work of transcriptome analysis was done by the industrial partner CeGaT in Tübingen. For transcriptome analysis iPSC-derived neurons from all donors (CTR 1-3, SZ 1-3, ASD 1-3) were differentiated for four weeks into cortical neurons, harvested and sent for analysis. Transcriptome analysis should identify potential gene expression similarities and differences in iPSC-derived neurons. Potential differences of gene expression of genes related to neurodevelopmental, synaptic, immune activation or functional processes were focused and may relate to disease relevant mechanisms. Whole transcriptomes of iPSC-derived neurons were analysed to test the specificity of gene expression changes. Gene

expression of donor within one group should exhibited a stronger accordance than to donor of other groups. After transcriptome analysis similarity of gene expression was compared via hierarchical clustering. Fig. 16 shows the hierarchical clustering of all samples based on similarity of expression data (Spearman's rank correlation coefficient) of all genes which are significantly changed in a group comparison. Donors exhibited small changes in gene expression clustered closer than donors with big differences. iPSC-derived neurons from patients with schizophrenia or autism and healthy individuals clustered according to their disease or non-disease origin. Observed changes in transcriptome analysis were disease specific. The Dendrogram shows, RNA expression profiles of patients with schizophrenia were more closely related to the healthy control group than those of patients with autism. In addition to a hierarchical clustering RNA expression of healthy individuals and patients with schizophrenia was compared to identify significantly deregulated genes.

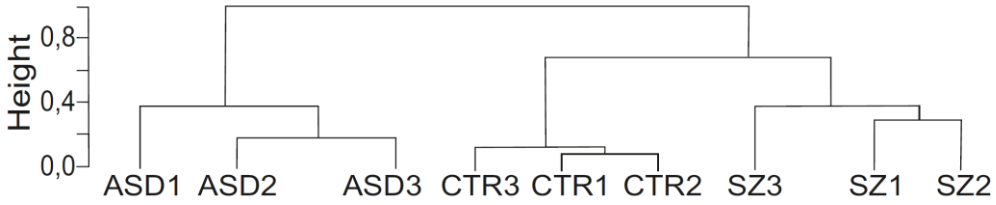

Fig. 16: Hierarchical clustering of all samples. The dendrogram shows the clustering of all donors based on similarity of RNA expression.

Tab. 20: Significant deregulated genes after group comparison of SZ and CTR.

gene ID	gene name	log2 Fold-Change
AC104809.3	homo sapiens BAC clone RP11-637O3 from 2	3.2
ARHGAP36	rho GTPase activating protein 36	-3.5
ASPN	asporin	3.4
C22orf42	chromosome 22 open reading frame 42	-3.2
CDC20B	cell division cycle 20B	4.1
CLEC2L	c-type lectin domain family 2 member L	-3.1
COL22A1	collagen type XXII alpha 1 chain	2.6
CPM	carboxypeptidase M	3.4
CYP4F24P	cytochrome P450 family 4 subfamily F member	3.7
DCT	dopachrome tautomerase	3.3
EEF1GP1	eukaryotic translation elongation factor 1	3.7
ENTPD2	ectonucleoside triphosphate	2.9
FAM156A	family with sequence similarity 156 member A	-2.8
FNDC9	fibronectin type III domain containing 9	-2.9
GALNTL6	polypeptide N-acetylgalactosaminyltransferase	-2.4
ITGA2	integrin subunit alpha 2	3.4
LEF1	lymphoid enhancer binding factor 1	3.4
LINC00473	long intergenic non-protein coding RNA 473	-3.4
NGB	neuroglobin	-3.5
RIT2	Ras like without CAAX 2	-2.8

RP11-19O2.2	pre-mRNA processing factor 31	-3.4
RP11-209K10.2	pre-mRNA processing factor 31	-3.8
RP11-262H14.5	pre-mRNA processing factor 31	-2.8
RP1-293L6.1	RP1, axonemal microtubule associated	-3.3
SPOCK3	SPARC/osteonectin, cwcv and kazal like	-2.4
ZPLD1	zona pellucida like domain containing 1	-3.3

Tab. 20 shows all deregulated genes after comparing all donors of the healthy control group with all donors with schizophrenia. The gene ID is shown on the left side, followed by the extended gene name and log2 Fold-change, which indicates the kind of deregulation. Detailed table is added as Supplement Tab. 1. All in all 26 genes indicated major differences in the transcriptomic profile ($p<0,05$), 11 genes were upregulated and 15 genes were downregulated. Transcriptomic changes were investigated in genes related to various signalling pathways or functional units. The 26 deregulated genes were submitted to panther gene ontology analysis version 12.0 (http://pantherdb.org). Statistical overrepresentation test showed no significant result ($p<0,05$). The functional classification tool grouped genes according to specific pathways, functionality or cellular compartments. Having a closer look to the ontology “Molecular function”, 8 out of 26 genes belonged to “catalytic activity” (GO:0003824) and 5 out 26 genes were members of the “binding category” (GO:0005488). Only 1 gene belonged to “structural molecule activity” (GO:0005198) and another gene to “transporter activity” (GO:0005215). The two prominent categories after selecting the ontology term “Biological Process” were “cellular process” (GO:0009987) (8 genes out of 26) and “metabolic process” (GO:0008152) (7 genes out of 26). The ontologies “Cellular Component”, “Protein Class” and “Pathways” exhibited no category with more than 4 genes. However, some of the deregulated genes identified were previously shown to be linked to SZ. For example the upregulated ecto-nucleosidase ENTPD2 was mentioned before in an antipsychotic study for schizophrenia [146]. As a member of the Ras-signaling family, RIT2 is important for neuronal development. In 2010 Glessner et al. analysed copy number variations in patients with schizophrenia and found also aberrations in the RIT2 gene [147]. Among these genes related to schizophrenia, upregulation of LEF1 was identified indicating aberrations in the WNT-signalling pathway [148]. During the last years, several papers described the WNT pathway as a crucial pathway in the pathogenesis of schizophrenia [149, 150].

Minor difference in transcriptome analysis after comparing healthy individuals with patients with schizophrenia may result on big gene expression differences between individual donors in each group. Each donor with schizophrenia (SZ 1, SZ 2 and SZ 3) was compared separately with the group of all healthy control individuals. Numbers of deregulated genes observed for each patient are depicted in Fig. 17. The transcriptomic profile of donor SZ 1 showed the

highest number of deregulated genes (149) in comparison to the healthy control group. Donor SZ 2 (49) and SZ 3 (37) exhibited less deregulated genes. Only two deregulated genes (ASPN, EEF1GP1) mentioned in previous studies were again significantly deregulated comparing single patients with schizophrenia with the healthy control group.

Indicating the big genetic variability between donors of one group, most deregulated genes were not shared among transcriptomic profiles. Only 4 identical genes were deregulated in SZ 1 and SZ 2, SZ 2 and SZ 3 shared only one deregulated gene. Most similarity existed between SZ 3 and SZ 1 (16 identical deregulated genes). For details of deregulated genes see Supplement Tab. 2-4. Analysis of shared deregulated genes using the PANTHER Overrepresentation Test showed no enrichment of any genes. But detailed analysis of the 149 deregulated genes between SZ 1 and CTR 1-3 exhibited significantly overrepresented genes. Genes involved in “muscle contraction” (GO:0006936) revealed 19.77-fold enrichment ($p=9.21 \times 10^{-16}$) and genes important for “actin cytoskeleton” (GO:0015629) a 10.56-fold enrichment ($p=1.33 \times 10^{-7}$, Bonferroni correction). Genes related to “calcium ion binding” (GO:0005509) and “cell differentiation” (GO:0030154) were significantly enriched, too. 8 deregulated genes belonged to “Wnt signaling pathway” (P00057), 30 genes to “developmental process” (GO:0032502), 8 genes to “calcium-binding protein” (PC00060) and 1 gene belonged to “synapse” (GO:0045202).

49 deregulated genes were found after a detailed comparison of SZ 2 and CTR 1-3. PANTHER overrepresentation test identified an enrichment of genes greater than 100-fold involved in antigen processing and presentation of peptide or polysaccharide antigen via MHC class II (GO:0002504) ($p=5.36 \times 10^{-16}$). Here 7 out of 49 genes belonging to category “developmental process” (GO:0032502). Genes related to calcium or WNT-signalling were not found.

Only 53 deregulated genes were found in transcriptome profile analysis of SZ 3 and the healthy control group. Deregulated genes were analysed via PANTHER overrepresentation test. Genes involved in “nervous system development” (GO:0007399) showed a 6.72-fold significant enrichment (p=0.00494). 12 genes were grouped to the category “developmental process” (GO:0032502), 1 gene to category “calcium-binding protein” (PC00060) and 2 genes belonged to category “Wnt signaling pathway” (P00057). Deregulated genes were found a variety of signalling and functional processes. These findings indicate the high diversity of patients with schizophrenia at the transcriptome level.

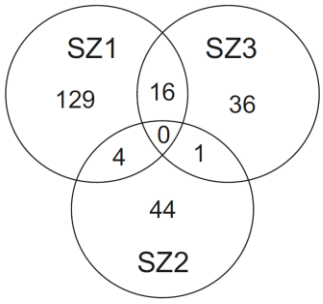

Fig. 17: Number of deregulated genes after transcriptomic profile comparison. Individual patients with schizophrenia are compared with the healthy control group. Numbers indicate deregulated genes belonging to major differences in transcriptomic profile ($p<0.05$).

Since group comparisons revealed only few differences, a paired comparison of one individual chosen from the healthy (CTR1) and the schizophrenia (SZ2) group was conducted. 1146 significantly deregulated genes (Supplement Tab. 5), found after transcriptome sequencing, were analysed with PANTHER overrepresentation test. Deregulated genes of following ontology groups were significantly deregulated (p=<0,05): “calcium-dependent phospholipid binding” (GO:0005544) (p=0.029), “antigen processing and presentation of peptide or polysaccharide antigen via MHC class II” (GO:0002504) (p= 0.000014), “nervous system development” (GO:0007399) ($p=8.05 \times 10^{-9}$) and “synaptic transmission” (GO:0007268) (p= 0.00345). Functional classification analysis identified 18 genes important for “calcium-binding proteins” (PC00060), 21 genes related to “Wnt signaling pathway” (P00057), 9 genes to “synapse” (GO:0045202), 159 genes to “developmental process” (GO:0032502) and 51 genes to “immune system process” (GO:0002376).

In conclusion, gene expression of patients with schizophrenia and healthy individuals exhibited big differences. Minimization and specification of analysed groups resulted in an increased number of significantly deregulated genes. Overrepresentation test and functional annotation figured out gene clusters, related to calcium signalling, cell development and MHC class II.

3.7 Reduced calcium mobilization in iPSC-derived neurons from patient with schizophrenia SZ 2

As mentioned in the previous chapter, a group of genes related to calcium binding was significant enriched. Since calcium ions are involved in neuronal transmission, aberrant calcium influx may account for functional defects observed in schizophrenia.

To test potential changes in calcium mobilization iPSC-derived neurons were differentiated for eight weeks and analysed regarding intracellular calcium mobilization. Cal520® AM was used as fluorescence-based assay to detect intracellular calcium ions in neurons. According to the

fluorescence intensity an influx and outflux of calcium were measured and analysed. As shown in Fig. 18A fluorescence intensity of Cal520® AM differs at different time point of the recording. Neuronal cells showed spontaneous activity and exhibited a changed amount of calcium ions inside the cell body. Exemplarily, quantification of Cal520® AM fluorescence intensity of iPSC-derived neurons from ASD 1 is shown in Fig. 18B. This visualization was used to count the frequency of calcium peaks and the length of a peak. Three independent experiments were performed for CTR 1, SZ 2 and ASD 1 to analyse potential differences in case of schizophrenia. As shown in Fig. 18C frequency in iPSC-derived neurons from patients with schizophrenia and autism is significantly reduced. In each experiment data were normalised to CTR 1. iPSC-derived neurons from donor SZ 2 significantly showed less mobilization of calcium ions. In comparison to healthy individuals, frequency was reduced by more than one-half (53 %). Frequency of iPSC-derived neuron from donor ASD 1 is also significantly diminished to 61 %. In contrast to the frequency, the length of a calcium peak is not significantly affected in iPSC-derived neuron from patients with schizophrenia (147 %) or autism (142 %) (Fig. 18D). Results of three independent experiments exhibited a high variability.

As supposed after transcriptomic analysis, calcium influx is affected in patients with schizophrenia. iPSC-derived neurons from patients with schizophrenia obtained a significant reduced frequency of calcium influx. The lengths of the calcium peaks were not affected.

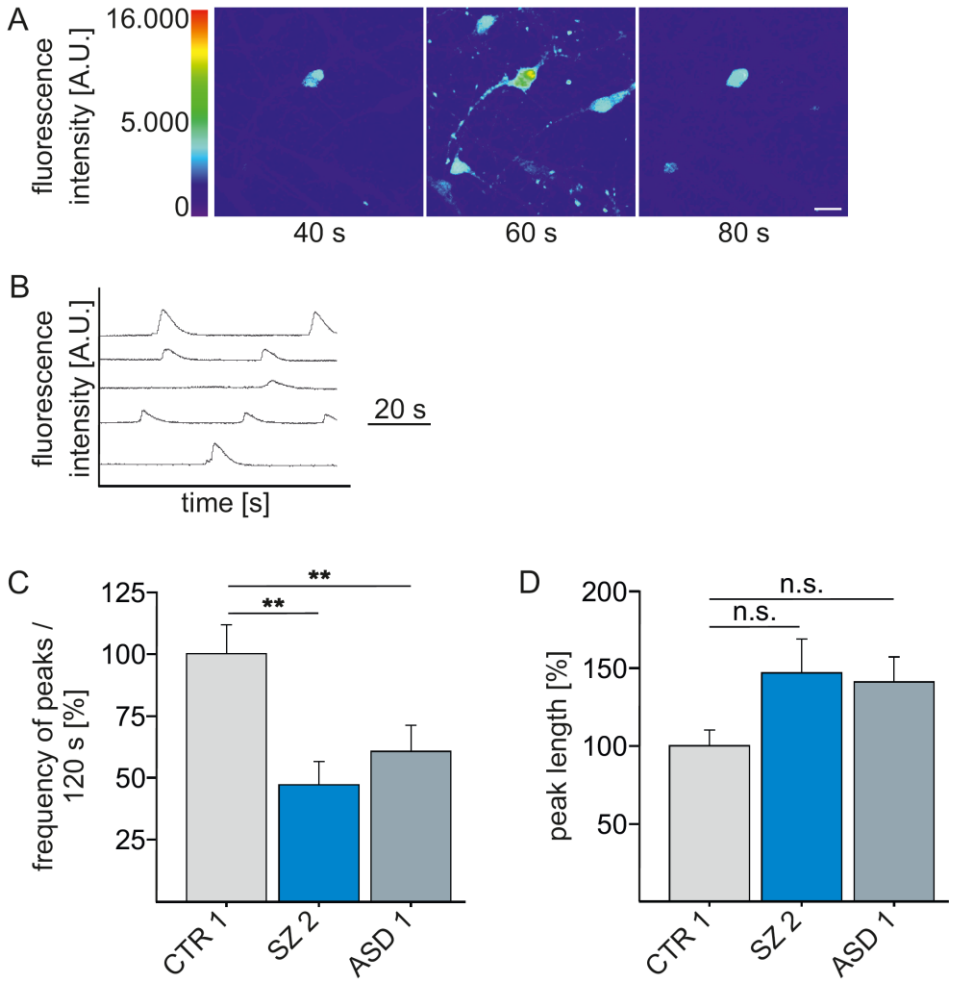

Fig. 18: Calcium mobilization in iPSC-derived neurons. (A) Fluorescence dye Cal520® AM is used to visualize intracellular calcium ions. Images of stained iPSC-derived neurons from donor CTR 1 are shown for time points 40, 60 and 80 seconds. Scale bar: 10 µm (B) Fluorescence intensity of Cal50® AM during a 120 second recording of iPSC-derived neurons from donor ASD 1. (C) Frequency of peaks measuring Cal520® AM fluorescence intensity in iPSC-derived neurons from CTR 1, SZ 2 and ASD 1. Data is normalised to CTR 1. $H(2)=13.7$, $n>14$. (D) Peak length normalised to CTR 1 during a Cal520® AM recording in iPSC-derived neurons from CTR 1, SZ 2 and ASD 1. $H(2)=1.9$, $n>33$. (C, D) Kruskal-Wallis Test and Dunn's post hoc test, $p<0.01$**, n.s.= not significant, error bars are s.e.m.

3.8 Increased MHCII expression in iPSC-derived NPCs and neurons from patient with schizophrenia SZ 2

In addition to deregulated calcium binding genes, transcriptome analysis identified an enrichment of MHCII related antigens. MHCII complex can be found on antigen presenting cells which are important for initiating the immune response. The formation and potential changes in MHCII complex expression have to be investigated in iPSC-derived NPC and neurons from patients with schizophrenia or autism in comparison to healthy individuals.

To test whether the upregulation of MHCII complexes is initiated early in neuronal development, MHCII expression in NPCs was analysed. Therefore, NPCs from SZ 2 and CTR 1 were stained with the Tü39 antibody specific for HLA-DR, DP and DQ heterodimeric

cell surface glycoproteins of the MHCII complex, without permeabilization. Cell nuclei were stained with Hoechst. Analysis focussed on a round shaped area surrounding the cell nucleus. Tü39 intensity of each ROI was measured automatically using the open source software Fiji. Mean intensity of Tü39 was calculated for 50 different cells for each donor and normalised to CTR 1 (100%). As shown in Fig. 19A the mean intensity of Tü39 is significantly upregulated by 29 % in iPSC-derived NPCs from SZ 2 (129 %). iPSC-derived NPCs from SZ 2 expressed significantly more MHCII complexes at their cell surfaces than CTR1. For further neuronal differentiation gene expression of MHCII has to be investigated. iPSC-derived NPC from patient with schizophrenia and healthy individual were differentiated to cortical neuronal cell for four weeks. The MHCII expression was analysed with immunocytochemical staining with Tü39 antibody. For exposure to the first antibody, neurons were not fixed and permeabilised to enable detection of functional MHCII complexes at the cell surface. Images show neuronal cells with typical neuron morphology (Fig. 19B). Cell nuclei were stained with Hoechst solution. MHCII complexes were spread all over the cell body independent of the donor, visible as green spots.

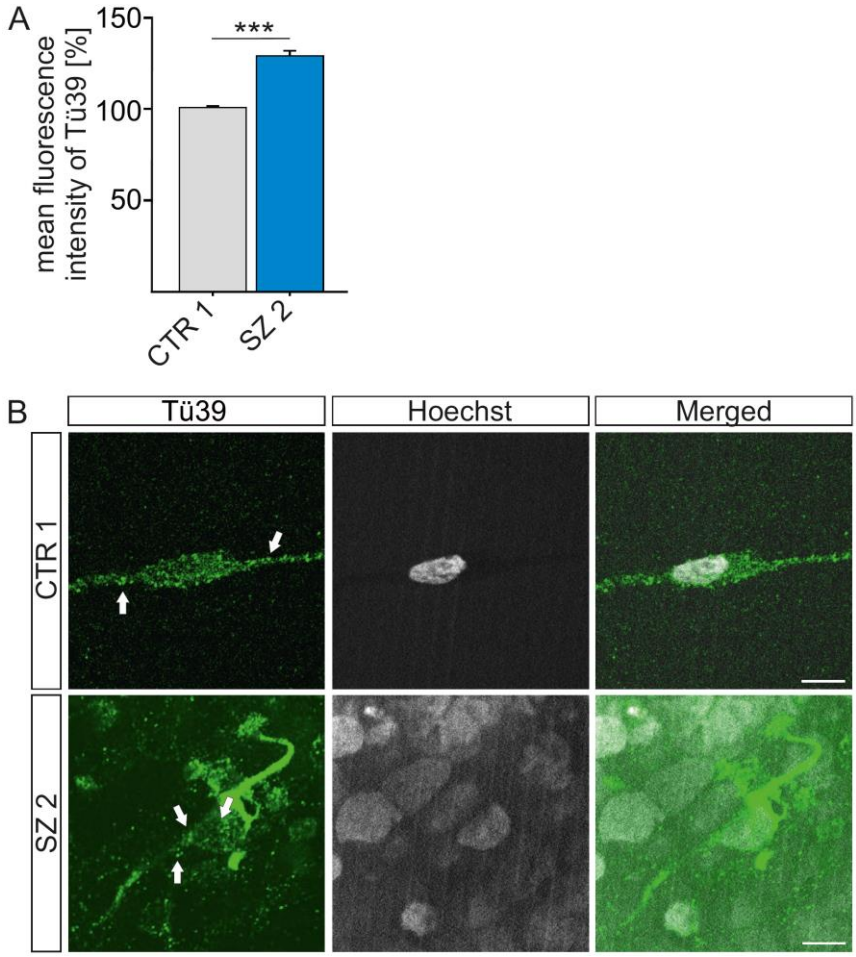

Fig. 19: MHCII expression in iPSC-derived cells. (A) Quantification of mean intensity of MHCII expression of NPCs from donor CTR 1 and SZ 2. Data is normalised to CTR 1. Mann-Whitney U-Test, $p<0.001$***, n=50, error bars are s.e.m. (B) Immunocytochemical staining of living four weeks old neurons from donor CTR 1 and SZ 2. Hoechst staining is done as nuclei staining. Scale bars: 10 µm.

3.9 Olanzapine and haloperidol significantly reduced early neurite outgrowth of iPSC-derived neurons from donor CTR 1

As mentioned before early neuronal development of iPSC-derived neurons from patients with schizophrenia is changed. Neurons exhibited deficits in the percentages of neurons with neurites and mean neurite length. Measuring the neurite outgrowth offers a robust method to investigate early neurodevelopmental processes. The effect of three known and three new substances on neurite outgrowth of iPSC-derived neurons was tested, to find new drugs for the treatment of schizophrenia. In the beginning, common drugs used for the treatment of schizophrenia were selected. One first generation antipsychotic haloperidol and two atypical antipsychotics clozapine and olanzapine were chosen. Mode of action differs between drugs. Second generation antipsychotics have a higher affinity to serotonin receptors and first generation antipsychotics bind preferentially more to dopamine receptors.

iPSC-derived neurons from donor CTR 1 and SZ 2 were differentiated for 72 hours and treated with different concentrations of antipsychotics for the subsequent 48 hours. Finally, cells were fixed, stained against surface marker β-III-tubulin and neurite outgrowth was automatically analysed with the ImageXpress system. The percentage of neurons with neurites >10 µm and the mean neurite length of all measured neurons were calculated for 75 images per individual experiment. Analysis was performed for CTR 1 and SZ 2 in three independent experiments. Effects of drugs on neurite outgrowth were tested in concentrations up to 4 µM.

Fig. 20A shows the percentage of neurons developing neurites after treatment with clozapine in the range from 0.15 µM up to 4 µM. All values were normalised to CTR 1 untreated. As shown before, the percentage of neurons with neurites from the patient with schizophrenia SZ 2 (59 %) was in untreated condition significant lower than percentage in the healthy control group (100 %). Significance was tested for drug treated versus untreated conditions individually per donor. The drug clozapine did not influence the percentage of neurites per neuron in any case independently of the drug concentration and the donor. Despite no significant results, little effects on the ability to form neurites could be observed. Low concentration of 0.15 µM clozapine had a negative effect on the ability of neurite formation in both donors (CTR 1=88 %, SZ 2=48 %). Higher concentration supported the percentages of neurons with neurites and increased the value for donor CTR 1 at 1 µM to a maximum of 115 % and for SZ 2 at 4 µM up to 75 %. Observed changes were not significant.

Olanzapine (Fig. 20B) had a significantly negative effect on neurite formation of donor CTR 1. The percentage of neurons with neurites from CTR 1 was significantly reduced after treatment with 0.125, 0.5 and 1 µM olanzapine in comparison to the untreated control. Highest reduction was measured after cultivation with 0.5 µM olanzapine. Neurite formation was significantly reduced by 36 %. In addition to CTR 1, the curve of the percentage of neurons with neurites from SZ 2 after olanzapine treatment showed a U shape with higher amounts of neurites in the low and high drug concentrations. Comparing untreated and drug treated conditions, iPSC-derived neurons from SZ 2 showed no significant differences.

The treatment with haloperidol (Fig. 20C) from 0.005 µM up to 4 µM had also a significantly negative effect on the formation of neurites from CTR 1. The percentage of neurons with neurites was significantly reduced in iPSC-derived neurons from CTR 1 after treatment with 0.027 and 0.067 µM haloperidol. In comparison to the untreated control highest reduction by 43 % was measured after treatment with 0.067 µM haloperidol. iPSC-derived neurons from SZ 2 exhibited no significant changes in neurite formation after treatment with haloperidol.

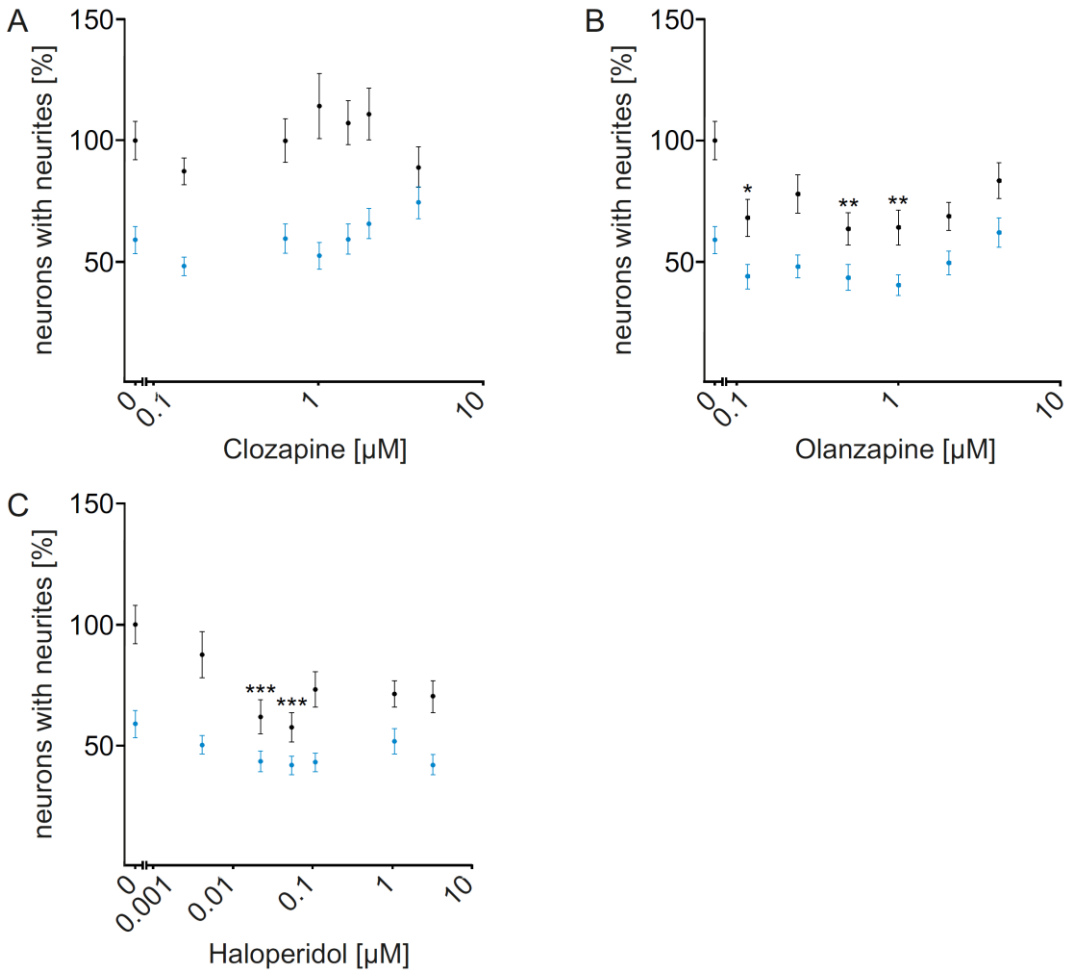

Fig. 20: Percentage neurons with neurites of iPSC-derived neurons from CTR 1 and SZ 2 after drug treatment. iPSC-derived neurons from patient with schizophrenia SZ 2 (blue) and healthy individual CTR 1 (black) were treated with clozapine (A, 0.15, 0.62, 1, 1.5, 2, 4 µM), olanzapine (B, 0.125, 0.25, 0.5,1,2,4 µM) and haloperidol (C, 0.005, 0.027, 0.067, 0.133, 1.3, 4 µM) for 48 hours and percentage of neurons with neurites was calculated for 75 images per individual experiment. Only significant spots are marked. Kruskal-Wallis Test and Dunn's post hoc test, $p<0.05$*, $p<0.01$**, $p<0.001$***, CTR 1 Clozapine $H(6)=8.3$, CTR 1 Olanzapine $H(6)=22.8$, CTR 1 Haloperidol $H(6)=25.2$, SZ 2 Clozapine $H(6)=10.9$, SZ 2 Olanzapine $H(6)=12.6$, SZ 2 Haloperidol $H(6)=10.6$, $n=75$, error bars are s.e.m.

In addition to neurite formation the mean neurite length was calculated after treatment with clozapine, olanzapine and haloperidol up to 4 µM. Treatment with clozapine showed no significant changes in neurite outgrowth in comparison to the untreated control for both donors (Fig. 21A).

Fig. 21B shows the mean neurite length of iPSC-derived neurons from CTR 1 and SZ 2 after treatment with olanzapine with the same concentration as described above. Mean neurite length of donor CTR 1 was significantly reduced after treatment with 0.125, 0.5, 1 and 2 µM olanzapine. Highest reduction (39 %) was measured after treatment with 1 µM olanzapine. iPSC-derived neurons from SZ 2 exhibited no significant changes.

Treatment with haloperidol also significantly reduced the mean neurite length in iPSC-derived neurons from CTR 1. A significant reduction of the mean neurite length was measured for donor CTR 1 after treatment with 0.027, 0.067, 0.133, 1.3 and 4 µM haloperidol. The mean neurite length of iPSC-derived neurons from CTR 1 was minimal reduced by 43 % after treatment with 0.067 µM haloperidol. In comparison to the untreated control, iPSC-derived neurons from SZ 2 showed no significant differences in neurite outgrowth.

Despite of the same affinity profiles clozapine and olanzapine showed no comparable effects on the ability to form neurites. Clozapine did not significantly influence the neurite formation and the mean neurite length at any concentrations. The drugs olanzapine and haloperidol significantly inhibited the process of neurite outgrowth for donor CTR 1. Reduction of neurons with neurites and mean neurite length followed a U-shaped turn suggesting compensatory effects at higher concentrations as described by hormetic drug response models [151].

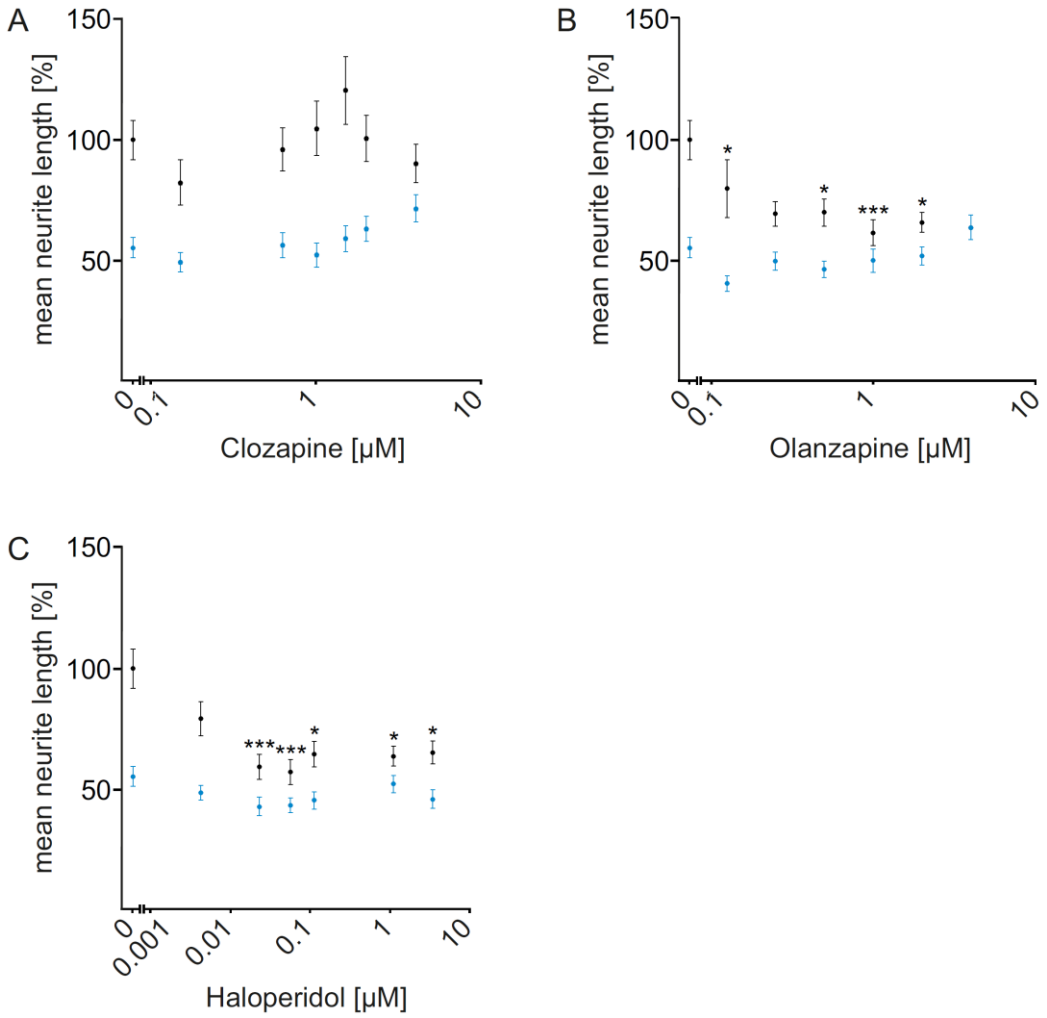

Fig. 21: Mean neurite length of iPSC-derived neurons from CTR 1 and SZ 2 after drug treatment. iPSC-derived neurons from patient with schizophrenia SZ 2 (blue) and healthy individual CTR 1 (black) were treated with clozapine (A, 0.15, 0.62, 1, 1.5, 2, 4 µM), olanzapine (B, 0.125, 0.25, 0.5,1,2,4 µM) and haloperidol (C, 0.005, 0.027, 0.067, 0.133, 1.3, 4 µM) for 48 hours and mean neurite outgrowth of all cells was calculated for 75 images per individual experiment. Only significant spots are marked. Kruskal-Wallis Test and Dunn's post hoc test, $p<0.05$*, $p<0.01$**, $p<0.001$***, CTR 1 Clozapine $H(6)=10.6$, CTR 1 Olanzapine $H(6)=23.2$, CTR 1 Haloperidol $H(6)=27.3$, SZ 2 Clozapine $H(6)=11.9$, SZ 2 Olanzapine $H(6)=17$, SZ 2 Haloperidol $H(6)=9.1$, $n=75$, error bars are s.e.m.

3.10 Increased percentage of neurons with neurites after treatment with mimetic peptides was not peptide specific

Three different mimetic peptides were added to the neuronal differentiation of iPSC-derived cells to test the influence on the neurite outgrowth, too. Narpin, neurexide and FN4-NF3 are synthetic mimetic peptides which target important receptors for neuronal development, like the FGF receptor.

The glycoprotein neuroplastin 55 was basis for the synthesis of the mimetic peptide narpin. Neuroplastin 55 is one isoform of neuroplastin which belongs to the immunoglobulin superfamily of cell adhesion molecules (CAMs). The mimetic peptide neurexide has the same sequence as the heterophilic neuroligin-1 binding site of neurexin 1. Neurexin 1 is a presynaptic membrane protein and its interaction with neurexin is essential for a neuron-neuron interaction and the formation of a synapse. The mimetic peptide FN4-NF3 is synthesised on basis of the sequence for neurofascin which is important for the synaptic development, too. Neurofascin is a cell adhesion molecule important for axon targeting in neuronal development.

Effects of mimetic peptides narpin, neurexide and FN4-NF3 in different concentrations were tested in iPSC-derived neurons from a healthy individual (CTR 1) and a patient with schizophrenia (SZ 2). According to the drug treatment, application of peptides started 24 hours after initiating neuronal differentiation and lasted for 48 hours. Cells were fixed, stained with β-III-tubulin antibody and Hoechst solution and automatically analysed using the MetaXpress system. Three experiments were performed independently. Data was normalised to the untreated value of CTR 1 or SZ 2 in each experiment. As experimental control, the neurite outgrowth after ROCK inhibitor treatment was analysed. An enhanced neurite outgrowth after ROCK inhibitor was shown before. Compared to DMSO, percentage of neurons with neurites after ROCK inhibitor treatment was significantly increased in iPSC-derived neurons from CTR 1 (73 %) and SZ 2 (70 %). An enhancing effect of the ROCK inhibitor on neurite outgrowth was confirmed. A scrambled version of the peptide was applied in the same concentration as control for a peptide specific effect. Fig. 22 shows the percentage of neurons with neurites after treatment with a scrambled version of the peptides and a functional version of the peptides narpin (A), neurexide (B) and FN4-NF3 (C). Independent of the treatment or the donor the number of neurons elaborating neurites was enhanced. Even if the percentage is significantly increased in some cases after peptide treatment in comparison to the untreated control, the effect was not peptide specific. Number of neurites was increased after treatment with the scrambled version of the peptide, too. A comparison between the percentage of neurons with

neurites after treatment with the scrambled version of the peptide and the functional version of the peptide showed no significant differences at any concentration.

Even if results were not significant little tendency could be observed. Only in neurons from patients with schizophrenia, treatment with narpin had a supportive effect. Effect was not peptide specific but increased by 46 % in SZ 2 after treatment with 12 µM narpin. A treatment with 12 µM scrambled narpin increased the number of neurons with neurites by 45 %. In comparison, highest level of neurons with neurites in CTR 1 was 116 % after treatment with 3 µM narpin.

Treatment of iPSC-derived neurons from donor SZ 2 and CTR 1 with scrambled or functional neurexide had a supportive effect on neurite formation, too. iPSC-derived neurons from CTR 1 exhibited nearly the same number of neurites (~123 %) after treatment with the three peptide concentrations. After treatment with the scrambled version of neurexide percentage of neurons with neurites was increased up to 127 %. Highest level of neurons with neurites (153 %) was reached after treatment with 9 µM neurexide for donor SZ 2. 9 µM scrambled neurexide increased number of neurons with neurites by 41 %. Difference was not significant and a peptide specific effect was excluded. Higher concentrations 27 µM and 50 µM neurexide did not increased the neurite formation as much as 9 µM neurexide.

Treatment of iPSC-derived neurons from CTR 1 with 3 µM FN4-NF3 had the most positive effect and increased the percentage of neurons with neurites up to 143 %. After treatment with 3 µM scrambled FN4-NF3 the number of neurons with neurites was enhanced by 32 %. Highest percentage of neurons with neurites (148 %) was measured after treatment with 18 µM in iPSC-derived neurons from SZ 2. Treatment with the same concentration of scrambled FN4-NF3 showed only an increase of neurites up to 128 %. Differences after treatment with scrambled or functional peptide were not significant and a peptide specific effect for neurite formation of FN4-NF3 was excluded.

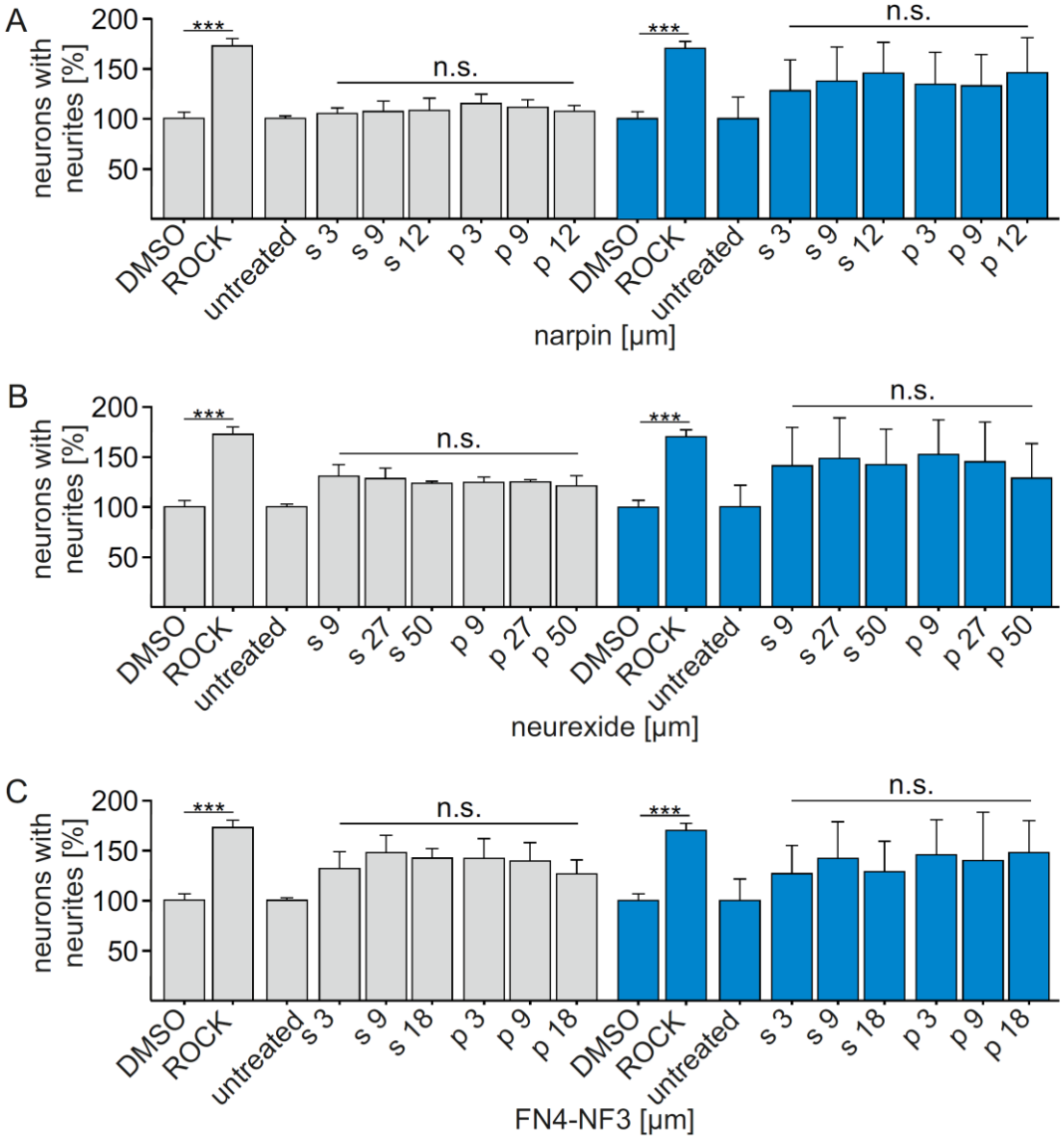

Fig. 22: Percentage of neurons with neurites of iPSC-derived neurons after treatment with mimetic peptides. iPSC-derived neurons from CTR 1 (grey bars) and SZ 2 (blue bars) are differentiated for 72 hours and treated with DMSO, ROCK inhibitor (10 µM) and different concentrations of narpin (A, 3, 9, 12 µM), neurexide (B, 9, 27, 50 µM) or FN4-NF3 (C, 3, 9, 18 µM) during the last 48 hours. Data is normalised to DMSO or the untreated control. s=scrambled peptide, p=peptide, Kruskal-Wallis Test and Dunn's post hoc test, $p<0.001$***, n.s.= not significant, narpin CTR 1:$H(5)=1.2$, narpin SZ 2:$H(5)=2.3$, neurexide CTR 1:$H(5)=1.1$, neurexide SZ 2:$H(5)=1.5$, FN4-NF3 CTR 1:$H(5)=2.1$, FN4-NF3 SZ 2:$H(5)=2.8$, $n=75$, error bars are s.e.m.

3.11 Knock-out of DISC1 generated same phenotypical characteristics as obtained in neurons from patients SZ 1-3

DISC1 is a known risk gene for schizophrenia and its functionality and interaction with other proteins is important for neurite development [152]. The influence of a DISC1 knock-out in iPSC-derived neurons on early neurodevelopmental processes has to be investigated. Exon 2 in iPSC derived from CTR 1 was deleted using CRISPR/Cas9 technology. Two self-designed guide RNAs targeted unique sequences in the beginning and in the end of exon 2 of the DISC1 gene (Fig 23A). gRNAs and Cas9 plasmid were delivered via electroporation to single cell iPSCs. Successful mutation of DISC 1 resulted in a deletion of 851 base pairs in exon 2. iPSC cells were cultivated until stable clonal growing occur again. iPSC of mutated donor CTR 1 (C-CTR 1) were differentiated to cortical neurons, via embryoid body formation and NPC generation. iPSC clones and NPCs were checked for a deletion of exon 2 in the DISC1 gene via genomic PCR. Experiments were performed by Kathrina Haag during her master thesis. Fig. 23B shows the results of genomic PCR of iPSC from CTR 1 and C-CTR 1 and NPC from C-CTR 1. PCR product of DISC 1 specific primers used for genomic PCR had a length of 1850 base pairs. After the deletion of exon 2 with a length of 851 base pairs the mutated fragment had a length of 999 base pairs. Wild type fragment of DISC1 gene was verified in samples of iPSCs from CTR 1. A second band with the length of 999 base pairs was present in samples of iPSCs and NPCs from mutated CTR 1. The wild type form of the DISC1 gene was still present, based on a CRISPR event only in one allele. The deletion of exon 2 which leads to a knock-out of DISC1 was shown in iPSCs and NPCs. Exon 2 of the DISC 1 gene in iPSC from donor CTR 1 was successfully deleted. Potential changes of morphological and functional characteristics of iPSC, NPC and cortical neurons in case of a DISC 1 mutation were analysed.

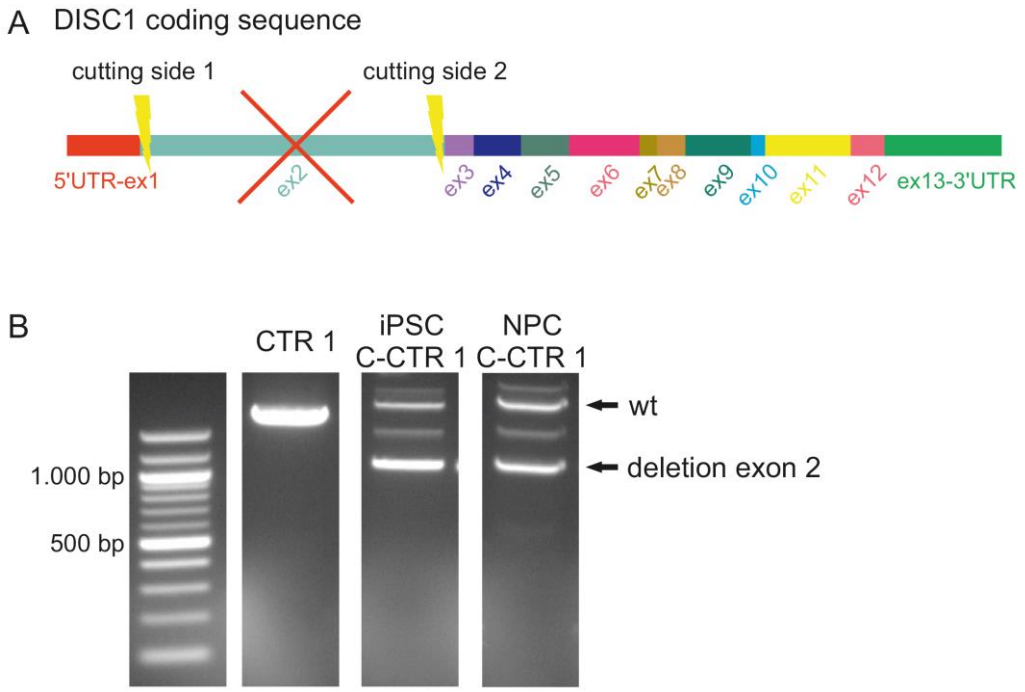

Fig. 23: Verification of DISC1 knockout in iPSCs and NPCs from donor CTR 1. (A) Schematic overview of the DISC1 coding sequence and induced cutting sides. (B) Agarose gel of genomic PCR products of iPSCs from CTR 1 and iPSCs and NPCs from C-CTR 1. Arrows indicate expected genomic PCR product length of wildtype and mutated Exon 2 fragments of the DISC 1 gene.

After testing of DISC 1 mutation iPSC were cultivated and passaged until the typical clonal morphology occurred. Stem cell specific marker expression was analysed via immunofluorescence staining against SSEA 4 and Tra 1-81. iPSC from C-CTR 1 show clonal growing and stem cell specific marker expression (Fig. 24A, B). Changes in growing abilities and marker expression in comparison to iPSC from CTR 1 (see Fig. 6) were not observed. In addition to immunocytochemical stainings, the expression of induced exogenous genes and typical endogenous embryonic stem cell marker genes were analysed in iPSC from C-CTR 1 by RT-PCR (Fig 24C). Exogenous genes OCT3/4, SOX 2, KLF4 and c-Myc induced during reprogramming process were still silenced. Endogenous gene expression of 17 embryonic stem cell marker genes were shown. NTERA cell line served as control for stem cell specific genes. In comparison to iPSC from CTR 1 less endogenous genes were expressed (see Fig. 7).

Based on morphological analysis and immunocytochemical staining no changes were observed in iPSC from C-CTR 1. Gene expression analysis showed minor differences in gene expression in comparison to iPSC from CTR 1. iPSC were used for neuronal differentiation, producing embryoid bodies and neuronal progenitor cells as described before.

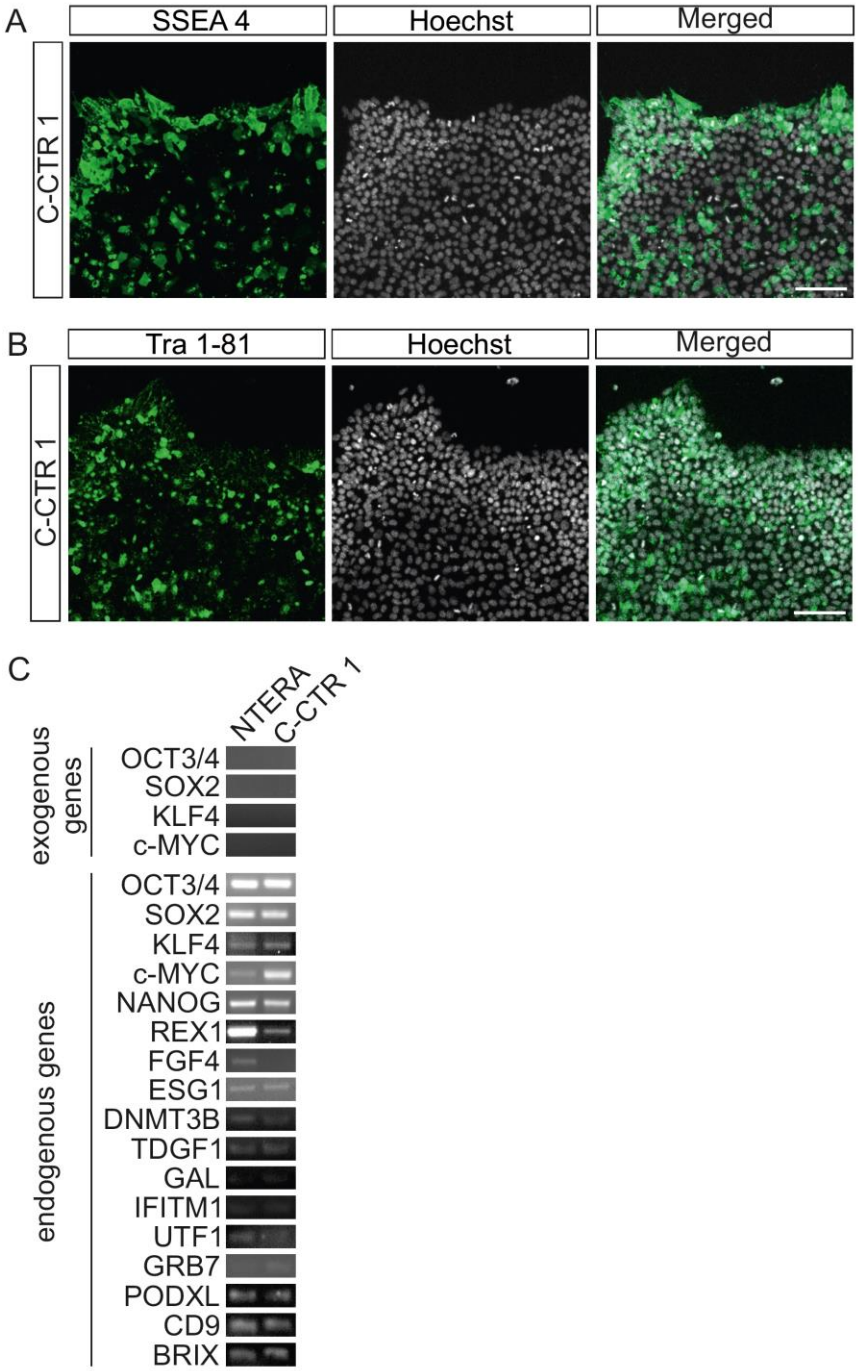

Fig. 24: Immunocytochemical staining and RT-PCR of mutated iPSC from donor CTR 1. Immunocytochemical staining of mutated iPSCs from CTR 1 (C-CTR 1) against stem cell specific marker genes SSEA 4 (A) and Tra 1-81 (B). Scale bars: 100 µm (C) RT-PCR of embryonic stem cell specific marker genes of mutated iPSCs from donor CTR 1. The silenced expression of exogenous markers can be confirmed. NTERA serves as positive control. NTERA=human embryonal carcinoma cell line.

As first step in the neuronal differentiation neuronal progenitor cells (NPC) were generated using high quality iPSC clones carrying DISC 1 mutation. To confirm a NPC phenotype, cells were stained against NPC marker genes ZO 1, PAX 6, Nestin and SOX 1 as described above. Results of immunocytochemical staining are shown in Fig. 25. Immunocytochemistry revealed that PAX 6 and SOX 1 were enriched in cell nuclei. ZO 1 and Nestin immunoreactivity was

spread all over the cell soma. Only some of the stained cells express NPC specific marker. Based on positive immunocytochemical staining, stem cell specific marker expression of iPSC-derived NPCs from C-CTR 1 is comparable to non-mutated NPCs (see Fig. 9). Number of cells expressing NPC marker seems to be reduced. In face of this changed abilities NPCs were used for final neuronal differentiation. Already after a short differentiation time cells exhibited neuronal morphology and built neurites.

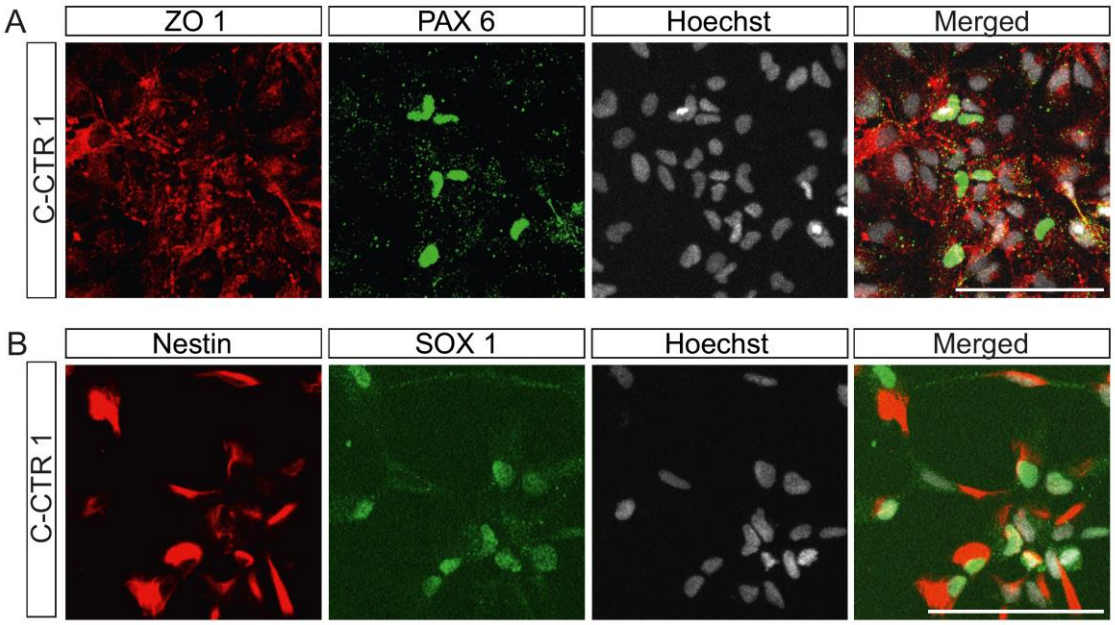

Fig. 25: Immunocytochemical staining of mutated donor CTR 1 against Neuronal Progenitor Cell marker genes ZO 1, PAX 6, Nestin and SOX 1. In (A) cell surface marker ZO 1 and transcription factor PAX 6 and in (B) Nestin and transcription factor SOX 1 were stained as NPC marker genes in NPCs of mutated cell from donor CTR 1. ZO 1=Zona Occludens 1, PAX 6=Paired box gene 6, SOX 1=SRY box 1, Scale bars: 100 µm.

As indicator for early neuronal developmental neurite formation and mean neurite length were analysed. Fig. 26A shows an immunocytochemical staining of three days old iPSC-neurons from CTR 1 and C-CTR 1 using cell surface marker β-III-tubulin and cell nuclei marker Hoechst. In contrast to CTR 1, iPSC-derived neurons from donor C-CTR 1 showed more cells with a NPC morphology than neuronal morphology. Cell bodies were flatter and expanded and the neuronal network was very limited. An impaired neuronal differentiation and development was tested via neurite outgrowth experiment. iPSC-derived neurons from C-CTR 1 were differentiated into cortical neurons for four days, fixed and stained. Percentage of neurons with neurites > 10 µm and mean neurite length was analysed as described before. Finding was confirmed in a quantification of three independent experiments. iPSC-derived neurons from CTR 1 served as control cells. Results of neurite outgrowth experiments are shown in Fig. 26B and C. iPSC-derived neurons from C-CTR 1 showed significantly reduced percentage of neurons with neurites (Fig. 26B). The percentage was significantly reduced by 67 %. The mean

neurite length of iPSC-neurons from C-CTR 1 was significantly reduced by 34 % (Fig. 26C). Differences in neurite outgrowth were observed in iPSC-derived neurons from C-CTR 1. Changes in early neuronal development resulted of DISC1 mutation in iPSC-derived neurons. In comparison to neurite outgrowth of iPSC-derived neurons from patients with schizophrenia (SZ 1-3), percentage of neurons with neurites and mean neurite length of iPSC-derived neurons from CTR 1 was more reduced. Mutated iPSC-derived neurons from donor CTR 1 can be used as potential *in vitro* model to simulate early neurite development in case of schizophrenia.

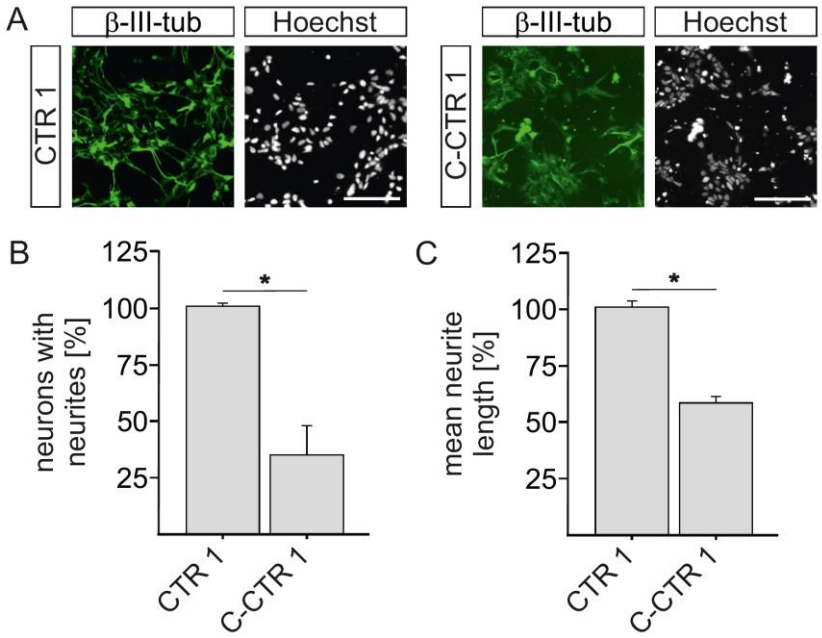

Fig. 26: High content analysis of neurite outgrowth of mutated iPSC-derived neurons from donor CTR 1. (A) Immunocytochemical staining using b-III-tubulin antibody and Hoechst in iPSC-derived neurons from CTR 1 (left) and mutated iPSC-derived neurons from CTR 1 (right). Scale bars: 100 µm Effect of DISC1 knock-out is shown via percentage of neurons with neurites (B) and mean neurite outgrowth (C) in three days old neurons derived from non-mutated and mutated iPSCs from donor CTR 1. (B, C) Data is normalised to CTR 1. Mann-Whitney U-Test, n=3, $p<0.05$*.

4. DISCUSSION

In the context of this thesis, an iPSC-derived neuronal system was developed to study changes in early neuronal development in case of schizophrenia. Therefore, fibroblasts from three healthy individuals, three patients with schizophrenia and three patients with autism were reprogrammed into high quality iPSC. These clones were differentiated into cortical neuronal cells and characterised for disease-specific properties. Beside neurite outgrowth, PSD95 cluster density and the calcium flux were decreased in iPSC-derived neurons from patients with schizophrenia. Transcriptome analysis identified changes in neuronal and synapse-specific genes and aberrations in the expression of genes related to calcium signalling and MHC clusters in case of schizophrenia. Treatment with antipsychotic drugs like olanzapine and haloperidol resulted in a reduced neurite outgrowth in iPSC-derived neurons from CTR 1. In the following section the observed results are critically discussed and compared with the current state of the literature in the field of iPSC technology for neurodevelopmental diseases.

4.1 Reprogramming of fibroblasts into iPSC

First part of this thesis focus on the generation of nine iPSC lines out of human fibroblasts from preselected patients with schizophrenia or autism and healthy individuals. Fibroblasts were reprogrammed via retroviral transduction using the four Yamanaka factors Sox2, OCT3/4, KLF4, and c-Myc and relevant genomic aberrations could be excluded in all iPSC lines. Only characterised iPSC clones with a typical stem cell morphology, right marker expression, and proof of pluripotency were used as starting material for a neuronal differentiation.

In 2007, the group of Yamanaka was the first one describing the successful reprogramming of human fibroblasts into iPSC [123]. Retroviral transduction was the first method to deliver the reprogramming factors into the host genome. Despite the high reprogramming efficiency, some problems developed using this system. The reprogramming viruses can randomly integrate into the genome and thereby induce changes in gene expression, *de novo* somatic coding mutations, copy number variations and chromosomal abnormalities [153-156]. Unpredictable genomic changes, aberrant transgene expression or tumor formation can occur. The induction of genetic aberration is very problematic, because reprogramming can affect undiscovered genetic modifications and epigenetic memory of schizophrenia. To circumvent genomic aberrations after retroviral transduction, alternative reprogramming strategies using non-integrative viruses like Sendai viruses [157], episomal vectors [158], modified mRNA transcripts [159] or proteins [160] have been developed. Another method is the direct lineage reprogramming, where an adult somatic cell is transformed into another lineage without going through the pluripotent state [161]. Generation of induced neurons (iN) directly out of iPSC

could be a valid alternative for modelling schizophrenia [162]. On one hand, direct conversion does not erase cellular ageing markers [163] and allows modelling of sporadic and epigenetic diseases. The process is much faster than retroviral transduction. On the other hand, it has limitations like a low reprogramming efficiency and a reduced neuronal maturation reflected in a small competence in synapse formation [164, 165]. The number of cells is limited to the amount of starting material and cannot be infinitely expanded like during the stem cell state. Direct reprogramming skips the pluripotent and neuronal progenitor stages [166] and make the modelling of early neurodevelopmental processes difficult. Because the cellular starting material was limited and the development and differentiation of neuronal progenitor cells were also focused on this thesis, retroviral reprogramming was chosen. Additionally, the reprogramming efficiency is high and this robust method enables the generation of iPSC independent from the genetic background of the patient. To exclude genomic aberrations because of viral integration, a non-integrative method should be selected for reprogramming in future.

4.2 Differentiation of iPSC into cortical neuronal cells

To study early neurodevelopmental processes of patients with schizophrenia, high quality iPSC were differentiated into cortical neurons with embryoid body formation and NPC generation. In addition to the manufacturer protocol, Dorsomorphin dihydrochloride, SB 431542 and recombinant Human Noggin Fc Chimera Protein were added to the medium to improve the generation of pure NPC. As described by Chambers et al. [167] dual inhibition of SMAD signalling using Noggin and SB 431542 leads to highly efficient neural conversion of iPSCs and an increase of NPC marker expression. Soluble BMP antagonists such as noggin, limit BMP signalling by ligand sequestration resulting in disturbed receptor heterodimerization. SB 431542 inhibits TGF-β signaling via blocking type I receptor activity which leads to a reduced phosphorylation and nuclear translocation of the SMADs. Additionally, the small molecule dorsomorphin inhibits SMAD-dependent BMP signal by directly disturbing the binding of SMAD 1/5/8 to its receptor [168]. A combination of these three factors enable the generation of pure NPCs. Every NPC line of each donor was immunocytochemically tested for the expression of relevant NPC markers to check the quality of the NPC culture. Only NPC cultures with the expression of all four NPC marker genes PAX 6, SOX 1, ZO 1 and Nestin were used for further differentiation into cortical neurons.

Cortical neuronal differentiation was performed according to the protocol of Shi et al., which followed all steps of the human brain development [140]. This way of differentiation is more precise to the early *in vivo* process. Transcriptome analysis of 4-weeks old iPSC-derived neuronal cells from healthy individuals as well as patients with schizophrenia and autism

showed typical gene expression of neuronal cells like calcium, synapse and nervous system-related genes. As shown by Handel et al., differentiated iPSC-derived neurons resembled cells of the fetal brain and can be used for modelling young stages of the disease phenotype [169]. They used a broad range of neuronal markers for single-cell transcriptomics to characterise different layer identities in iPSC-derived cortical neuronal cultures. After differentiation of iPSC into neuronal cells 93.6 % of single cells expressed genes indicate neuronal identity, mostly excitatory glutamatergic receptor and synaptic genes. In comparison to single-cell RNA-sequencing data from primary human brain tissue, iPSC-derived cortical neurons, differentiated cells recapitulate the single-cell transcriptomic signature of human fetal cortical neurons, and expressed many genes associated with neuronal and synaptic function [169]. Based on these findings, iPSC-derived cortical neurons are a suitable source to investigate changes in gene expression in early neuronal developmental stages.

Following, the protocol of Shi et al. enables a differentiation into a mixture of cortical neurons, which may have variable roles in disease pathogenesis. A variety of neuronal markers of excitatory, inhibitory neurons and astrocytes were observed after immunocytochemical staining. Exact percentage proportion was not determined but a variety of neuronal cell types were obvious. The experimental diversity complicated a comparison between diverse differentiation approaches. Additionally, the generation of disease relevant cell types in a defined amount may improve the modelling because of a better representation of the disease phenotype. The establishment of lineage-specific differentiation enables the production of specific subtype of neuronal cells [170]. But lineage-specific differentiation and investigations using only one neuronal subtype do not represent the heterogeneous *in vivo* conditions and the complex disease phenotype. Further improvement of the differentiation protocol and standardization will increase the comparability between different experiments and *in vivo* conditions.

Besides a proper differentiation protocol, the duration of neuronal differentiation is essential for marker gene expression and neuronal functionality. To follow neurodevelopmental processes, iPSC-derived neurons were positively stained against brain layer V marker gene Ctip2. Brain layer V is the second developed brain layer during cortex maturation and exhibiting subcortical projection neurons expressing Ctip2 [141]. The time point of marker expression of neurons from CTR 1 was comparable to studies performed by Shi et al. [140] and increased with further differentiation time. The expression of Ctip2 verified the differentiation into the targeted neuronal layer and indicated early stages of neuronal development. Functionality of iPSC-derived neuronal cells was tested using calcium imaging with an immunofluorescent calcium dye. Spontaneous calcium influx and efflux were positively tested in all iPSC-derived

neuronal cultures after eight weeks differentiation. In addition to a correct neuronal marker expression, the functionality of the neuronal cells is essential for studying neurodevelopmental diseases like schizophrenia with iPSC-derived neurons. Until today, iPSC-derived neurons failed to fully recapitulate the whole three-dimensional brain architecture [171], cellular maturation and aging [172] even after an extended cultivation time. The differentiation time in an *in vitro* culture from 14 to greater than 100 days [140, 167, 173] is much shorter than the human neurodevelopment of the brain. Therefore, the study of later disease phases for example early adolescence would be much more difficult. Focus of this thesis was to investigate potential changes in early neuronal development of iPSC-derived neurons from patients with schizophrenia, therefore the expression of early neuronal markers and first neuronal functionality is sufficient. All these characteristics were observed after eight weeks of neuronal differentiation in iPSC derived cells from healthy individuals as well as patients with schizophrenia or autism. Only neuronal cultures exhibiting all morphological and functional neuronal characteristics were selected for experiments to study neurodevelopmental changes.

4.3 Expression of disease relevant characteristics like neurite outgrowth and synaptic formation

iPSC-derived neurons from patients with schizophrenia were used to study changes in early neurodevelopmental processes in comparison to iPSC-derived neurons from healthy individuals. Proliferation, differentiation of precursor cells into neuronal cells, migration and elaboration of neurites are some of the key cellular processes of neuronal development [174]. Important for a normal development of the nervous system is a dynamic process and coordinated expression of molecular and cellular events at the correct time and place [175, 176]. The neurite outgrowth experiment is a simplified model to investigate processes of nervous system development in a 2D system. As indicator for early neuronal development the percentage of neurons with neurites and the mean neurite length were selected as phenotypical assay. Both values were significantly decreased in neurons derived from patients with schizophrenia in comparison to healthy individuals. Neurite outgrowth is the most performed assay because it is directly linked with cellular function and cellular health [177-179]. In brain development, a reduced neurite development can lead to a diminished formation of the neurite network and reduced maturation. Changes in dendritic arborizations were already observed in studies of post-mortem brains from patients with schizophrenia [62]. Additionally, iPSC showed high potential in phenotypical screenings like neurite outgrowth because pathophysiology of the disease is focused [180]. Brennand et al. observed reduced neurite outgrowth in iPSC-derived neurons from patients with schizophrenia [68]. In contrast to the experimental procedure described in this thesis, Brennand et al. differentiated iPSC-

derived neurons for three-months in a co-culture with astrocytes. For the analysis they counted the number of neurites growing out of the cell soma in iPSC-derived neurons from patients with schizophrenia. Despite varied differentiation periods and analysis methods in both cases a diminished ability to form neurites was observed and could be linked to neurons with a schizophrenic genetic background. Even if the percentage of neurons with neurites was significantly reduced in group wise comparison, the percentage of reduction differs. Cultivation and differentiation method were identical, and differences may be based on genetic heterogeneity between individual donors. The generation of an isogenetic disease cell line may increase the comparability of mutation related effects. For this thesis, a schizophrenic disease cell line was generated with inducing a mutation in the known risk gene DISC1 [181] in iPSC from donor CTR 1 using CRIPSR/Cas9 technology. Genome editing with CRIPSR/Cas9 is an easy tool to induce specific mutation or to correct known aberrations [182]. With this, each cell line can serve as its own control because of a shared genetic origin. Specific morphological changes can be investigated regarding the induction of a known mutation in this case DISC1 knock-out. Off-target effects should be studied and excluded before using a cell line.

DISC1 is an important gene for neuronal differentiation, signalling and synaptic function [183], that is why changes in neurite outgrowth were analysed using the neurite outgrowth experiment. As expected the percentage of neurons with neurites and the mean neurite outgrowth were significantly reduced in comparison to CTR 1. Mice lines with DISC1 mutation showed alterations in neuronal architecture for example a reduction in the apical dendrite length of layer V pyramidal neurons [184]. Wen et al. reprogrammed somatic cells of individuals carrying a DISC1 mutation and differentiated them into forebrain-specific neuronal cells. For each donor two independent iPSC lines were generated. As control somatic cells of unaffected relatives were reprogrammed and differentiated. Similar to immunocytochemical staining used in this thesis, Wen et al. did not observe any changes in iPSC or NPC generation. Neurite outgrowth was analysed as total dendritic length of forebrain neurons derived from each individual at one up to four weeks of neuronal differentiation. In contrast to the mean neurite outgrowth after three days of neuronal differentiation of iPSC-derived neurons carrying an artificial induced DISC1 mutation, Wen et al. observed an increased total dendritic length during the first two weeks of neuronal differentiation. Effects became indistinguishable from control iPSC cell lines after three and four weeks. Various differentiation and analysis procedures as well as diverse analysis time points make a comparison between both experiments difficult. Both experiments showed the relevance of DISC1 in neuronal development. Described findings support theories of changed neurite outgrowth observed in previous studies of patients with schizophrenia.

A reduced neuronal development may lead to aberrations in synaptogenesis and cellular connectivity. As representative marker gene of the postsynaptic density, the formation of PSD95 clusters were analysed in 8-weeks old iPSC-derived neurons. Significant reduction was observed in the number of PSD95 cluster density of iPSC-derived cortical neurons from individual patients. Key finding of a reduced synaptic density was already described by Roberts et al. using electron microscopy [185]. Additionally, this observation correlates with the findings of Brennand et al., who observed a diminished PSD95-protein level in iPSC-derived neurons, even if the analysis was performed for the whole PSD95:MAP2 ratio of all stained neurons [68]. Furthermore, Wen et al. analysed reduced synaptic density indicated by PSD95/Synapsin 1 (SYN1) co-staining in iPSC-derived neurons carrying DISC1 mutation in comparison to healthy family members. Diminished PSD95 protein expression can also lead to changes with interaction partners like NMDA receptor or neuregulin 1 [186]. A reduced PSD95 expression was described in several publications and seems to be a characteristic of neuronal cells derived from patients with schizophrenia. Additionally, a decreased PSD95 cluster density may cause dysregulation of synaptic function and structure. Synapses are the basic functional units of the brain and are important for signalling processes with neurotransmitter. Neurotransmitter are important for the intracellular signalling processes like gating calcium channels and with this regulating the synaptic activity. Calcium ions have a large concentration gradient among the plasma membrane of all cells [187]. In neurons calcium ions regulate the electrical activity by opening and closing sodium and potassium channels, inducing action potentials [188].

In this work, spontaneous calcium influx and efflux of eight weeks old iPSC-derived neurons were significantly reduced in case of schizophrenia. The immature neuronal phenotype of all neurons independent of the genetic origin were indicated by a low frequency of calcium peaks and missing synchronism. Aberrations in calcium signalling was correlated to the molecular pathology of schizophrenia before [189]. Functional imaging studies and post-mortem studies identified brain and synapse deficits in prefrontal cortex region of patients with schizophrenia [63, 66]. The publication of Wen et al. observed iPSC-derived forebrain neurons carrying a DISC1 mutation with reduced synaptic boutons after four and six weeks differentiation and deficits in synaptic vesicle release [98]. Similar to the results of iPSC-derived neurons from patients with schizophrenia described in this thesis, the frequency of excitatory spontaneous synaptic currents was reduced in iPSC-derived neurons with DISC1 mutation in comparison to neurons derived from healthy family members. Brennand et al. did not observe any changes in spontaneous calcium transient imaging in iPSC-derived neurons [68]. In contrast to these experiments, they used the calcium dye Fluo-4AM to visualise calcium traces of fluorescent intensity from three-month-old iPSC-derived neurons co-cultured with astrocytes. The spike amplitude of spontaneous calcium transients and the total number of calcium transients

showed no significant differences. Potentially correlated to the age, iPSC-derived neuronal cells were more synchronic in co-culture.

Maybe based on different genetic backgrounds and various differentiation procedures, results of calcium transients differed between individual approaches. In all experiments spontaneous calcium release was measured to analyse calcium influx and efflux indicating the functionality of generated neuronal cells. Even if a changed calcium release needs more experimental explanations, first steps in the generation of functional cortical neuronal cells were made. Next step would be the quantification of firing response to current injections, stimulation or inhibitory substances to get a better understanding of the synaptic function and processes related to calcium signalling. Additionally, the number of analysed patients per functional analysis should be increased to exclude individuum specific results. A genetic predisposition in the family seemed to be a relevant selection criteria to see differences in functional assays and should be maintained.

4.4 Transcriptome analysis identify changes in MHC locus in case of schizophrenia

iPSC technology offers an easy system for studying the expression profile of neurodevelopmental and cellular processes in the pathophysiology of schizophrenia. A lot of changes in the transcriptome, including gene expression of synapse, calcium signalling and cell development are known for schizophrenia until today. Four weeks-old iPSC-derived neurons from SZ 2 exhibited a significant upregulation of HLA related genes like HLA-DM, HLA-DQ and HLA-DR, in comparison to CTR 1 after transcriptome analysis. Immunocytochemical staining of NPC derived from SZ 2 confirmed an increased amount of functional MHCII expression at early stages of neuronal development. Transcriptome analysis was performed to identify new relevant changes in gene expression in neuronal cells in case of schizophrenia. Aberrations may explain neurodevelopmental or phenotypical changes.

First evidence for a changed Human Leukocyte Antigen (HLA) locus in schizophrenia was published in 1974 from Cazzullo et al. [190]. Since then, several HLA alleles like HLA-DRB1 and HLA-DQB1 were directly linked to schizophrenia. HLA-DRB1 is important for antigen presentation and processing and build with HLA-DPA1 a dimer of the MHCII complex [191]. Multiple alleles and polymorphism of the HLA-DRB1 promotor makes the gene expression complex. The rheumatoid arthritism which negatively correlated with the incidence of schizophrenia, is related to the expression of the HLA-DRB1 allele [192, 193].

In 2009 the International Schizophrenia Consortium performed a GWAS using 3,322 European individuals with schizophrenia and 3,587 healthy controls. The HLA locus was identified as most powerful region of association for schizophrenia. Aberrations in genes involved in the antigen presentation shows a close link to innate and adaptive immune functions [91]. Furthermore, other studies figure the HLA locus out as one of the most significant determinant of susceptibility for schizophrenia [194, 195]. Most prominent SNPs were identified in regions near immune-related genes [194]. MHCII genes have important roles in the immune response and a variation in its density influences the intensity of the T-cell response. Its interaction with the T-cell receptor results in an activation and stimulation of CD4 T-cells [196]. An increase of the MHCII density would result in hyperactive T-cells resulting in increased immune reactions. These findings correlate to the enteropathogenesis. Dysregulation of innate and adaptive immune systems was described before by different working groups [197-199]. Prenatal infections [27], an increased risk for autoimmune diseases [200] and altered levels of inflammatory biomarkers [75] have been found as well in schizophrenia pathology.

Beside immunological functionality, the MHC locus is also linked to non-immune functions. For example, the MHCI complex is involved in fundamental functions of the CNS, including neuronal differentiation, maturation and synaptic plasticity [201-203]. In 2016 Sekar et al. identified a linearly relation between the risk of schizophrenia and the expression of MHC region gene C4 [204]. The expression of C4 leads to an excessive synaptic pruning in neurons, giving straightforward evidence that the expression of an immune gene influences brain development. Another study observed significant SNPs closely to the gene NOTCH4 (neurogenic locus notch homolog 4) [205, 206]. NOTCH4 codes for a transmembrane protein which is critical for neurodevelopment. Because NOTCH4 is a non-HLA gene that only maps to the HLA locus may suggest non-immune function as well.

iPSC-derived neuronal cells showed same transcriptomic changes as described in previous studies indicating the explanatory power of these cells as cellular system to detect disease specific genomic changes. Findings support the relevance of gene expression aberrations in MHC-related genes in case of schizophrenia. In contrast to GWAS performed with somatic cells, the differentiation into neuronal cells and following transcriptome analysis enables investigations of disease relevant cell types. Schizophrenia is known as polygenetic disease and the disease origin cannot be only related to changes in one genomic region [80]. The genetic complexity of the disease has to be investigated in future to fully understand all observed genetic changes.

4.5 iPSC technology as cellular system for drug development of neurodevelopmental diseases

In addition to morphological and functional tests, iPSC can be used to test drug effects *in vitro* and to identify new drug targets or molecular predictors in pharmacogenomics [180]. Animal models and post-mortem studies were mostly used for the investigation of schizophrenia but have limitations in qualified drug testing. Animal models can be used for the analysis of disease-specific molecular pathways or neuronal circuits, but fail to fully recapitulate all features of the psychiatric disorder schizophrenia. Changes in brain morphology, neuronal network, and synapse plasticity are already described using post-mortem brain tissue. Studies with post-mortem tissue only investigate the endpoint of the disease. Effects of drugs on early neuronal developmental or signalling processes can be better studied using living cells. Phenotypical assays for drug development must be relevant for clinical diagnosis and robust in therapeutic screenings [180]. The parameter neurite outgrowth of neuronal cells exhibit these properties and can be used as an indicator for the action of drugs or chemical compounds in developmental processes [178].

To investigate the effect of antipsychotics on early neuronal development, drugs were applied after 24 hours of differentiation and neurite outgrowth of iPSC-derived neurons from CTR 1 and SZ 2 was analysed after 72 hours. One first generation antipsychotic drug, haloperidol, and a second-generation antipsychotic drug, namely olanzapine, significantly reduced neurite outgrowth of iPSC-derived neurons from CTR 1. The antipsychotic clozapine had no effect on the neurite outgrowth. iPSC-derived neurons from SZ 2 were not significantly changed in neurite outgrowth after treatment with clozapine, olanzapine or haloperidol.

Intrinsic and extrinsic factors which regulate the assembly of cytoskeletal elements, control the initiation and elongation of neurites [207, 208]. Additionally, changes in gene expression, membrane receptors, ion channels and complex intracellular signalling processes can result in aberrant neurite initiation and growth [209]. The complex nature of the regulation of neurite outgrowth, causes a wide range of potential targets to perturb this process.

All three antipsychotics bind as antagonists with a moderate affinity to the dopamine D1 receptor. Olanzapine has the highest affinity in comparison to Haloperidol and Clozapine. The DRD1 receptor is highly expressed in the prefrontal brain region [210] and dopamine plays a prominent role in the pathophysiology of schizophrenia [211, 212]. Already post-mortem studies identified a decreased expression of DRD1 receptor [213] in patients with schizophrenia mostly linked with an impairment of cognitive function and the presence of

negative symptoms [214, 215]. The functionality of DRD1 is directly linked to the control of working memory [216, 217], which dysfunction is a prominent feature in schizophrenia [218]. The dopamine D1 receptor belongs to the heptahelical receptor family which modulated the activity of adenylate cyclase by activating specific G-proteins. The stimulation of DRD1 leads to the activation of adenyl cyclase (AC) which increases the production of cyclic adenosine monophosphate (cAMP). A higher cAMP activation increased the activation of protein kinase A (PKA). Both molecules play an extensive role in neuronal development and neuroplasticity [219]. For example, neurite outgrowth [220], neuronal differentiation [221] and survival [222] are mediated by cAMP in neurons. Stronger activation of the cAMP/PKA pathway promotes the neurite outgrowth in human embryonal carcinoma stem cells [223]. The application of an DRD1 antagonist such as olanzapine [224] and haloperidol [225] decreased the neurite outgrowth as expected. Despite the inhibitory effect on DRD1 of clozapine, the application of this drug resulted in no significant changes of neurite outgrowth. A reduction was only observed in iPSC-derived neurons from healthy individuals. Transcriptome analysis showed a reduced DRD2 expression in iPSC-derived neurons from donor SZ 2. Changes in DRD1 expression were not detected. In contrast to DRD1 the activation of DRD2 receptor inhibits AC [226] and may result in a decreased amount of cAMP. The proportions of DRD1:DRD2 receptors are essential for the cAMP activation and may be the reason for different effects in neurite outgrowth after drug application.

Brennand et al. studied also neuronal development of iPSC-derived neurons from patients with schizophrenia after treatment with antipsychotics. Treatment with loxapine improved neuronal connectivity and gene expression, similar Clozapine and olanzapine had no effect on neuronal connectivity after adding during the last three weeks of neuronal differentiation [68]. Loxapine has a strong binding affinity for dopamine D4 and serotonin 5-HT2 receptors [227] and mode of action differs to other antipsychotics. Above described results are difficult to compare to the results of this thesis because differentiation protocol and time point of analysis differed. Furthermore, the co-cultivation with astrocytes may have an impact on the neuronal development of iPSC-derived cells which may lead to different experimental results.

After an extended period without new developments, some new drugs are already in clinical trial phases II and III. At the CNS summit 2016 efforts of the new drug named ITI-007 manufactured by IntraCellular Therapies were presented. ITI-007 showed significant improvements in comparison to the placebo control and reduce positive and negative symptoms in acute and residual schizophrenia (compare clinical trials gov. Identifier: NCT02469155, [228]). Comparable to further drugs ITI-007 mode of action includes the D2 dopamine receptor and is agonist at the presynaptic side and antagonist at the postsynaptic

side. Additionally, it has serotonin antagonistic effects and increases the phosphorylation of GluN2B [229]. The appearance of side effects is limited under ITI-007 treatment.

4.6 Outlook

In this thesis the development of an iPSC-based cellular system for modelling schizophrenia is described using patient-derived cells. Modelling of complex neurodevelopmental disease *in vitro* is still challenging because of missing maturation of neuronal cells and robust analysis systems.

The development of 3-dimensional cerebral organoids as described by Lancaster et al. [230] mimics the *in vivo* conditions in a more specific way and recapitulate fundamental mechanisms of human brain development, neuronal circuits and neuronal interaction partners. Organoids were successfully used to model a neuron specific disease phenotype and supports the development of disease-specific drugs. Pasca et al. developed a method to generate human cortical spheroids using pluripotent stem cell, which mimic the cerebral cortex structure of a human brain [231]. Developed structures contain cell types of deep and superficial cortical layers. Transcriptome analysis data correlated with results of fetal derived cells. Beside morphological characteristics, functionality of neurons was observed by electrophysiological experiments which display spontaneous activity and functional synapses.

With the improvement of differentiation also the analysis setup of prominent neuronal network formation has to be more robust, efficient and replicable. The multielectrode array (MEA) technology offers a perfect tool to measure neuronal network activity. Here, iPSC-derived neurons are cultivated of an electrode field enable a non-invasive measurement of connectivity of functional neural networks during the whole cultivation time. Aspects of development, maturation, as well as, responses to pharmaceuticals can be investigated in a long-term culture.

To increase the explanatory power of the cellular system with patient-specific cells an automation and upscaling is necessary, potentially with automatization. Although it will be very challenging to optimize and standardize the differentiation protocols, culture conditions and differentiation strategies to produce more mature, healthy and stable neurons at a much faster time scale.

5. SUPPLEMENT

5.1 Supplement figures

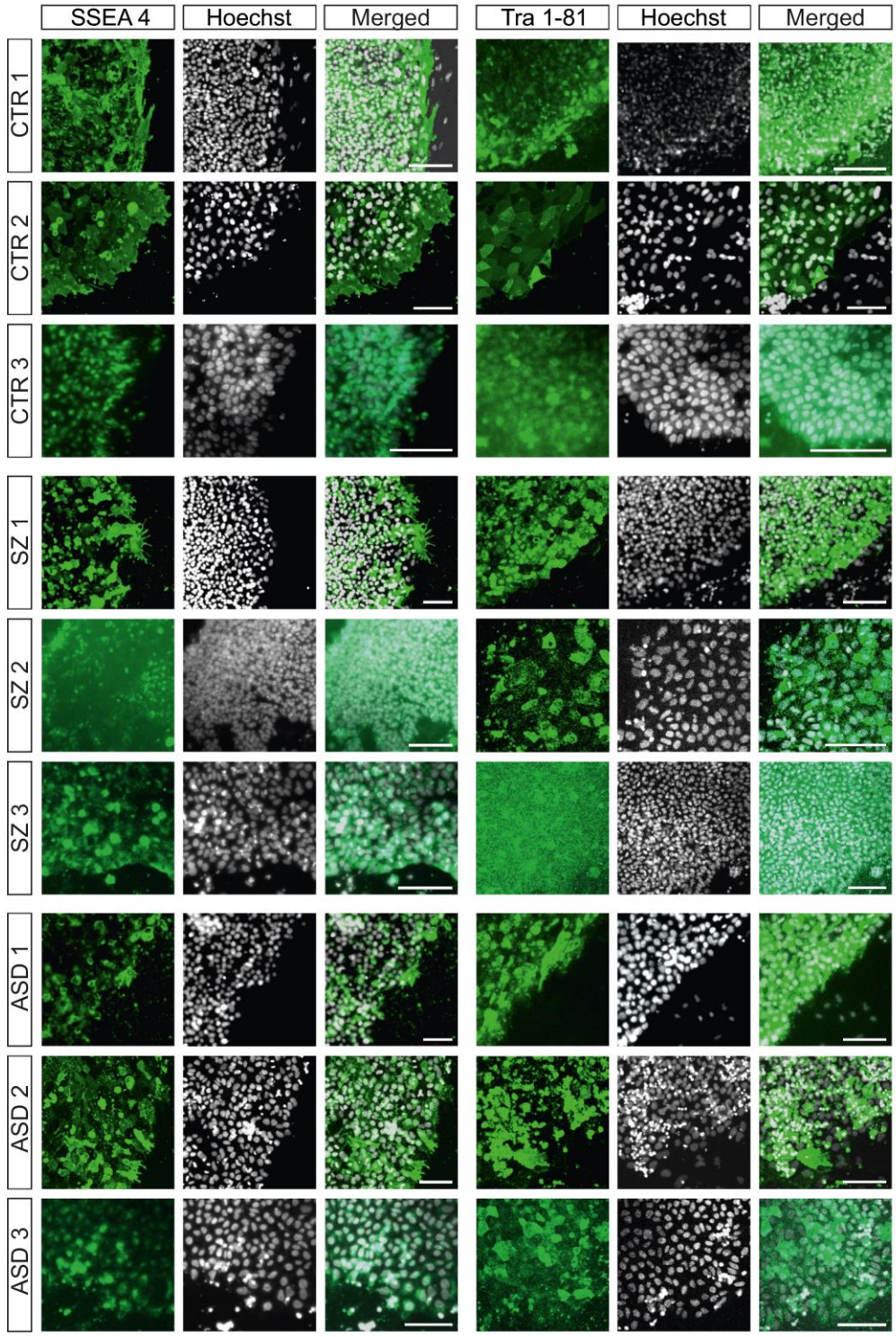

Supplement Fig. 1: Immunocytochemical staining of iPSCs from all donors against stem cell marker genes SSEA 4 and Tra 1-81. iPSC clones of donor CTR 1-3, SZ 1-3 and ASD 1-3 are shown. The expression of stem cell marker genes SSEA 4 (left) and Tra 1-81 (right) is demonstrated with immunocytochemical staining. Scale bars: 100 µm.

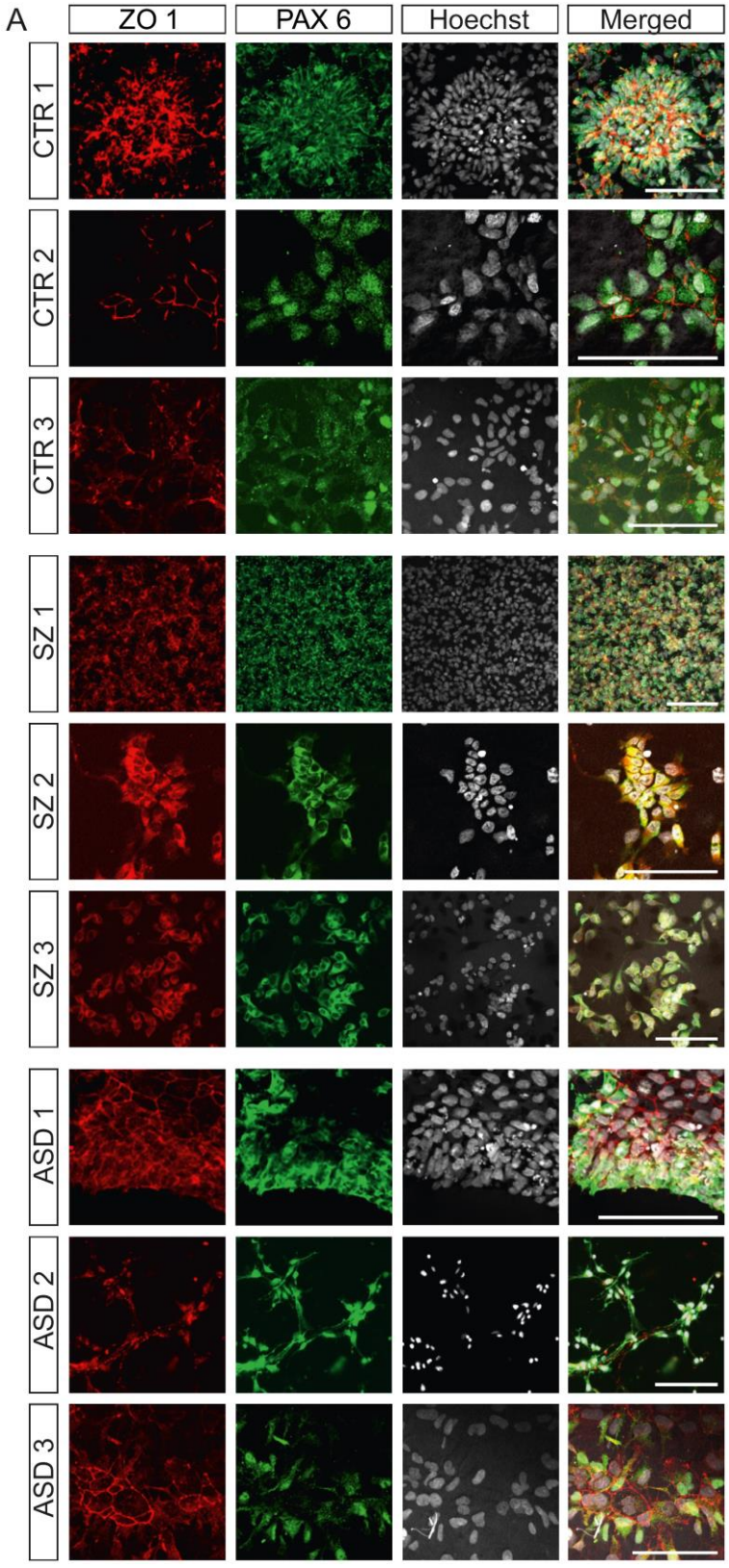

Supplement Fig. 2: Immunocytochemical staining of NPCs from all donors against marker genes ZO 1 and PAX 6. Expression of NPC marker genes like cell surface marker ZO 1 and transcription factor PAX 6 was validated via immunocytochemical staining of NPCs derived from donor CTR 1-3, SZ 1-3 and ASD 1-3. ZO 1=Zona Occludens 1, PAX 6=Paired box gene 6, Scale bars: 100 µm.

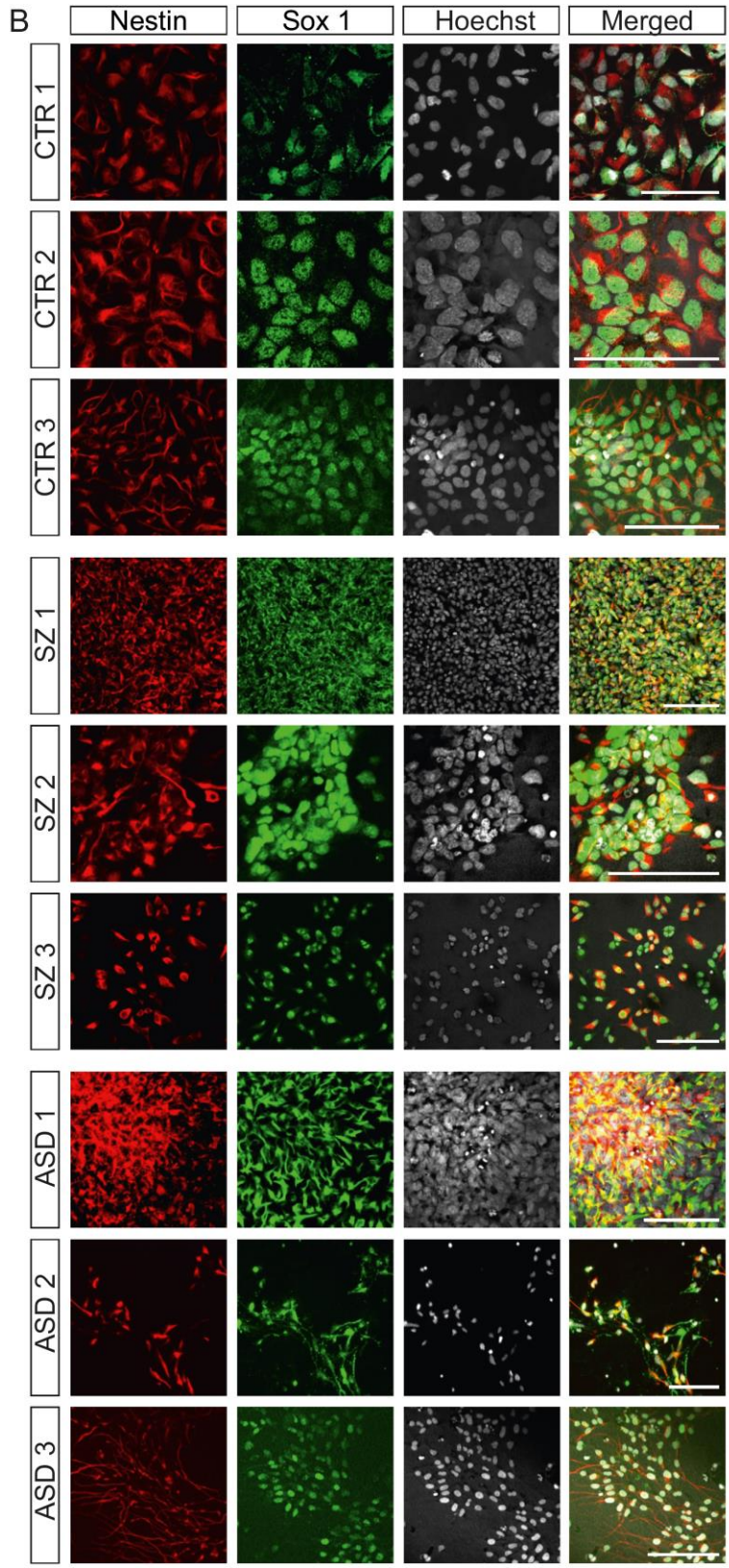

Supplement Fig. 3: Immunocytochemical staining of NPCs from all donors against marker genes Nestin and SOX 1. Expression of NPC marker genes like Nestin and transcription factor SOX 1 was validated via immunocytochemical staining of NPCs derived from donor CTR 1-3, SZ 1-3 and ASD 1-3. SOX 1=SRY box 1, Scale bars: 100 µm.

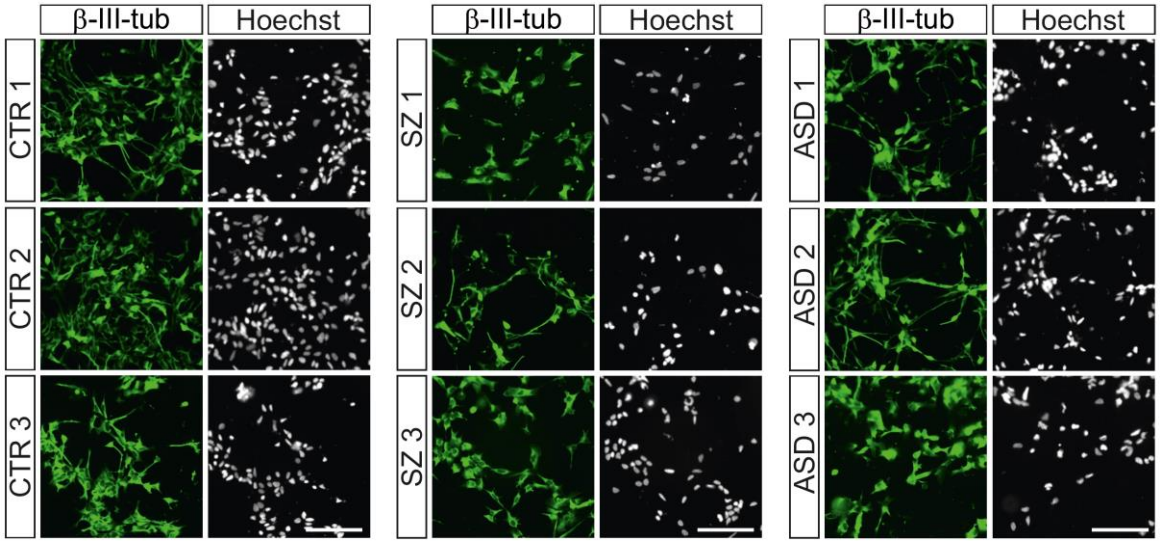

Supplement Fig. 4: Immunocytochemical staining of iPSC-derived neurons from all donors against β-III-tubulin. iPSC-derived neurons from CTR 1-3, SZ 1-3 and ASD 1-3 were differentiated for four days and stained against β-III-tubulin. Hoechst solution was used for nuclei staining. Images were automatically obtained by ImageXpress micro XL microscope and used for segmentation with the MetaXpress Software. Scale bars: 100 µm.

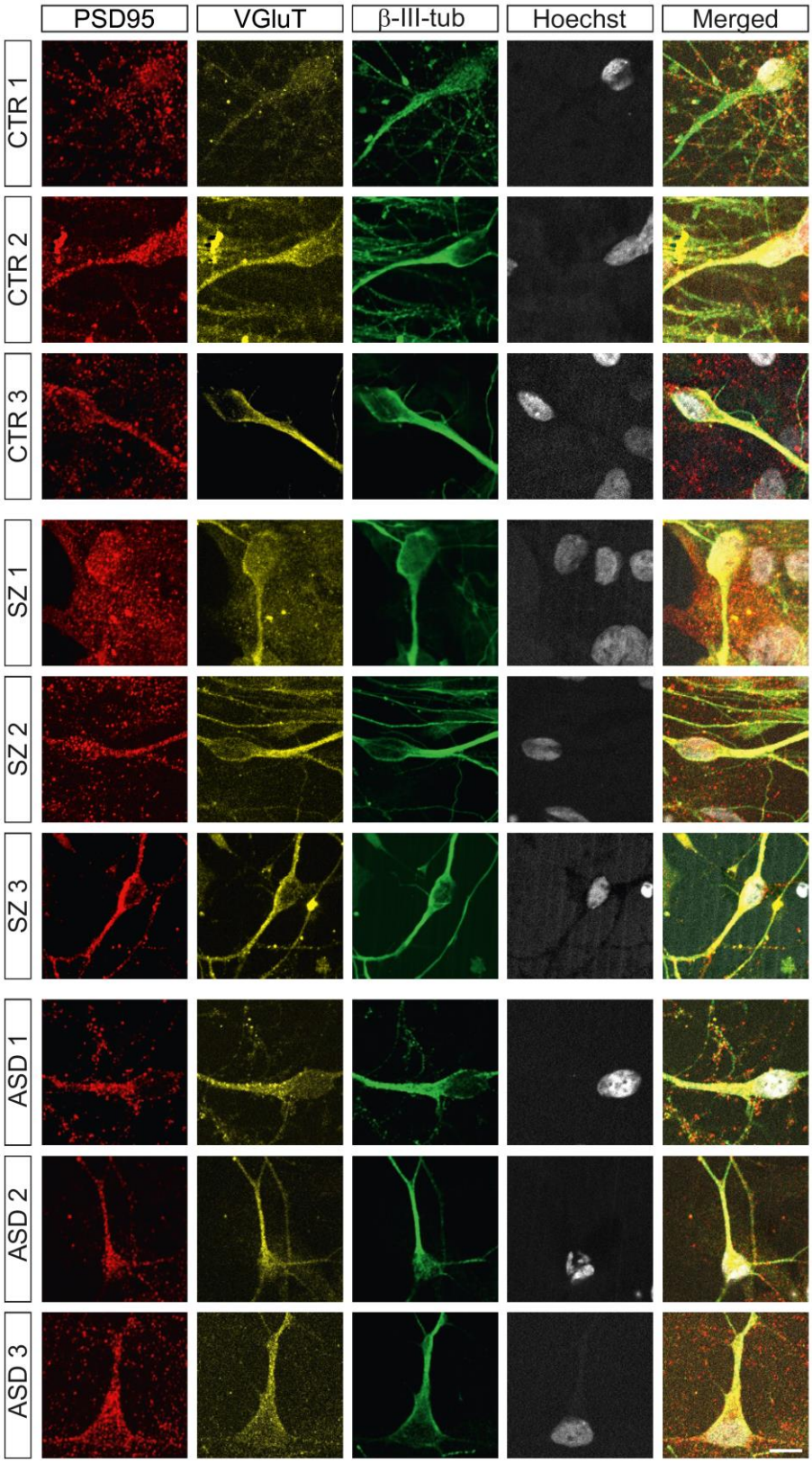

Supplement Fig. 5: Immunocytochemical staining of iPSC-derived neurons against synaptical and neuronal markers. Immunocytochemical staining of eight weeks old iPSC-derived neurons from donor CTR 1-3, SZ 1-3 and ASD 1-3 against synaptic marker PSD95, VGluT and neuronal marker β-III-tubulin. Hoechst was used for nuclei staining. Scale bars: 10 µm.

5.2 Supplement tables

Supplement Tab. 1: Significant deregulated genes of iPSC-derived neurons from all SZ versus all CTR after transcriptome analysis.

gene ID	gene	log2FoldChange	pvalue	padj
ENSG00000226321	AC104809.3	3.2	4.73E-05	4.60E-02
ENSG00000147256	ARHGAP36	-3.5	2.53E-06	9.13E-03
ENSG00000106819	ASPN	3.4	3.34E-05	3.67E-02
ENSG00000205856	C22orf42	-3.2	1.27E-05	2.01E-02
ENSG00000164287	CDC20B	4.1	1.16E-06	7.64E-03
ENSG00000236279	CLEC2L	-3.1	9.38E-06	1.69E-02
ENSG00000169436	COL22A1	2.6	4.22E-05	4.26E-02
ENSG00000135678	CPM	3.4	1.72E-08	4.33E-04
ENSG00000267594	CYP4F24P	3.7	1.08E-05	1.81E-02
ENSG00000080166	DCT	3.3	4.84E-06	1.35E-02
ENSG00000186676	EEF1GP1	3.7	1.21E-06	7.64E-03
ENSG00000054179	ENTPD2	2.9	1.87E-05	2.78E-02
ENSG00000182646	FAM156A	-2.8	3.91E-05	4.12E-02
ENSG00000172568	FNDC9	-2.9	7.56E-06	1.47E-02
ENSG00000174473	GALNTL6	-2.4	2.55E-05	3.22E-02
ENSG00000164171	ITGA2	3.4	1.57E-06	7.92E-03
ENSG00000138795	LEF1	3.4	1.70E-07	2.15E-03
ENSG00000223414	LINC00473	-3.4	2.20E-05	2.93E-02
ENSG00000165553	NGB	-3.5	3.21E-06	1.01E-02
ENSG00000152214	RIT2	-2.8	3.08E-05	3.54E-02
ENSG00000250448	RP11-19O2.2	-3.4	2.74E-05	3.30E-02
ENSG00000259203	RP11-209K10.2	-3.8	5.36E-06	1.35E-02
ENSG00000229422	RP11-262H14.5	-2.8	7.44E-06	1.47E-02
ENSG00000234688	RP1-293L6.1	-3.3	6.07E-06	1.39E-02
ENSG00000196104	SPOCK3	-2.4	1.99E-05	2.80E-02
ENSG00000170044	ZPLD1	-3.3	2.05E-06	8.62E-03

Supplement Tab. 2: Significant deregulated genes of iPSC-derived neurons from SZ 1 versus all CTR after transcriptome analysis.

gene ID	gene	log2FoldChange	pvalue	padj
ENSG00000234281	AC007970.1	4.7	1.15E-05	3.33E-03
ENSG00000143632	ACTA1	4.1	4.91E-05	1.09E-02
ENSG00000159251	ACTC1	4.8	2.73E-06	1.11E-03
ENSG00000077522	ACTN2	4.2	1.22E-05	3.50E-03
ENSG00000157510	AFAP1L1	3.7	1.28E-04	2.38E-02
ENSG00000165092	ALDH1A1	5.6	2.18E-08	2.37E-05
ENSG00000147256	ARHGAP36	-4.4	8.32E-06	2.55E-03
ENSG00000005981	ASB4	3.8	1.94E-04	3.30E-02
ENSG00000164122	ASB5	4.1	8.87E-05	1.77E-02

ENSG00000106819	ASPN	4.3	1.67E-06	7.91E-04
ENSG00000101892	ATP1B4	6.6	2.03E-10	4.06E-07
ENSG00000043039	BARX2	5.3	4.73E-07	2.82E-04
ENSG00000182492	BGN	3.8	2.68E-05	6.94E-03
ENSG00000177354	C10orf71	4.6	1.47E-05	4.04E-03
ENSG00000161992	C16orf11	5.1	1.69E-06	7.91E-04
ENSG00000180999	C1orf105	4.4	1.53E-05	4.15E-03
ENSG00000169085	C8orf46	-3.4	1.96E-04	3.30E-02
ENSG00000077274	CAPN6	4.7	5.31E-06	1.86E-03
ENSG00000118729	CASQ2	4.6	6.88E-07	3.79E-04
ENSG00000164287	CDC20B	5.0	3.48E-06	1.32E-03
ENSG00000129910	CDH15	4.6	3.43E-07	2.36E-04
ENSG00000135902	CHRND	5.1	1.75E-06	8.03E-04
ENSG00000104879	CKM	4.6	1.31E-05	3.66E-03
ENSG00000159212	CLIC6	4.6	1.81E-05	4.87E-03
ENSG00000187955	COL14A1	4.0	6.80E-06	2.24E-03
ENSG00000105664	COMP	7.8	1.06E-15	7.77E-12
ENSG00000129170	CSRP3	5.7	2.26E-08	2.37E-05
ENSG00000268518	CTD-2545M3.8	5.6	2.84E-08	2.84E-05
ENSG00000186377	CYP4X1	-3.6	3.36E-04	4.97E-02
ENSG00000067048	DDX3Y	6.2	2.40E-09	3.59E-06
ENSG00000175084	DES	4.4	1.51E-06	7.54E-04
ENSG00000231764	DLX6-AS1	-4.2	3.57E-05	8.74E-03
ENSG00000121570	DPPA4	-4.0	8.29E-06	2.55E-03
ENSG00000186676	EEF1GP1	3.5	1.34E-04	2.46E-02
ENSG00000198692	EIF1AY	7.3	1.21E-13	6.65E-10
ENSG00000127507	EMR2	3.8	3.13E-04	4.69E-02
ENSG00000108515	ENO3	4.5	5.06E-07	2.94E-04
ENSG00000065361	ERBB3	4.0	3.27E-05	8.25E-03
ENSG00000157554	ERG	4.4	2.17E-05	5.76E-03
ENSG00000106038	EVX1	3.9	1.23E-04	2.31E-02
ENSG00000122176	FMOD	5.7	2.61E-09	3.59E-06
ENSG00000143140	GJA5	3.9	2.13E-04	3.53E-02
ENSG00000177291	GJD4	5.5	1.53E-07	1.22E-04
ENSG00000132975	GPR12	-3.6	5.59E-05	1.22E-02
ENSG00000130600	H19	4.6	1.84E-06	8.27E-04
ENSG00000164107	HAND2	5.2	2.91E-07	2.07E-04
ENSG00000237125	HAND2-AS1	5.1	2.38E-06	1.03E-03
ENSG00000204287	HLA-DRA	-4.0	1.14E-05	3.33E-03
ENSG00000130528	HRC	4.6	1.10E-06	5.79E-04
ENSG00000157219	HTR5A	-3.4	2.56E-04	3.99E-02
ENSG00000167244	IGF2	4.6	3.83E-07	2.51E-04
ENSG00000115221	ITGB6	3.6	1.05E-04	2.01E-02
ENSG00000241859	KALP	5.0	2.58E-06	1.07E-03
ENSG00000182255	KCNA4	-3.5	1.79E-04	3.12E-02

ENSG00000185774	KCNIP4	-3.5	2.27E-04	3.71E-02
ENSG00000115474	KCNJ13	4.0	2.38E-04	3.83E-02
ENSG00000012817	KDM5D	6.6	5.51E-11	1.35E-07
ENSG00000168427	KLHL30	3.9	7.44E-05	1.53E-02
ENSG00000157119	KLHL40	4.6	1.40E-06	7.20E-04
ENSG00000239474	KLHL41	4.8	4.00E-07	2.51E-04
ENSG00000131650	KREMEN2	3.6	4.97E-05	1.09E-02
ENSG00000122367	LDB3	4.1	8.84E-06	2.67E-03
ENSG00000262152	LINC00514	4.9	4.48E-06	1.62E-03
ENSG00000233117	LINC00702	4.1	1.88E-04	3.26E-02
ENSG00000249378	LINC01060	4.2	9.48E-05	1.85E-02
ENSG00000170807	LMOD2	4.0	1.49E-04	2.67E-02
ENSG00000214548	MEG3	8.4	2.00E-16	2.20E-12
ENSG00000265142	MIR1-2	4.3	6.99E-05	1.47E-02
ENSG00000211574	MIR770	4.9	7.42E-06	2.37E-03
ENSG00000136297	MMD2	-3.5	2.47E-04	3.91E-02
ENSG00000086967	MYBPC2	4.0	7.98E-05	1.61E-02
ENSG00000111049	MYF5	6.0	2.03E-08	2.36E-05
ENSG00000109063	MYH3	5.4	2.75E-07	2.02E-04
ENSG00000168530	MYL1	4.2	6.74E-05	1.44E-02
ENSG00000160808	MYL3	3.7	1.36E-04	2.48E-02
ENSG00000198336	MYL4	4.8	4.31E-06	1.58E-03
ENSG00000180209	MYLPF	4.8	3.39E-06	1.31E-03
ENSG00000133454	MYO18B	4.1	3.13E-05	8.02E-03
ENSG00000129152	MYOD1	6.1	6.82E-10	1.25E-06
ENSG00000122180	MYOG	5.0	3.24E-06	1.30E-03
ENSG00000142661	MYOM3	4.8	7.01E-06	2.27E-03
ENSG00000172399	MYOZ2	3.7	4.60E-05	1.05E-02
ENSG00000138347	MYPN	5.2	2.73E-07	2.02E-04
ENSG00000183091	NEB	3.6	3.19E-04	4.75E-02
ENSG00000087303	NID2	3.8	3.91E-05	9.30E-03
ENSG00000122585	NPY	4.0	3.95E-05	9.30E-03
ENSG00000226306	NPY6R	4.2	1.07E-04	2.04E-02
ENSG00000106809	OGN	4.1	4.73E-05	1.06E-02
ENSG00000183801	OLFML1	3.7	1.26E-04	2.35E-02
ENSG00000188269	OR7A5	4.0	2.43E-04	3.89E-02
ENSG00000171540	OTP	-4.6	3.37E-06	1.31E-03
ENSG00000108405	P2RX1	4.0	3.12E-04	4.69E-02
ENSG00000253537	PCDHGA7	3.8	2.80E-04	4.29E-02
ENSG00000069011	PITX1	6.4	7.50E-11	1.65E-07
ENSG00000147588	PMP2	-3.7	1.43E-04	2.59E-02
ENSG00000099725	PRKY	4.7	6.08E-06	2.03E-03
ENSG00000172179	PRL	5.8	3.25E-08	3.11E-05
ENSG00000171864	PRND	4.4	2.43E-06	1.03E-03
ENSG00000165917	RAPSN	5.0	1.58E-06	7.75E-04

ENSG00000254202	RP11-120I21.2	5.0	3.72E-06	1.39E-03
ENSG00000269994	RP11-276H19.2	-3.3	2.80E-04	4.29E-02
ENSG00000254586	RP11-358H18.3	4.3	9.29E-05	1.83E-02
ENSG00000253619	RP11-369K17.1	4.5	3.29E-05	8.25E-03
ENSG00000269466	RP11-432M8.17	4.5	4.28E-05	9.94E-03
ENSG00000257951	RP11-554D14.4	4.9	5.17E-06	1.84E-03
ENSG00000267287	RP11-567M16.1	4.2	7.42E-05	1.53E-02
ENSG00000258732	RP11-603B24.1	4.0	2.59E-04	4.02E-02
ENSG00000259669	RP11-643A5.2	4.5	3.47E-05	8.59E-03
ENSG00000248713	RP11-766F14.2	3.9	1.96E-04	3.30E-02
ENSG00000259847	RP11-95H3.1	4.0	2.91E-04	4.43E-02
ENSG00000129824	RPS4Y1	7.2	2.07E-13	9.12E-10
ENSG00000070031	SCT	3.9	2.20E-04	3.62E-02
ENSG00000108823	SGCA	4.9	6.78E-07	3.79E-04
ENSG00000126778	SIX1	3.9	5.72E-05	1.23E-02
ENSG00000091482	SMPX	4.1	8.93E-05	1.77E-02
ENSG00000115593	SMYD1	5.0	1.55E-07	1.22E-04
ENSG00000185739	SRL	5.2	6.38E-09	7.81E-06
ENSG00000184343	SRPK3	3.8	2.01E-04	3.36E-02
ENSG00000139874	SSTR1	-3.5	1.57E-04	2.79E-02
ENSG00000166317	SYNPO2L	5.1	7.44E-08	6.31E-05
ENSG00000163630	SYNPR	-4.0	1.30E-05	3.66E-03
ENSG00000092377	TBL1Y	4.5	3.90E-05	9.30E-03
ENSG00000135111	TBX3	3.9	2.49E-04	3.92E-02
ENSG00000121075	TBX4	4.2	3.97E-05	9.30E-03
ENSG00000188681	TEKT4P2	5.7	3.94E-08	3.62E-05
ENSG00000142910	TINAGL1	4.8	5.40E-06	1.86E-03
ENSG00000187616	TMEM8C	5.2	4.05E-07	2.51E-04
ENSG00000154620	TMSB4Y	6.2	2.53E-09	3.59E-06
ENSG00000101470	TNNC2	4.5	8.33E-06	2.55E-03
ENSG00000159173	TNNI1	5.3	4.72E-09	6.12E-06
ENSG00000130598	TNNI2	5.3	4.93E-08	4.35E-05
ENSG00000105048	TNNT1	3.8	4.44E-05	1.02E-02
ENSG00000118194	TNNT2	4.5	2.44E-05	6.40E-03
ENSG00000130595	TNNT3	5.1	2.00E-06	8.81E-04
ENSG00000186439	TRDN	3.9	7.56E-05	1.54E-02
ENSG00000147573	TRIM55	4.1	6.83E-05	1.45E-02
ENSG00000158022	TRIM63	4.0	1.59E-04	2.80E-02
ENSG00000155657	TTN	4.2	5.75E-06	1.95E-03
ENSG00000118271	TTR	4.6	9.84E-06	2.93E-03
ENSG00000176728	TTTY14	5.3	4.09E-07	2.51E-04
ENSG00000233864	TTTY15	8.6	5.71E-18	1.26E-13
ENSG00000131002	TXLNG2P	7.2	8.45E-13	3.10E-09
ENSG00000141161	UNC45B	5.2	7.44E-07	4.00E-04
ENSG00000114374	USP9Y	6.8	6.54E-12	2.02E-08

ENSG00000181408	UTS2R	3.9	9.90E-05	1.91E-02
ENSG00000183878	UTY	6.8	7.35E-12	2.02E-08
ENSG00000135925	WNT10A	3.6	1.89E-04	3.26E-02
ENSG00000163092	XIRP2	4.0	2.33E-04	3.78E-02
ENSG00000067646	ZFY	6.2	1.99E-09	3.38E-06

Supplement Tab. 3: Significant deregulated genes of iPSC-derived neurons from SZ 2 versus all CTR after transcriptome analysis.

gene ID	gene	log2FoldChange	pvalue	padj
ENSG00000224911	AC015936.3	4.2	3.64E-05	2.19E-02
ENSG00000106819	ASPN	4.1	5.44E-06	4.72E-03
ENSG00000125730	C3	4.3	1.28E-05	9.24E-03
ENSG00000151062	CACNA2D4	4.1	2.02E-05	1.37E-02
ENSG00000019582	CD74	6.0	2.08E-10	1.51E-06
ENSG00000164287	CDC20B	6.0	1.16E-08	2.28E-05
ENSG00000133048	CHI3L1	5.8	6.09E-10	2.21E-06
ENSG00000179583	CIITA	5.7	1.30E-09	4.03E-06
ENSG00000115844	DLX2	4.2	1.04E-05	8.39E-03
ENSG00000105880	DLX5	4.2	1.08E-05	8.39E-03
ENSG00000006377	DLX6	4.0	7.31E-05	3.78E-02
ENSG00000231764	DLX6-AS1	5.1	1.33E-08	2.41E-05
ENSG00000070886	EPHA8	-3.5	8.75E-05	4.36E-02
ENSG00000164308	ERAP2	5.4	1.78E-08	2.76E-05
ENSG00000230316	FEZF1-AS1	4.4	4.01E-05	2.35E-02
ENSG00000143631	FLG	4.6	2.72E-05	1.73E-02
ENSG00000164694	FNDC1	3.7	5.29E-05	3.02E-02
ENSG00000134612	FOLH1B	5.6	2.29E-07	2.62E-04
ENSG00000176165	FOXG1	4.1	1.05E-04	4.82E-02
ENSG00000117226	GBP3	4.2	9.92E-06	8.29E-03
ENSG00000131095	GFAP	3.8	3.04E-05	1.89E-02
ENSG00000184674	GSTT1	-4.8	1.66E-07	2.00E-04
ENSG00000206337	HCP5	4.3	1.14E-05	8.50E-03
ENSG00000204257	HLA-DMA	4.2	3.12E-06	2.83E-03
ENSG00000242574	HLA-DMB	4.5	5.40E-07	5.86E-04
ENSG00000204252	HLA-DOA	6.3	1.66E-11	1.80E-07
ENSG00000231389	HLA-DPA1	5.6	3.18E-10	1.56E-06
ENSG00000196735	HLA-DQA1	5.5	6.88E-09	1.49E-05
ENSG00000237541	HLA-DQA2	5.2	7.06E-07	7.30E-04
ENSG00000232629	HLA-DQB2	6.0	4.75E-09	1.15E-05
ENSG00000204287	HLA-DRA	5.5	3.59E-10	1.56E-06
ENSG00000196126	HLA-DRB1	4.0	5.46E-05	3.04E-02
ENSG00000198502	HLA-DRB5	4.3	1.32E-05	9.24E-03
ENSG00000229391	HLA-DRB6	5.6	2.49E-08	3.60E-05
ENSG00000204642	HLA-F	3.8	1.07E-04	4.82E-02

ENSG00000132204	LINC00470	4.7	2.13E-06	2.10E-03
ENSG00000012223	LTF	6.8	6.85E-12	1.49E-07
ENSG00000053438	NNAT	-4.7	1.01E-07	1.29E-04
ENSG00000111331	OAS3	4.2	2.47E-06	2.33E-03
ENSG00000160951	PTGER1	3.9	8.83E-05	4.36E-02
ENSG00000198774	RASSF9	3.7	5.68E-05	3.08E-02
ENSG00000250138	RP11-848G14.5	4.3	9.73E-05	4.70E-02
ENSG00000177409	SAMD9L	3.7	1.02E-04	4.82E-02
ENSG00000126778	SIX1	3.8	1.09E-04	4.82E-02
ENSG00000226287	TMEM191A	-3.7	6.81E-05	3.61E-02
ENSG00000150244	TRIM48	6.2	2.17E-09	5.89E-06
ENSG00000148704	VAX1	5.7	1.77E-08	2.76E-05
ENSG00000106018	VIPR2	-4.2	2.19E-05	1.44E-02
ENSG00000197134	ZNF257	5.8	5.21E-08	7.08E-05

Supplement Tab. 4: Significant deregulated genes of iPSC-derived neurons from SZ 3 versus all CTR after transcriptome analysis.

gene ID	**gene**	**log2FoldChange**	**pvalue**	**padj**
ENSG00000251621	AC009487.5	4.9	8.98E-05	3.92E-02
ENSG00000178522	AMBN	8.6	2.92E-19	3.13E-15
ENSG00000004848	ARX	4.6	3.55E-06	2.62E-03
ENSG00000169085	C8orf46	-3.9	5.23E-05	2.49E-02
ENSG00000117266	CDK18	4.1	1.39E-05	8.37E-03
ENSG00000168539	CHRM1	5.2	2.34E-06	1.79E-03
ENSG00000259436	CTC-378H22.2	-4.8	2.01E-05	1.16E-02
ENSG00000250377	CTC-467M3.3	6.1	4.02E-07	3.44E-04
ENSG00000080166	DCT	4.2	1.18E-04	4.86E-02
ENSG00000067048	DDX3Y	7.6	9.36E-12	1.43E-08
ENSG00000142700	DMRTA2	7.2	1.28E-12	2.11E-09
ENSG00000186676	EEF1GP1	5.3	2.79E-08	2.84E-05
ENSG00000198692	EIF1AY	7.9	4.08E-14	8.72E-11
ENSG00000170370	EMX2	8.5	1.55E-15	5.35E-12
ENSG00000229847	EMX2OS	8.8	3.73E-16	1.99E-12
ENSG00000163064	EN1	-5.2	1.66E-06	1.32E-03
ENSG00000163508	EOMES	5.0	7.00E-06	4.68E-03
ENSG00000153266	FEZF2	8.3	4.46E-18	3.18E-14
ENSG00000176165	FOXG1	6.5	2.51E-08	2.68E-05
ENSG00000144820	GPR128	7.5	7.10E-11	1.01E-07
ENSG00000164171	ITGA2	4.4	1.10E-05	6.92E-03
ENSG00000241859	KALP	5.2	1.41E-05	8.37E-03
ENSG00000012817	KDM5D	7.6	6.10E-13	1.09E-09
ENSG00000138795	LEF1	4.4	4.10E-06	2.83E-03
ENSG00000106689	LHX2	6.1	1.07E-08	1.21E-05
ENSG00000214548	MEG3	7.0	2.64E-10	3.53E-07

ENSG00000111341	MGP	-4.4	3.45E-05	1.84E-02
ENSG00000164600	NEUROD6	3.9	4.10E-05	2.04E-02
ENSG00000133636	NTS	4.5	4.04E-06	2.83E-03
ENSG00000171540	OTP	-5.6	2.30E-07	2.14E-04
ENSG00000163803	PLB1	-4.6	4.21E-05	2.05E-02
ENSG00000099725	PRKY	6.2	3.65E-08	3.54E-05
ENSG00000134438	RAX	4.7	1.04E-04	4.45E-02
ENSG00000185304	RGPD2	5.5	7.27E-06	4.71E-03
ENSG00000152214	RIT2	-4.1	3.83E-05	2.00E-02
ENSG00000263711	RP11-169F17.1	6.8	1.16E-09	1.46E-06
ENSG00000260197	RP11-424G14.1	5.2	3.18E-05	1.74E-02
ENSG00000205663	RP11-706O15.5	5.7	1.02E-06	8.38E-04
ENSG00000231227	RP11-85O21.4	4.8	7.68E-05	3.49E-02
ENSG00000129824	RPS4Y1	8.1	3.04E-15	8.13E-12
ENSG00000066230	SLC9A3	4.9	2.60E-05	1.46E-02
ENSG00000136535	TBR1	8.0	5.16E-14	1.00E-10
ENSG00000157150	TIMP4	-4.4	1.18E-04	4.86E-02
ENSG00000154620	TMSB4Y	6.1	2.78E-07	2.48E-04
ENSG00000176728	TTTY14	4.7	1.21E-04	4.86E-02
ENSG00000233864	TTTY15	9.7	1.22E-19	2.61E-15
ENSG00000131002	TXLNG2P	8.3	1.97E-14	4.68E-11
ENSG00000262519	TXNP4	-4.4	6.97E-05	3.24E-02
ENSG00000114374	USP9Y	8.2	1.75E-15	5.35E-12
ENSG00000183878	UTY	8.4	1.17E-15	5.00E-12
ENSG00000227165	WDR11-AS1	-4.6	4.04E-05	2.04E-02
ENSG00000204186	ZDBF2	-4.4	8.31E-05	3.70E-02
ENSG00000067646	ZFY	6.6	8.84E-09	1.05E-05

Supplement Tab. 5: Significant deregulated genes of iPSC-derived neurons from SZ 2 versus CTR 1 after transcriptome analysis.

gene ID	gene	log2FoldChange	pvalue
ENSG00000175899	A2M	2.5	1.63E-02
ENSG00000181409	AATK	-2.2	2.81E-02
ENSG00000108846	ABCC3	3.3	2.84E-03
ENSG00000006071	ABCC8	-2.7	1.18E-02
ENSG00000154175	ABI3BP	3.0	5.24E-03
ENSG00000163995	ABLIM2	-2.0	4.53E-02
ENSG00000173210	ABLIM3	-2.5	1.59E-02
ENSG00000187905	AC002472.13	2.8	1.15E-02
ENSG00000188477	AC003003.5	3.4	2.66E-03
ENSG00000261790	AC005606.14	-2.4	3.59E-02
ENSG00000261342	AC006538.1	-2.2	3.62E-02
ENSG00000236544	AC008060.8	2.4	4.29E-02
ENSG00000223642	AC008277.1	2.6	2.60E-02

ENSG00000224911	AC015936.3	3.2	3.89E-03
ENSG00000234710	AC060834.3	3.0	1.10E-02
ENSG00000228528	AC068057.1	-2.6	2.56E-02
ENSG00000229267	AC072062.1	2.5	2.87E-02
ENSG00000222043	AC079305.10	-2.4	4.37E-02
ENSG00000204460	AC079586.1	-2.8	1.62E-02
ENSG00000229370	AC092635.1	-2.7	2.23E-02
ENSG00000226321	AC104809.3	2.5	3.47E-02
ENSG00000236710	AC108448.2	-2.6	2.49E-02
ENSG00000232938	AC139099.3	-2.9	1.30E-02
ENSG00000197142	ACSL5	2.4	4.11E-02
ENSG00000154930	ACSS1	2.3	2.68E-02
ENSG00000159251	ACTC1	-2.6	1.56E-02
ENSG00000163017	ACTG2	2.7	1.12E-02
ENSG00000077080	ACTL6B	-2.1	3.61E-02
ENSG00000073670	ADAM11	-2.3	2.56E-02
ENSG00000148848	ADAM12	2.0	4.73E-02
ENSG00000138316	ADAMTS14	2.4	2.16E-02
ENSG00000145536	ADAMTS16	2.9	5.87E-03
ENSG00000158859	ADAMTS4	2.2	3.89E-02
ENSG00000134917	ADAMTS8	-2.3	3.53E-02
ENSG00000105963	ADAP1	-2.9	6.97E-03
ENSG00000141433	ADCYAP1	-2.4	1.83E-02
ENSG00000118492	ADGB	2.7	1.83E-02
ENSG00000106624	AEBP1	2.2	2.86E-02
ENSG00000135439	AGAP2	-2.3	2.45E-02
ENSG00000255737	AGAP2-AS1	2.1	4.68E-02
ENSG00000165923	AGBL2	2.7	1.96E-02
ENSG00000124942	AHNAK	2.4	1.97E-02
ENSG00000106546	AHR	2.0	4.79E-02
ENSG00000154027	AK5	-2.0	4.76E-02
ENSG00000162641	AKNAD1	2.8	1.06E-02
ENSG00000151632	AKR1C2	-2.7	1.00E-02
ENSG00000179148	ALOXE3	-2.6	2.79E-02
ENSG00000104899	AMH	-2.5	1.78E-02
ENSG00000167772	ANGPTL4	2.1	4.74E-02
ENSG00000187984	ANKRD19P	-2.8	1.92E-02
ENSG00000230006	ANKRD36BP2	-2.2	3.81E-02
ENSG00000164512	ANKRD55	-2.3	3.02E-02
ENSG00000230062	ANKRD66	3.0	9.60E-03
ENSG00000011426	ANLN	2.0	4.94E-02
ENSG00000131620	ANO1	2.3	3.31E-02
ENSG00000231991	ANXA2P2	2.0	4.92E-02
ENSG00000273295	AP000350.5	-2.6	2.50E-02
ENSG00000213983	AP1G2	-2.3	2.55E-02

ENSG00000107282	APBA1	-2.0	4.33E-02
ENSG00000198768	APCDD1L	2.6	1.97E-02
ENSG00000134817	APLNR	2.5	2.00E-02
ENSG00000239713	APOBEC3G	2.3	4.42E-02
ENSG00000130203	APOE	2.6	1.21E-02
ENSG00000100342	APOL1	3.0	1.07E-02
ENSG00000221963	APOL6	2.6	1.43E-02
ENSG00000198576	ARC	-2.3	2.41E-02
ENSG00000081181	ARG2	-2.1	3.79E-02
ENSG00000198826	ARHGAP11A	2.5	1.68E-02
ENSG00000187951	ARHGAP11B	2.1	4.07E-02
ENSG00000137727	ARHGAP20	-2.2	3.14E-02
ENSG00000137962	ARHGAP29	2.1	3.99E-02
ENSG00000147256	ARHGAP36	-2.9	7.61E-03
ENSG00000242173	ARHGDIG	-3.2	3.42E-03
ENSG00000165309	ARMC3	3.1	4.75E-03
ENSG00000172995	ARPP21	-2.1	3.53E-02
ENSG00000140450	ARRDC4	2.2	3.21E-02
ENSG00000004848	ARX	3.0	6.38E-03
ENSG00000108684	ASIC2	-2.3	2.28E-02
ENSG00000108381	ASPA	2.7	2.13E-02
ENSG00000174939	ASPHD1	-2.3	2.52E-02
ENSG00000066279	ASPM	3.0	5.02E-03
ENSG00000106819	ASPN	3.1	4.06E-03
ENSG00000179774	ATOH7	-2.8	1.58E-02
ENSG00000118322	ATP10B	2.3	2.75E-02
ENSG00000105409	ATP1A3	-2.3	2.33E-02
ENSG00000067842	ATP2B3	-2.4	2.17E-02
ENSG00000180389	ATP5EP2	-2.2	3.22E-02
ENSG00000132932	ATP8A2	-2.0	4.11E-02
ENSG00000081923	ATP8B1	2.2	3.81E-02
ENSG00000178999	AURKB	2.0	4.80E-02
ENSG00000176383	B3GNT4	-2.6	1.60E-02
ENSG00000086062	B4GALT1	2.5	1.53E-02
ENSG00000181790	BAI1	-2.4	2.08E-02
ENSG00000198604	BAZ1A	2.0	4.35E-02
ENSG00000166546	BEAN1	-2.4	2.13E-02
ENSG00000183092	BEGAIN	-2.2	3.04E-02
ENSG00000133169	BEX1	-2.1	3.90E-02
ENSG00000133134	BEX2	-2.1	3.90E-02
ENSG00000184515	BEX5	-2.3	2.68E-02
ENSG00000182492	BGN	2.8	8.09E-03
ENSG00000139618	BRCA2	2.4	2.16E-02
ENSG00000136492	BRIP1	2.1	4.09E-02
ENSG00000160469	BRSK1	-2.0	4.89E-02

ENSG00000169679	BUB1	2.2	2.86E-02
ENSG00000137691	C11orf70	2.3	2.84E-02
ENSG00000183644	C11orf88	2.6	1.83E-02
ENSG00000188596	C12orf55	2.2	3.01E-02
ENSG00000177875	C12orf68	-2.1	3.91E-02
ENSG00000156206	C15orf26	2.9	8.77E-03
ENSG00000221916	C19orf73	-2.4	3.34E-02
ENSG00000203963	C1orf141	2.3	4.62E-02
ENSG00000157330	C1orf158	2.6	1.39E-02
ENSG00000163263	C1orf189	2.3	4.59E-02
ENSG00000188931	C1orf192	2.1	3.62E-02
ENSG00000142609	C1orf222	2.6	1.68E-02
ENSG00000228594	C1orf233	-2.2	3.05E-02
ENSG00000162598	C1orf87	2.5	3.33E-02
ENSG00000144119	C1QL2	-2.6	1.42E-02
ENSG00000172247	C1QTNF4	-2.3	2.28E-02
ENSG00000159403	C1R	2.7	1.12E-02
ENSG00000139178	C1RL	2.1	4.03E-02
ENSG00000205885	C1RL-AS1	2.8	1.13E-02
ENSG00000182326	C1S	2.1	3.92E-02
ENSG00000171695	C20orf201	-2.9	9.81E-03
ENSG00000198547	C20orf203	-2.8	1.16E-02
ENSG00000182912	C21orf90	-2.9	1.05E-02
ENSG00000154642	C21orf91	2.5	1.56E-02
ENSG00000205856	C22orf42	-2.3	2.95E-02
ENSG00000183186	C2CD4C	-2.0	4.26E-02
ENSG00000125730	C3	3.2	4.34E-03
ENSG00000224389	C4B	2.4	2.27E-02
ENSG00000181577	C6orf223	2.4	3.10E-02
ENSG00000164746	C7orf57	2.6	1.44E-02
ENSG00000160401	C9orf117	2.4	2.39E-02
ENSG00000204352	C9orf129	-2.7	1.45E-02
ENSG00000204711	C9orf135	2.3	4.40E-02
ENSG00000188523	C9orf171	2.2	3.44E-02
ENSG00000063180	CA11	-2.3	2.38E-02
ENSG00000157782	CABP1	-2.7	1.36E-02
ENSG00000141837	CACNA1A	-2.0	4.88E-02
ENSG00000006283	CACNA1G	-2.1	3.41E-02
ENSG00000100346	CACNA1I	-2.9	7.21E-03
ENSG00000007402	CACNA2D2	-2.0	4.15E-02
ENSG00000157445	CACNA2D3	-2.3	2.55E-02
ENSG00000151062	CACNA2D4	3.0	6.70E-03
ENSG00000166862	CACNG2	-2.2	3.24E-02
ENSG00000104327	CALB1	-2.4	2.08E-02
ENSG00000172137	CALB2	-2.3	2.23E-02

ENSG00000122786	CALD1	2.0	4.66E-02
ENSG00000130643	CALY	-3.0	5.75E-03
ENSG00000070808	CAMK2A	-2.4	1.90E-02
ENSG00000058404	CAMK2B	-2.7	1.02E-02
ENSG00000163888	CAMK2N2	-2.4	1.88E-02
ENSG00000076826	CAMSAP3	-2.2	2.93E-02
ENSG00000180881	CAPS2	2.5	1.96E-02
ENSG00000152611	CAPSL	2.5	2.27E-02
ENSG00000204397	CARD16	2.6	2.27E-02
ENSG00000137812	CASC5	2.6	1.24E-02
ENSG00000167971	CASKIN1	-2.6	1.27E-02
ENSG00000137752	CASP1	2.2	3.20E-02
ENSG00000196954	CASP4	2.4	3.02E-02
ENSG00000121691	CAT	3.9	6.46E-04
ENSG00000105974	CAV1	2.5	1.72E-02
ENSG00000102924	CBLN1	-2.9	6.48E-03
ENSG00000141668	CBLN2	3.5	2.88E-03
ENSG00000054803	CBLN4	3.0	9.67E-03
ENSG00000105479	CCDC114	2.3	3.32E-02
ENSG00000159625	CCDC135	2.3	2.62E-02
ENSG00000120262	CCDC170	2.2	3.08E-02
ENSG00000213085	CCDC19	2.4	2.32E-02
ENSG00000173421	CCDC36	2.7	2.38E-02
ENSG00000186710	CCDC42B	2.3	3.47E-02
ENSG00000135127	CCDC64	-2.3	2.45E-02
ENSG00000055813	CCDC85A	-2.0	4.92E-02
ENSG00000110148	CCKBR	-2.5	2.13E-02
ENSG00000131142	CCL25	-2.4	3.57E-02
ENSG00000151882	CCL28	3.1	8.15E-03
ENSG00000145386	CCNA2	2.1	3.89E-02
ENSG00000156535	CD109	3.0	5.91E-03
ENSG00000120217	CD274	2.2	4.38E-02
ENSG00000174059	CD34	2.2	3.81E-02
ENSG00000019582	CD74	3.9	5.72E-04
ENSG00000153563	CD8A	-2.1	3.84E-02
ENSG00000010278	CD9	2.4	1.97E-02
ENSG00000117399	CDC20	2.1	4.09E-02
ENSG00000164287	CDC20B	3.5	3.09E-03
ENSG00000231007	CDC20P1	2.2	3.73E-02
ENSG00000184661	CDCA2	2.3	2.77E-02
ENSG00000163814	CDCP1	2.7	1.55E-02
ENSG00000149654	CDH22	-2.3	2.45E-02
ENSG00000187492	CDHR4	2.5	3.50E-02
ENSG00000170312	CDK1	2.0	4.44E-02
ENSG00000171450	CDK5R2	-2.2	2.90E-02

ENSG00000124762	CDKN1A	-2.0	4.48E-02
ENSG00000147889	CDKN2A	2.1	4.27E-02
ENSG00000129355	CDKN2D	-2.5	1.76E-02
ENSG00000186567	CEACAM19	-2.2	3.29E-02
ENSG00000007129	CEACAM21	-3.1	5.56E-03
ENSG00000093072	CECR1	2.0	4.55E-02
ENSG00000101489	CELF4	-2.6	1.27E-02
ENSG00000161082	CELF5	-2.1	3.51E-02
ENSG00000184524	CEND1	-2.4	1.89E-02
ENSG00000117724	CENPF	2.6	1.22E-02
ENSG00000151725	CENPU	2.0	4.80E-02
ENSG00000138180	CEP55	2.8	8.61E-03
ENSG00000188452	CERKL	2.1	4.66E-02
ENSG00000205403	CFI	2.1	3.95E-02
ENSG00000003402	CFLAR	3.7	9.59E-04
ENSG00000138028	CGREF1	-2.0	4.72E-02
ENSG00000186940	CHCHD2P9	-3.1	5.84E-03
ENSG00000116254	CHD5	-2.3	2.49E-02
ENSG00000100604	CHGA	-2.6	1.41E-02
ENSG00000089199	CHGB	-2.5	1.54E-02
ENSG00000133048	CHI3L1	3.8	8.12E-04
ENSG00000064886	CHI3L2	3.1	4.89E-03
ENSG00000154645	CHODL	3.7	1.40E-03
ENSG00000101204	CHRNA4	-3.2	3.32E-03
ENSG00000175264	CHST1	-2.2	2.81E-02
ENSG00000179583	CIITA	3.9	6.84E-04
ENSG00000125931	CITED1	-2.0	4.52E-02
ENSG00000169607	CKAP2L	2.0	4.71E-02
ENSG00000223572	CKMT1A	-2.3	2.73E-02
ENSG00000237289	CKMT1B	-2.6	1.47E-02
ENSG00000013297	CLDN11	2.3	3.16E-02
ENSG00000164007	CLDN19	2.5	2.52E-02
ENSG00000160318	CLDND2	-2.2	4.37E-02
ENSG00000105472	CLEC11A	-2.2	3.46E-02
ENSG00000261210	CLEC19A	2.8	1.50E-02
ENSG00000236279	CLEC2L	-3.5	1.95E-03
ENSG00000239265	CLRN1-AS1	-3.1	7.94E-03
ENSG00000070729	CNGB1	-2.6	1.41E-02
ENSG00000146910	CNPY1	3.2	3.91E-03
ENSG00000060718	COL11A1	2.0	4.89E-02
ENSG00000111799	COL12A1	3.0	4.89E-03
ENSG00000187955	COL14A1	2.4	1.83E-02
ENSG00000108821	COL1A1	2.4	2.12E-02
ENSG00000169436	COL22A1	2.2	3.41E-02
ENSG00000144810	COL8A1	2.3	2.57E-02

ENSG00000049089	COL9A2	2.0	4.36E-02
ENSG00000092758	COL9A3	2.9	6.86E-03
ENSG00000158270	COLEC12	2.5	1.61E-02
ENSG00000105664	COMP	3.5	2.23E-03
ENSG00000106789	CORO2A	-2.2	3.52E-02
ENSG00000258981	COX5AP2	-3.0	9.84E-03
ENSG00000047457	CP	3.2	3.31E-03
ENSG00000128510	CPA4	2.8	9.55E-03
ENSG00000168993	CPLX1	-3.2	3.71E-03
ENSG00000124772	CPNE5	-2.7	1.07E-02
ENSG00000178773	CPNE7	-3.0	5.61E-03
ENSG00000166426	CRABP1	-3.1	4.33E-03
ENSG00000143320	CRABP2	2.1	3.45E-02
ENSG00000175874	CREG2	-2.5	1.69E-02
ENSG00000147571	CRH	-2.2	4.81E-02
ENSG00000120088	CRHR1	-2.3	3.11E-02
ENSG00000146215	CRIP3	-2.3	4.82E-02
ENSG00000095713	CRTAC1	-2.9	6.76E-03
ENSG00000109846	CRYAB	2.8	8.43E-03
ENSG00000233280	CRYBG3	2.9	7.57E-03
ENSG00000080200	CRYBG3	2.1	3.55E-02
ENSG00000183117	CSMD1	2.9	8.95E-03
ENSG00000173546	CSPG4	2.5	2.03E-02
ENSG00000114646	CSPG5	-1.9	4.92E-02
ENSG00000273287	CTA-268H5.14	-2.7	1.41E-02
ENSG00000260708	CTA-29F11.1	-2.1	4.26E-02
ENSG00000259871	CTA-363E6.1	2.9	1.36E-02
ENSG00000268262	CTC-246B18.8	-2.4	3.82E-02
ENSG00000269814	CTC-273B12.10	-2.3	4.63E-02
ENSG00000259436	CTC-378H22.2	-2.6	1.81E-02
ENSG00000247311	CTC-441N14.2	2.2	4.97E-02
ENSG00000267481	CTC-559E9.5	2.6	2.44E-02
ENSG00000232615	CTD-2012J19.1	2.3	4.17E-02
ENSG00000267121	CTD-2020K17.1	-2.6	2.27E-02
ENSG00000233175	CTD-2020K17.3	-2.4	2.22E-02
ENSG00000261439	CTD-2050B12.2	-2.6	2.78E-02
ENSG00000253525	CTD-2114J12.1	3.1	6.65E-03
ENSG00000267890	CTD-2126E3.4	-2.9	1.04E-02
ENSG00000267254	CTD-2162K18.5	3.2	5.81E-03
ENSG00000271743	CTD-2541M15.3	-2.1	4.95E-02
ENSG00000267640	CTD-2554C21.2	3.2	6.43E-03
ENSG00000229481	CTD-2554C21.3	3.6	2.09E-03
ENSG00000268119	CTD-2561J22.5	2.2	4.37E-02
ENSG00000268041	CTD-2575K13.6	-2.6	1.55E-02
ENSG00000267522	CTD-2621I17.6	-2.7	2.05E-02

ENSG00000234773	CTD-2666L21.1	2.4	2.71E-02
ENSG00000255372	CTD-3064C13.1	-2.3	3.86E-02
ENSG00000180458	CTD-3064H18.4	2.6	2.63E-02
ENSG00000188897	CTD-3088G3.8	2.2	4.10E-02
ENSG00000103811	CTSH	3.0	5.51E-03
ENSG00000158290	CUL4B	-2.5	1.61E-02
ENSG00000107562	CXCL12	3.1	4.13E-03
ENSG00000081041	CXCL2	2.4	3.11E-02
ENSG00000165164	CXorf22	2.5	3.02E-02
ENSG00000188011	CXXC11	-2.0	4.94E-02
ENSG00000071967	CYBRD1	2.4	2.17E-02
ENSG00000161544	CYGB	-2.9	7.30E-03
ENSG00000138061	CYP1B1	2.1	3.52E-02
ENSG00000187553	CYP26C1	-3.8	9.29E-04
ENSG00000036530	CYP46A1	-2.2	3.25E-02
ENSG00000187048	CYP4A11	-2.5	3.01E-02
ENSG00000186377	CYP4X1	-2.1	4.22E-02
ENSG00000173198	CYSLTR1	2.5	3.47E-02
ENSG00000166265	CYYR1	2.8	9.63E-03
ENSG00000153071	DAB2	2.1	4.15E-02
ENSG00000126733	DACH2	-2.1	3.49E-02
ENSG00000164488	DACT2	2.6	1.20E-02
ENSG00000123977	DAW1	2.6	1.26E-02
ENSG00000163673	DCLK3	-2.4	2.33E-02
ENSG00000237737	DCTN1-AS1	-2.2	4.20E-02
ENSG00000145358	DDIT4L	2.5	1.91E-02
ENSG00000203797	DDO	2.7	2.09E-02
ENSG00000137628	DDX60	2.1	4.18E-02
ENSG00000024526	DEPDC1	2.7	1.09E-02
ENSG00000175084	DES	2.7	1.10E-02
ENSG00000273164	DGCR10	-2.7	2.08E-02
ENSG00000204466	DGKK	-2.0	4.72E-02
ENSG00000139734	DIAPH3	2.1	4.03E-02
ENSG00000116544	DLGAP3	-2.0	4.74E-02
ENSG00000126787	DLGAP5	2.4	2.22E-02
ENSG00000144355	DLX1	2.0	4.50E-02
ENSG00000115844	DLX2	3.0	5.37E-03
ENSG00000105880	DLX5	3.3	3.11E-03
ENSG00000006377	DLX6	3.5	2.31E-03
ENSG00000231764	DLX6-AS1	3.8	7.16E-04
ENSG00000161249	DMKN	-2.1	4.56E-02
ENSG00000176399	DMRTA1	2.5	2.02E-02
ENSG00000158856	DMTN	-2.4	2.02E-02
ENSG00000105877	DNAH11	2.8	1.11E-02
ENSG00000174844	DNAH12	2.6	1.69E-02

ENSG00000149927	DOC2A	-2.3	2.38E-02
ENSG00000272636	DOC2B	-2.6	1.47E-02
ENSG00000141096	DPEP3	2.7	2.19E-02
ENSG00000143196	DPT	-2.3	4.26E-02
ENSG00000188641	DPYD	2.7	1.05E-02
ENSG00000149295	DRD2	-2.3	2.80E-02
ENSG00000046604	DSG2	2.9	6.61E-03
ENSG00000163840	DTX3L	2.4	2.03E-02
ENSG00000158050	DUSP2	-2.6	1.66E-02
ENSG00000158560	DYNC1I1	-2.2	2.73E-02
ENSG00000165891	E2F7	2.0	4.50E-02
ENSG00000129173	E2F8	2.1	4.01E-02
ENSG00000106823	ECM2	2.3	2.69E-02
ENSG00000114346	ECT2	2.2	3.21E-02
ENSG00000101210	EEF1A2	-2.3	2.18E-02
ENSG00000186676	EEF1GP1	2.5	2.27E-02
ENSG00000034239	EFCAB1	2.6	1.20E-02
ENSG00000185055	EFCAB10	2.6	1.65E-02
ENSG00000115380	EFEMP1	2.7	9.38E-03
ENSG00000143590	EFNA3	-2.0	4.28E-02
ENSG00000198759	EGFL6	-2.4	2.15E-02
ENSG00000255150	EID3	2.5	3.06E-02
ENSG00000166897	ELFN2	-2.6	1.30E-02
ENSG00000158711	ELK4	2.0	4.65E-02
ENSG00000227295	ELL2P1	2.3	4.55E-02
ENSG00000049540	ELN	2.4	1.83E-02
ENSG00000230314	ELOVL2-AS1	-2.4	2.93E-02
ENSG00000134531	EMP1	2.0	4.41E-02
ENSG00000170370	EMX2	2.8	1.11E-02
ENSG00000229847	EMX2OS	2.8	1.55E-02
ENSG00000164778	EN2	3.0	4.82E-03
ENSG00000119888	EPCAM	-2.4	2.13E-02
ENSG00000183317	EPHA10	-2.5	1.55E-02
ENSG00000070886	EPHA8	-3.3	2.56E-03
ENSG00000177106	EPS8L2	-2.4	2.08E-02
ENSG00000164308	ERAP2	3.9	6.53E-04
ENSG00000171320	ESCO2	2.2	3.29E-02
ENSG00000143845	ETNK2	-2.0	4.64E-02
ENSG00000134954	ETS1	2.8	8.13E-03
ENSG00000115363	EVA1A	2.4	2.83E-02
ENSG00000106038	EVX1	-3.1	8.16E-03
ENSG00000174279	EVX2	-3.2	6.48E-03
ENSG00000110723	EXPH5	2.2	3.97E-02
ENSG00000057593	F7	-3.0	1.13E-02
ENSG00000165591	FAAH2	-2.2	4.26E-02

ENSG00000121769	FABP3	-2.0	4.75E-02
ENSG00000172782	FADS6	-2.4	4.02E-02
ENSG00000135472	FAIM2	-2.1	3.99E-02
ENSG00000189057	FAM111B	2.3	2.54E-02
ENSG00000135842	FAM129A	2.7	9.80E-03
ENSG00000185519	FAM131C	-2.8	9.87E-03
ENSG00000147724	FAM135B	3.7	1.27E-03
ENSG00000182646	FAM156A	-2.9	1.27E-02
ENSG00000182183	FAM159A	-2.5	2.79E-02
ENSG00000196990	FAM163B	-2.6	1.66E-02
ENSG00000215187	FAM166B	2.8	1.59E-02
ENSG00000186973	FAM183A	2.2	3.44E-02
ENSG00000104059	FAM189A1	-2.1	3.74E-02
ENSG00000219438	FAM19A5	-3.9	6.39E-04
ENSG00000179813	FAM216B	3.4	2.33E-03
ENSG00000250486	FAM218A	-2.2	3.45E-02
ENSG00000183508	FAM46C	2.3	3.36E-02
ENSG00000149926	FAM57B	-2.0	4.11E-02
ENSG00000142530	FAM71E1	-2.5	1.90E-02
ENSG00000153347	FAM81B	2.3	2.76E-02
ENSG00000153789	FAM92B	2.2	4.29E-02
ENSG00000078098	FAP	2.6	1.79E-02
ENSG00000180178	FAR2P1	-3.1	4.97E-03
ENSG00000188573	FBLL1	-2.4	1.83E-02
ENSG00000166147	FBN1	2.0	4.15E-02
ENSG00000138829	FBN2	2.1	3.41E-02
ENSG00000127585	FBXL16	-2.1	3.67E-02
ENSG00000156804	FBXO32	2.1	3.85E-02
ENSG00000163013	FBXO41	-2.0	4.85E-02
ENSG00000101311	FERMT1	2.3	3.28E-02
ENSG00000128610	FEZF1	3.1	7.55E-03
ENSG00000230316	FEZF1-AS1	3.0	8.37E-03
ENSG00000154783	FGD5	-2.3	2.91E-02
ENSG00000129682	FGF13	-2.2	2.97E-02
ENSG00000158815	FGF17	-2.4	2.24E-02
ENSG00000162344	FGF19	2.8	1.61E-02
ENSG00000138675	FGF5	3.1	5.96E-03
ENSG00000143631	FLG	2.8	1.84E-02
ENSG00000102755	FLT1	2.7	1.91E-02
ENSG00000122025	FLT3	-2.7	1.70E-02
ENSG00000248905	FMN1	2.6	1.78E-02
ENSG00000184922	FMNL1	-2.2	3.35E-02
ENSG00000115414	FN1	3.3	2.26E-03
ENSG00000164694	FNDC1	2.8	9.17E-03
ENSG00000172568	FNDC9	-2.9	8.65E-03

ENSG00000134612	FOLH1B	3.1	8.48E-03
ENSG00000110195	FOLR1	2.8	1.15E-02
ENSG00000204612	FOXB2	-3.2	5.80E-03
ENSG00000129654	FOXJ1	2.0	4.74E-02
ENSG00000254685	FPGT	2.0	4.44E-02
ENSG00000139926	FRMD6	2.3	2.60E-02
ENSG00000156869	FRRS1	2.7	1.42E-02
ENSG00000237637	FRY-AS1	-2.3	4.73E-02
ENSG00000174951	FUT1	-2.6	2.07E-02
ENSG00000180549	FUT7	-2.7	1.87E-02
ENSG00000089327	FXYD5	2.7	1.09E-02
ENSG00000221946	FXYD7	-2.2	3.04E-02
ENSG00000163251	FZD5	2.2	3.24E-02
ENSG00000109458	GAB1	2.0	4.56E-02
ENSG00000136928	GABBR2	-2.0	4.80E-02
ENSG00000011677	GABRA3	-2.2	2.92E-02
ENSG00000186297	GABRA5	-2.5	1.71E-02
ENSG00000146276	GABRR1	-2.6	2.37E-02
ENSG00000182870	GALNT9	-2.3	3.00E-02
ENSG00000174473	GALNTL6	-2.6	1.23E-02
ENSG00000223460	GAPDHP69	2.3	4.19E-02
ENSG00000139354	GAS2L3	2.5	1.52E-02
ENSG00000117228	GBP1	3.3	3.00E-03
ENSG00000162645	GBP2	3.1	5.18E-03
ENSG00000117226	GBP3	3.7	9.74E-04
ENSG00000187210	GCNT1	2.2	3.75E-02
ENSG00000140297	GCNT3	-2.3	4.70E-02
ENSG00000119125	GDA	2.1	3.85E-02
ENSG00000131095	GFAP	3.1	3.91E-03
ENSG00000099998	GGT5	2.6	1.72E-02
ENSG00000121743	GJA3	2.4	3.97E-02
ENSG00000165474	GJB2	2.3	3.46E-02
ENSG00000101958	GLRA2	-2.4	1.79E-02
ENSG00000135423	GLS2	-2.4	2.05E-02
ENSG00000130755	GMFG	-2.5	2.86E-02
ENSG00000205835	GMNC	3.5	1.80E-03
ENSG00000155265	GOLGA7B	-2.4	2.15E-02
ENSG00000269783	GOLGA7B	-2.5	2.31E-02
ENSG00000174567	GOLT1A	-2.6	2.44E-02
ENSG00000136235	GPNMB	2.6	1.42E-02
ENSG00000256925	GPR123-AS1	-2.2	4.89E-02
ENSG00000144230	GPR17	2.7	1.63E-02
ENSG00000156097	GPR61	-2.3	2.64E-02
ENSG00000173698	GPR64	-2.1	4.29E-02
ENSG00000164199	GPR98	2.3	2.36E-02

ENSG00000155324	GRAMD3	2.2	3.29E-02
ENSG00000166923	GREM1	2.1	3.59E-02
ENSG00000176884	GRIN1	-2.2	3.39E-02
ENSG00000198785	GRIN3A	3.7	1.22E-03
ENSG00000144596	GRIP2	-2.4	1.89E-02
ENSG00000124493	GRM4	-2.5	1.81E-02
ENSG00000196277	GRM7	3.5	2.26E-03
ENSG00000104518	GSDMD	2.7	1.33E-02
ENSG00000169181	GSG1L	-2.6	1.40E-02
ENSG00000177602	GSG2	2.1	4.13E-02
ENSG00000184674	GSTT1	-3.6	1.52E-03
ENSG00000180613	GSX2	3.0	1.00E-02
ENSG00000145736	GTF2H2	2.1	4.84E-02
ENSG00000253203	GUSBP3	2.8	1.62E-02
ENSG00000132702	HAPLN2	-2.4	2.41E-02
ENSG00000105509	HAS1	-2.4	2.93E-02
ENSG00000099822	HCN2	-2.9	6.22E-03
ENSG00000206337	HCP5	3.4	2.26E-03
ENSG00000121764	HCRTR1	-2.5	2.18E-02
ENSG00000173706	HEG1	1.9	4.92E-02
ENSG00000127311	HELB	2.1	4.74E-02
ENSG00000019991	HGF	3.0	7.24E-03
ENSG00000223345	HIST2H2BA	2.5	3.47E-02
ENSG00000159399	HK2	2.4	2.08E-02
ENSG00000234745	HLA-B	2.7	9.24E-03
ENSG00000204525	HLA-C	2.3	2.26E-02
ENSG00000204257	HLA-DMA	3.5	1.45E-03
ENSG00000242574	HLA-DMB	3.4	2.40E-03
ENSG00000204252	HLA-DOA	3.9	6.03E-04
ENSG00000231389	HLA-DPA1	3.9	5.89E-04
ENSG00000223865	HLA-DPB1	3.5	1.70E-03
ENSG00000196735	HLA-DQA1	3.9	8.37E-04
ENSG00000237541	HLA-DQA2	3.8	9.29E-04
ENSG00000179344	HLA-DQB1	3.2	3.73E-03
ENSG00000232629	HLA-DQB2	3.7	1.37E-03
ENSG00000204287	HLA-DRA	3.9	6.21E-04
ENSG00000196126	HLA-DRB1	3.9	5.66E-04
ENSG00000198502	HLA-DRB5	3.9	6.63E-04
ENSG00000229391	HLA-DRB6	3.9	7.02E-04
ENSG00000204592	HLA-E	2.2	3.11E-02
ENSG00000204642	HLA-F	3.8	8.61E-04
ENSG00000143341	HMCN1	3.2	3.52E-03
ENSG00000149948	HMGA2	2.7	1.11E-02
ENSG00000072571	HMMR	2.5	1.81E-02
ENSG00000233429	HOTAIRM1	-3.3	3.44E-03

ENSG00000253293	HOXA10	-3.5	2.09E-03
ENSG00000253187	HOXA10-AS	-2.6	2.42E-02
ENSG00000105996	HOXA2	-3.7	1.52E-03
ENSG00000106004	HOXA5	-3.6	1.78E-03
ENSG00000106006	HOXA6	-2.7	2.22E-02
ENSG00000122592	HOXA7	-3.8	1.08E-03
ENSG00000078399	HOXA9	-3.7	1.36E-03
ENSG00000253552	HOXA-AS2	-2.5	3.12E-02
ENSG00000173917	HOXB2	-3.0	6.07E-03
ENSG00000120093	HOXB3	-3.5	1.85E-03
ENSG00000182742	HOXB4	-3.1	7.22E-03
ENSG00000120075	HOXB5	-3.8	9.79E-04
ENSG00000108511	HOXB6	-3.6	1.89E-03
ENSG00000260027	HOXB7	-3.7	1.56E-03
ENSG00000120068	HOXB8	-3.5	2.66E-03
ENSG00000170689	HOXB9	-3.8	9.99E-04
ENSG00000230148	HOXB-AS1	-2.4	3.52E-02
ENSG00000198353	HOXC4	-2.7	2.02E-02
ENSG00000037965	HOXC8	-3.1	7.64E-03
ENSG00000128710	HOXD10	-3.1	7.52E-03
ENSG00000128652	HOXD3	-3.2	4.95E-03
ENSG00000128709	HOXD9	-3.0	9.59E-03
ENSG00000121905	HPCA	-2.6	1.32E-02
ENSG00000115756	HPCAL1	-2.2	3.17E-02
ENSG00000116983	HPCAL4	-2.1	3.36E-02
ENSG00000101180	HRH3	-2.1	4.39E-02
ENSG00000122254	HS3ST2	-2.3	2.75E-02
ENSG00000171004	HS6ST2	-2.0	4.83E-02
ENSG00000141854	hsa-mir-1199	-2.6	1.42E-02
ENSG00000237973	hsa-mir-6723	-3.0	5.46E-03
ENSG00000102878	HSF4	-2.3	2.62E-02
ENSG00000004776	HSPB6	2.2	4.14E-02
ENSG00000142798	HSPG2	2.3	2.40E-02
ENSG00000157219	HTR5A	-2.8	1.02E-02
ENSG00000090339	ICAM1	3.4	1.97E-03
ENSG00000163565	IFI16	2.3	2.68E-02
ENSG00000159217	IGF2BP1	2.0	4.66E-02
ENSG00000163453	IGFBP7	2.6	1.35E-02
ENSG00000204869	IGFL4	-3.1	7.25E-03
ENSG00000142549	IGLON5	-2.1	3.59E-02
ENSG00000147255	IGSF1	-2.3	2.42E-02
ENSG00000110324	IL10RA	-2.5	2.22E-02
ENSG00000115594	IL1R1	2.5	1.87E-02
ENSG00000091181	IL5RA	2.6	1.74E-02
ENSG00000168685	IL7R	2.3	4.23E-02

ENSG00000139269	INHBE	2.3	2.74E-02
ENSG00000168918	INPP5D	-2.9	9.26E-03
ENSG00000124313	IQSEC2	-2.1	4.06E-02
ENSG00000120645	IQSEC3	-2.7	9.37E-03
ENSG00000164675	IQUB	2.3	2.70E-02
ENSG00000128604	IRF5	-2.2	4.15E-02
ENSG00000113430	IRX4	-2.4	2.36E-02
ENSG00000159387	IRX6	-2.6	1.61E-02
ENSG00000100593	ISM2	-2.7	1.76E-02
ENSG00000213949	ITGA1	2.7	1.19E-02
ENSG00000137809	ITGA11	2.4	1.97E-02
ENSG00000164171	ITGA2	3.1	5.10E-03
ENSG00000132470	ITGB4	2.3	2.62E-02
ENSG00000198542	ITGBL1	2.5	2.00E-02
ENSG00000123243	ITIH5	2.9	7.48E-03
ENSG00000184916	JAG2	-2.1	3.94E-02
ENSG00000152969	JAKMIP1	-2.1	3.61E-02
ENSG00000154118	JPH3	-2.5	1.68E-02
ENSG00000092051	JPH4	-2.0	4.43E-02
ENSG00000186994	KANK3	-2.3	3.21E-02
ENSG00000169282	KCNAB1	-2.1	3.86E-02
ENSG00000166006	KCNC2	-2.6	1.38E-02
ENSG00000131398	KCNC3	-3.0	5.56E-03
ENSG00000116396	KCNC4	-2.5	1.48E-02
ENSG00000162975	KCNF1	-2.4	2.14E-02
ENSG00000135519	KCNH3	-2.5	1.67E-02
ENSG00000089558	KCNH4	-2.3	3.74E-02
ENSG00000162728	KCNJ9	-2.1	4.13E-02
ENSG00000171303	KCNK3	-2.1	3.87E-02
ENSG00000169427	KCNK9	-2.1	3.46E-02
ENSG00000197584	KCNMB2	-2.2	3.46E-02
ENSG00000107147	KCNT1	-2.9	7.56E-03
ENSG00000104756	KCTD9	2.0	4.84E-02
ENSG00000100196	KDELR3	2.0	4.79E-02
ENSG00000235750	KIAA0040	3.2	3.94E-03
ENSG00000255103	KIAA0754	2.1	3.86E-02
ENSG00000122733	KIAA1045	-2.8	8.82E-03
ENSG00000103888	KIAA1199	2.4	2.12E-02
ENSG00000138160	KIF11	2.2	2.83E-02
ENSG00000118193	KIF14	2.6	1.28E-02
ENSG00000163808	KIF15	2.0	4.24E-02
ENSG00000121621	KIF18A	2.3	2.69E-02
ENSG00000112984	KIF20A	2.2	3.25E-02
ENSG00000138182	KIF20B	2.1	4.17E-02
ENSG00000150361	KLHL1	-2.0	4.66E-02

ENSG00000272079	LA16c-380H5.5	-3.1	7.03E-03
ENSG00000125869	LAMP5	-2.3	2.63E-02
ENSG00000138136	LBX1	-3.9	7.45E-04
ENSG00000227128	LBX1-AS1	-3.8	9.22E-04
ENSG00000166796	LDHC	2.4	4.07E-02
ENSG00000138795	LEF1	2.0	4.90E-02
ENSG00000143768	LEFTY2	2.3	2.74E-02
ENSG00000168481	LGI3	-3.2	3.92E-03
ENSG00000156959	LHFPL4	-2.3	2.36E-02
ENSG00000106852	LHX6	3.4	3.22E-03
ENSG00000162624	LHX8	3.0	9.42E-03
ENSG00000104863	LIN7B	-2.6	1.45E-02
ENSG00000178947	LINC00086	-2.0	4.11E-02
ENSG00000196421	LINC00176	-2.1	4.28E-02
ENSG00000180422	LINC00304	-2.5	2.47E-02
ENSG00000153363	LINC00467	2.0	4.99E-02
ENSG00000132204	LINC00470	3.5	2.33E-03
ENSG00000223414	LINC00473	-2.5	2.53E-02
ENSG00000259714	LINC00594	-2.2	3.91E-02
ENSG00000250337	LINC01021	-2.8	1.26E-02
ENSG00000232903	LINC01166	-2.7	1.73E-02
ENSG00000169783	LINGO1	-2.3	2.36E-02
ENSG00000101670	LIPG	2.0	4.71E-02
ENSG00000225110	LL0XNC01-16G2.1	-2.7	1.31E-02
ENSG00000142235	LMTK3	-1.9	4.99E-02
ENSG00000072201	LNX1	-2.1	3.61E-02
ENSG00000134013	LOXL2	2.2	2.92E-02
ENSG00000138131	LOXL4	2.2	3.39E-02
ENSG00000198670	LPA	-2.7	2.07E-02
ENSG00000145012	LPP	2.0	4.32E-02
ENSG00000128011	LRFN1	-2.0	4.28E-02
ENSG00000156564	LRFN2	-2.7	1.07E-02
ENSG00000155530	LRGUK	2.2	3.58E-02
ENSG00000186648	LRRC16B	-2.2	2.96E-02
ENSG00000163827	LRRC2	2.7	1.27E-02
ENSG00000171757	LRRC34	2.5	1.87E-02
ENSG00000176809	LRRC37A3	-2.0	4.90E-02
ENSG00000162494	LRRC38	-3.0	1.08E-02
ENSG00000229356	LRRC3-AS1	-2.8	1.69E-02
ENSG00000171962	LRRC48	2.2	3.58E-02
ENSG00000127399	LRRC61	-2.9	7.48E-03
ENSG00000160838	LRRC71	2.8	1.80E-02
ENSG00000171017	LRRC8E	2.8	1.61E-02
ENSG00000131951	LRRC9	2.1	4.30E-02
ENSG00000133640	LRRIQ1	2.0	4.31E-02

ENSG00000162620	LRRIQ3	2.8	1.40E-02
ENSG00000166159	LRTM2	-2.3	3.35E-02
ENSG00000111321	LTBR	2.9	9.07E-03
ENSG00000012223	LTF	3.8	1.11E-03
ENSG00000150556	LYPD6B	-2.2	4.06E-02
ENSG00000180660	MAB21L1	-2.8	7.74E-03
ENSG00000181541	MAB21L2	-2.9	6.97E-03
ENSG00000182759	MAFA	-2.3	3.25E-02
ENSG00000111837	MAK	3.1	4.53E-03
ENSG00000176601	MAP3K19	2.8	8.28E-03
ENSG00000184368	MAP7D2	-2.3	2.33E-02
ENSG00000181085	MAPK15	2.2	3.14E-02
ENSG00000186868	MAPT	-2.2	2.72E-02
ENSG00000264589	MAPT-AS1	-2.3	3.72E-02
ENSG00000105613	MAST1	-2.1	3.36E-02
ENSG00000007264	MATK	-2.8	8.84E-03
ENSG00000166603	MC4R	-3.2	4.44E-03
ENSG00000214548	MEG3	2.7	1.74E-02
ENSG00000134138	MEIS2	-2.6	1.20E-02
ENSG00000166823	MESP1	-2.1	3.95E-02
ENSG00000111341	MGP	-2.0	4.92E-02
ENSG00000204516	MICB	2.9	1.34E-02
ENSG00000240972	MIF	-2.1	3.75E-02
ENSG00000215417	MIR17HG	2.3	4.26E-02
ENSG00000264063	MIR3687	2.6	2.09E-02
ENSG00000129534	MIS18BP1	2.2	3.15E-02
ENSG00000187098	MITF	2.3	2.83E-02
ENSG00000148773	MKI67	2.6	1.30E-02
ENSG00000150051	MKX	2.4	2.31E-02
ENSG00000146147	MLIP	2.2	3.98E-02
ENSG00000096395	MLN	-2.6	2.98E-02
ENSG00000009950	MLXIPL	-3.3	4.18E-03
ENSG00000136297	MMD2	-2.2	3.88E-02
ENSG00000196611	MMP1	2.5	3.64E-02
ENSG00000137745	MMP13	2.5	3.57E-02
ENSG00000123342	MMP19	2.4	2.18E-02
ENSG00000125966	MMP24	-2.0	4.05E-02
ENSG00000100985	MMP9	2.5	3.07E-02
ENSG00000138722	MMRN1	2.1	3.76E-02
ENSG00000138587	MNS1	2.7	1.28E-02
ENSG00000075643	MOCOS	3.0	8.26E-03
ENSG00000161647	MPP3	-2.1	3.58E-02
ENSG00000153029	MR1	3.3	3.23E-03
ENSG00000254305	MRPL9P1	-2.8	1.21E-02
ENSG00000178860	MSC	2.5	2.03E-02

ENSG00000087250	MT3	-3.0	6.24E-03
ENSG00000162576	MXRA8	2.1	3.64E-02
ENSG00000133055	MYBPH	-2.3	4.40E-02
ENSG00000214114	MYCBP	2.3	2.81E-02
ENSG00000109063	MYH3	-2.0	4.95E-02
ENSG00000133020	MYH8	-3.2	5.80E-03
ENSG00000168530	MYL1	-2.9	1.36E-02
ENSG00000198336	MYL4	-2.5	2.89E-02
ENSG00000065534	MYLK	2.1	3.50E-02
ENSG00000180209	MYLPF	-3.4	3.27E-03
ENSG00000122180	MYOG	-3.0	1.16E-02
ENSG00000145911	N4BP3	-2.1	3.79E-02
ENSG00000177694	NAALADL2	2.3	3.16E-02
ENSG00000173559	NABP1	2.2	3.49E-02
ENSG00000187556	NANOS3	-2.7	1.16E-02
ENSG00000125814	NAPB	-2.0	4.50E-02
ENSG00000158747	NBL1	-2.1	3.61E-02
ENSG00000154654	2	3.8	1.09E-03
ENSG00000103034	NDRG4	-2.0	4.56E-02
ENSG00000103154	NECAB2	-2.7	1.02E-02
ENSG00000139350	NEDD1	2.0	4.84E-02
ENSG00000104725	NEFL	-2.0	4.36E-02
ENSG00000104722	NEFM	-2.1	3.49E-02
ENSG00000107954	NEURL1	-2.2	2.91E-02
ENSG00000171532	NEUROD2	-2.2	3.33E-02
ENSG00000123307	NEUROD4	3.1	4.46E-03
ENSG00000181965	NEUROG1	2.7	2.09E-02
ENSG00000178403	NEUROG2	2.0	4.62E-02
ENSG00000101096	NFATC2	2.2	3.52E-02
ENSG00000165553	NGB	-3.6	1.43E-03
ENSG00000066248	NGEF	-2.3	2.68E-02
ENSG00000171786	NHLH1	2.1	4.03E-02
ENSG00000177551	NHLH2	2.4	2.26E-02
ENSG00000185942	NKAIN3	2.0	4.65E-02
ENSG00000148826	NKX6-2	2.5	1.79E-02
ENSG00000022556	NLRP2	3.8	9.95E-04
ENSG00000123609	NMI	2.0	4.65E-02
ENSG00000053438	NNAT	-3.8	7.32E-04
ENSG00000166741	NNMT	3.0	6.22E-03
ENSG00000089250	NOS1	-2.6	1.46E-02
ENSG00000183793	NPIPA5	-2.4	2.70E-02
ENSG00000158806	NPM2	-2.4	2.31E-02
ENSG00000163273	NPPC	-2.4	3.15E-02
ENSG00000187258	NPSR1	2.3	4.19E-02
ENSG00000171246	NPTX1	-2.4	1.95E-02

ENSG00000221890	NPTXR	-2.1	3.63E-02
ENSG00000122585	NPY	2.6	1.72E-02
ENSG00000112333	NR2E1	3.4	3.70E-03
ENSG00000154146	NRGN	-2.1	3.82E-02
ENSG00000110076	NRXN2	-2.1	3.31E-02
ENSG00000168824	NSG1	-2.2	2.97E-02
ENSG00000170091	NSG2	-2.1	3.44E-02
ENSG00000143228	NUF2	2.4	1.87E-02
ENSG00000184923	NUTM2A	-2.2	4.48E-02
ENSG00000130950	NUTM2F	-2.8	1.45E-02
ENSG00000144227	NXPH2	-2.2	3.95E-02
ENSG00000182575	NXPH3	-2.7	1.15E-02
ENSG00000089127	OAS1	2.3	3.04E-02
ENSG00000111331	OAS3	3.3	2.62E-03
ENSG00000130558	OLFM1	-2.6	1.37E-02
ENSG00000125510	OPRL1	-2.2	3.15E-02
ENSG00000196071	OR2L13	3.2	4.47E-03
ENSG00000238243	OR2W3	2.2	4.74E-02
ENSG00000183444	OR7E38P	2.4	3.10E-02
ENSG00000145623	OSMR	2.6	1.36E-02
ENSG00000165899	OTOGL	2.8	1.12E-02
ENSG00000182447	OTOL1	-2.5	3.18E-02
ENSG00000115507	OTX1	2.5	2.14E-02
ENSG00000165588	OTX2	3.2	4.81E-03
ENSG00000083454	P2RX5	-2.7	1.63E-02
ENSG00000149380	P4HA3	2.2	3.71E-02
ENSG00000124507	PACSIN1	-2.7	1.15E-02
ENSG00000137843	PAK6	-2.7	1.17E-02
ENSG00000100767	PAPLN	2.7	1.37E-02
ENSG00000059378	PARP12	2.1	4.74E-02
ENSG00000173193	PARP14	2.0	4.64E-02
ENSG00000138964	PARVG	-2.5	3.26E-02
ENSG00000075891	PAX2	-3.3	2.78E-03
ENSG00000135903	PAX3	2.5	1.61E-02
ENSG00000125618	PAX8	-2.4	2.38E-02
ENSG00000250120	PCDHA10	2.2	3.59E-02
ENSG00000239389	PCDHA13	-2.7	1.64E-02
ENSG00000113248	PCDHB15	2.2	2.96E-02
ENSG00000255622	PCDHB17	2.3	3.00E-02
ENSG00000113209	PCDHB5	3.9	5.93E-04
ENSG00000253873	PCDHGA11	2.9	1.02E-02
ENSG00000254245	PCDHGA3	3.9	7.03E-04
ENSG00000248485	PCP4L1	-2.2	2.89E-02
ENSG00000102109	PCSK1N	-2.0	4.65E-02
ENSG00000197646	PDCD1LG2	2.2	4.27E-02

ENSG00000105650	PDE4C	-2.9	8.01E-03
ENSG00000134853	PDGFRA	2.0	4.83E-02
ENSG00000104213	PDGFRL	2.6	1.56E-02
ENSG00000185615	PDIA2	-3.0	4.78E-03
ENSG00000101327	PDYN	-2.8	1.07E-02
ENSG00000186862	PDZD7	-2.6	1.52E-02
ENSG00000187800	PEAR1	2.6	2.26E-02
ENSG00000154330	PGM5	2.2	3.62E-02
ENSG00000144824	PHLDB2	2.2	2.83E-02
ENSG00000109132	PHOX2B	-2.0	4.90E-02
ENSG00000175287	PHYHD1	2.2	4.30E-02
ENSG00000103335	PIEZO1	2.4	2.02E-02
ENSG00000167103	PIP5KL1	-2.1	3.69E-02
ENSG00000181191	PJA1	-2.0	4.79E-02
ENSG00000254681	PKD1P5	3.3	3.21E-03
ENSG00000188257	PLA2G2A	2.4	3.84E-02
ENSG00000122861	PLAU	2.6	1.27E-02
ENSG00000121316	PLBD1	2.6	1.93E-02
ENSG00000152952	PLOD2	2.1	3.48E-02
ENSG00000102007	PLP2	2.1	3.51E-02
ENSG00000004399	PLXND1	2.7	9.40E-03
ENSG00000141682	PMAIP1	2.2	3.56E-02
ENSG00000130822	PNCK	-2.6	1.31E-02
ENSG00000198883	PNMA5	-2.7	1.23E-02
ENSG00000257088	PNMA6D	-2.7	2.29E-02
ENSG00000128567	PODXL	2.2	2.93E-02
ENSG00000051341	POLQ	2.5	1.86E-02
ENSG00000205578	POM121B	2.6	2.17E-02
ENSG00000177380	PPFIA3	-2.1	3.41E-02
ENSG00000088808	PPP1R13B	-2.2	3.15E-02
ENSG00000101445	PPP1R16B	-2.4	2.25E-02
ENSG00000225361	PPP1R26-AS1	-2.5	1.69E-02
ENSG00000074211	PPP2R2C	-2.7	9.97E-03
ENSG00000214140	PRCD	-2.1	4.41E-02
ENSG00000046889	PREX2	2.1	4.02E-02
ENSG00000126583	PRKCG	-2.4	2.21E-02
ENSG00000067606	PRKCZ	-2.0	4.30E-02
ENSG00000171864	PRND	2.7	1.65E-02
ENSG00000143125	PROK1	-3.2	5.49E-03
ENSG00000007062	PROM1	2.1	3.85E-02
ENSG00000135406	PRPH	2.7	1.10E-02
ENSG00000112619	PRPH2	-3.1	6.54E-03
ENSG00000186654	PRR5	-2.0	4.84E-02
ENSG00000224940	PRRT4	-2.7	1.09E-02
ENSG00000059915	PSD	-2.1	3.80E-02

ENSG00000146005	PSD2	-2.0	4.91E-02
ENSG00000204264	PSMB8	2.3	2.45E-02
ENSG00000240065	PSMB9	3.0	6.83E-03
ENSG00000165983	PTER	2.4	2.73E-02
ENSG00000107317	PTGDS	3.1	4.53E-03
ENSG00000160951	PTGER1	2.9	9.19E-03
ENSG00000152104	PTPN14	2.1	3.36E-02
ENSG00000110786	PTPN5	-2.4	2.08E-02
ENSG00000155093	PTPRN2	-2.5	1.74E-02
ENSG00000139304	PTPRQ	2.4	3.89E-02
ENSG00000196090	PTPRT	3.7	1.03E-03
ENSG00000139832	RAB20	2.4	2.43E-02
ENSG00000134594	RAB33A	-2.0	4.14E-02
ENSG00000105649	RAB3A	-2.2	2.80E-02
ENSG00000169213	RAB3B	-2.0	4.48E-02
ENSG00000122679	RAMP3	2.5	2.13E-02
ENSG00000111344	RASAL1	-2.4	2.98E-02
ENSG00000100302	RASD2	-2.3	2.40E-02
ENSG00000146090	RASGEF1C	-2.8	8.44E-03
ENSG00000058335	RASGRF1	-2.7	1.02E-02
ENSG00000068831	RASGRP2	-2.4	2.06E-02
ENSG00000198774	RASSF9	3.1	4.26E-03
ENSG00000167281	RBFOX3	-2.9	6.30E-03
ENSG00000138207	RBP4	-2.9	9.34E-03
ENSG00000115386	REG1A	-3.2	6.79E-03
ENSG00000225465	RFPL1S	-2.0	4.75E-02
ENSG00000128253	RFPL2	-2.2	3.70E-02
ENSG00000090104	RGS1	2.4	3.95E-02
ENSG00000132554	RGS22	2.3	3.07E-02
ENSG00000104140	RHOV	-2.4	2.31E-02
ENSG00000101098	RIMS4	-2.3	2.39E-02
ENSG00000183421	RIPK4	2.5	2.63E-02
ENSG00000152214	RIT2	-2.8	1.07E-02
ENSG00000159753	RLTPR	-2.7	1.01E-02
ENSG00000249803	RP11-114H21.2	3.1	8.90E-03
ENSG00000259280	RP11-122D10.1	-3.2	6.23E-03
ENSG00000273238	RP11-1263C18.1	-2.5	2.19E-02
ENSG00000178715	RP11-169K16.8	-2.5	2.32E-02
ENSG00000259234	RP11-17L5.4	-2.4	4.13E-02
ENSG00000269916	RP11-193M21.1	2.3	4.11E-02
ENSG00000187186	RP11-195F19.5	-2.6	1.86E-02
ENSG00000261829	RP11-223I10.1	-2.3	2.94E-02
ENSG00000203900	RP11-261N11.8	-2.9	1.21E-02
ENSG00000234531	RP11-288G11.3	2.7	1.44E-02
ENSG00000215146	RP11-313J2.1	3.6	2.25E-03

ENSG00000226530	RP11-348F1.2	2.6	2.81E-02
ENSG00000226425	RP11-348J12.2	-2.6	2.76E-02
ENSG00000271369	RP11-350D17.3	-2.1	4.67E-02
ENSG00000203688	RP11-351J23.1	2.7	1.17E-02
ENSG00000235531	RP11-383H13.1	3.0	7.77E-03
ENSG00000264745	RP11-403A21.2	-2.4	4.20E-02
ENSG00000261003	RP1-140C12.2	-2.6	2.64E-02
ENSG00000273108	RP11-416N2.4	-2.4	2.09E-02
ENSG00000242512	RP11-416O18.1	2.5	3.08E-02
ENSG00000260987	RP11-423G4.7	-2.2	3.37E-02
ENSG00000215866	RP11-426L16.8	-2.6	2.80E-02
ENSG00000254973	RP11-429J17.7	-2.4	3.77E-02
ENSG00000259577	RP11-430B1.2	-2.7	1.58E-02
ENSG00000132832	RP11-445H22.3	-2.3	3.99E-02
ENSG00000244558	RP11-445H22.4	-2.5	2.68E-02
ENSG00000266045	RP11-466P24.7	-2.1	4.12E-02
ENSG00000242828	RP11-47P18.1	-2.4	4.45E-02
ENSG00000260769	RP11-491F9.5	-2.5	3.64E-02
ENSG00000206113	RP11-503N18.1	2.7	1.52E-02
ENSG00000249428	RP11-503N18.3	2.3	4.32E-02
ENSG00000213642	RP11-561N12.5	-2.1	4.12E-02
ENSG00000273087	RP11-566J3.4	-2.4	2.42E-02
ENSG00000257499	RP11-571M6.8	-2.4	2.33E-02
ENSG00000269975	RP11-58B17.2	-2.5	1.54E-02
ENSG00000261374	RP11-64K12.10	-2.1	4.04E-02
ENSG00000254682	RP11-660L16.2	-2.2	3.40E-02
ENSG00000260081	RP11-66N11.8	-2.1	4.33E-02
ENSG00000268555	RP11-678G14.3	2.4	4.29E-02
ENSG00000273456	RP11-686O6.2	-2.4	2.67E-02
ENSG00000234449	RP11-706O15.3	-3.1	4.16E-03
ENSG00000271474	RP11-710C12.1	-2.5	2.26E-02
ENSG00000251129	RP11-734I18.1	-3.7	1.24E-03
ENSG00000254349	RP11-758M4.1	2.3	3.96E-02
ENSG00000253706	RP11-758M4.4	2.1	4.96E-02
ENSG00000266970	RP11-806H10.4	2.5	2.87E-02
ENSG00000266456	RP11-806L2.2	-2.2	4.71E-02
ENSG00000257935	RP11-82C23.2	-2.2	3.61E-02
ENSG00000250138	RP11-848G14.5	2.6	2.46E-02
ENSG00000254510	RP11-867G23.10	-2.0	4.87E-02
ENSG00000262222	RP11-876N24.4	2.8	1.73E-02
ENSG00000259439	RP11-89K21.1	2.5	2.91E-02
ENSG00000250546	RP11-8L2.1	2.5	3.61E-02
ENSG00000267651	RP11-95O2.1	-2.6	1.77E-02
ENSG00000228659	RP1-23K20.2	-2.8	1.71E-02
ENSG00000233508	RP1-269M15.3	2.4	4.44E-02

ENSG00000243902	RP1-63G5.5	-2.3	3.59E-02
ENSG00000227012	RP1-97J1.2	-2.7	2.36E-02
ENSG00000234546	RP3-510D11.2	-2.6	2.26E-02
ENSG00000261675	RP5-1119A7.17	-2.6	1.41E-02
ENSG00000225988	RP5-1119D9.4	-2.3	4.63E-02
ENSG00000231302	RPL36P2	-2.7	2.35E-02
ENSG00000177519	RPRM	-2.2	3.18E-02
ENSG00000198208	RPS6KL1	-2.1	3.94E-02
ENSG00000132026	RTBDN	-2.8	1.07E-02
ENSG00000139970	RTN1	-2.0	4.51E-02
ENSG00000159216	RUNX1	2.2	3.35E-02
ENSG00000196218	RYR1	-2.2	3.32E-02
ENSG00000164483	SAMD3	-2.4	2.87E-02
ENSG00000205413	SAMD9	2.9	7.25E-03
ENSG00000177409	SAMD9L	2.7	1.18E-02
ENSG00000164764	SBSPON	2.5	1.57E-02
ENSG00000198794	SCAMP5	-2.0	4.05E-02
ENSG00000159307	SCUBE1	-2.6	1.46E-02
ENSG00000167680	SEMA6B	-2.4	1.88E-02
ENSG00000250722	SEPP1	2.4	2.10E-02
ENSG00000188488	SERPINA5	2.7	1.23E-02
ENSG00000106366	SERPINE1	3.5	1.63E-03
ENSG00000180440	SERTM1	-2.3	2.86E-02
ENSG00000063015	SEZ6	-2.0	4.87E-02
ENSG00000174938	SEZ6L2	-2.3	2.21E-02
ENSG00000120057	SFRP5	-2.6	1.83E-02
ENSG00000129810	SGOL1	2.1	3.81E-02
ENSG00000163535	SGOL2	2.0	4.46E-02
ENSG00000125731	SH2D3A	-3.2	5.10E-03
ENSG00000104611	SH2D4A	2.5	2.43E-02
ENSG00000189410	SH2D5	-2.0	4.57E-02
ENSG00000156463	SH3RF2	2.4	3.15E-02
ENSG00000161681	SHANK1	-2.6	1.32E-02
ENSG00000072858	SIDT1	-2.4	2.62E-02
ENSG00000126778	SIX1	3.1	4.91E-03
ENSG00000138083	SIX3	2.4	2.97E-02
ENSG00000100625	SIX4	2.7	1.27E-02
ENSG00000124140	SLC12A5	-2.3	2.41E-02
ENSG00000141526	SLC16A3	2.8	1.04E-02
ENSG00000168679	SLC16A4	2.4	1.99E-02
ENSG00000187714	SLC18A3	-2.4	2.08E-02
ENSG00000106688	SLC1A1	-2.0	4.92E-02
ENSG00000105143	SLC1A6	-2.7	9.60E-03
ENSG00000197847	SLC22A20	-2.2	4.52E-02
ENSG00000185052	SLC24A3	-2.3	2.40E-02

ENSG00000181240	SLC25A41	-2.7	1.36E-02
ENSG00000147606	SLC26A7	2.5	2.17E-02
ENSG00000115194	SLC30A3	-2.7	1.40E-02
ENSG00000164756	SLC30A8	-3.6	1.57E-03
ENSG00000151812	SLC35F4	-2.9	7.76E-03
ENSG00000138449	SLC40A1	2.0	4.55E-02
ENSG00000162426	SLC45A1	-2.1	3.97E-02
ENSG00000115665	SLC5A7	-2.2	3.80E-02
ENSG00000197106	SLC6A17	-2.8	8.76E-03
ENSG00000165970	SLC6A5	-3.7	1.44E-03
ENSG00000011083	SLC6A7	-3.4	2.45E-03
ENSG00000151012	SLC7A11	2.1	4.04E-02
ENSG00000099960	SLC7A4	-2.4	2.44E-02
ENSG00000118160	SLC8A2	-2.4	2.13E-02
ENSG00000100678	SLC8A3	-2.2	3.00E-02
ENSG00000101187	SLCO4A1	-2.4	2.44E-02
ENSG00000172716	SLFN11	3.1	4.79E-03
ENSG00000113810	SMC4	2.2	2.96E-02
ENSG00000204323	SMIM5	2.7	1.44E-02
ENSG00000188176	SMTNL2	-2.9	7.87E-03
ENSG00000145335	SNCA	-2.4	1.79E-02
ENSG00000074317	SNCB	-3.1	4.07E-03
ENSG00000173267	SNCG	-2.9	7.17E-03
ENSG00000172803	SNX32	-2.3	2.39E-02
ENSG00000184557	SOCS3	2.4	1.85E-02
ENSG00000108018	SORCS1	3.3	2.59E-03
ENSG00000198944	SOWAHA	-2.5	1.90E-02
ENSG00000100146	SOX10	3.1	7.00E-03
ENSG00000203883	SOX18	2.4	2.78E-02
ENSG00000067066	SP100	2.5	1.93E-02
ENSG00000077327	SPAG6	2.9	7.05E-03
ENSG00000185594	SPATA8	-2.4	4.13E-02
ENSG00000167642	SPINT2	-2.4	2.08E-02
ENSG00000183018	SPNS2	-2.4	2.12E-02
ENSG00000134668	SPOCD1	3.2	4.56E-03
ENSG00000244094	SPRR2F	-2.7	2.02E-02
ENSG00000070182	SPTB	-2.4	2.08E-02
ENSG00000160460	SPTBN4	-2.2	3.06E-02
ENSG00000157005	SST	-3.0	5.42E-03
ENSG00000139874	SSTR1	-2.2	2.98E-02
ENSG00000147488	ST18	2.0	4.95E-02
ENSG00000070731	ST6GALNAC2	3.0	7.64E-03
ENSG00000081320	STK17B	2.1	4.36E-02
ENSG00000250535	STK19P	-2.9	1.41E-02
ENSG00000104435	STMN2	-2.0	4.64E-02

ENSG00000015592	STMN4	-2.3	2.58E-02
ENSG00000133115	STOML3	3.2	3.69E-03
ENSG00000099365	STX1B	-2.3	2.44E-02
ENSG00000136854	STXBP1	-2.0	4.84E-02
ENSG00000060140	STYK1	-2.6	1.58E-02
ENSG00000159164	SV2A	-2.0	4.28E-02
ENSG00000166111	SVOP	-2.2	3.23E-02
ENSG00000008056	SYN1	-2.1	3.41E-02
ENSG00000157152	SYN2	-2.4	2.07E-02
ENSG00000100321	SYNGR1	-2.1	3.96E-02
ENSG00000127561	SYNGR3	-2.8	9.11E-03
ENSG00000102003	SYP	-2.7	1.09E-02
ENSG00000173227	SYT12	-2.6	1.34E-02
ENSG00000213023	SYT3	-3.2	3.41E-03
ENSG00000132872	SYT4	-2.1	3.55E-02
ENSG00000129990	SYT5	-2.6	1.28E-02
ENSG00000134207	SYT6	-2.3	2.40E-02
ENSG00000011347	SYT7	-2.7	9.91E-03
ENSG00000006128	TAC1	-2.2	3.19E-02
ENSG00000204261	TAPSAR1	2.3	3.74E-02
ENSG00000133138	TBC1D8B	2.8	9.63E-03
ENSG00000121068	TBX2	2.3	3.10E-02
ENSG00000204065	TCEAL5	-2.0	4.78E-02
ENSG00000176769	TCERG1L	2.8	1.53E-02
ENSG00000152760	TCTEX1D1	3.2	3.74E-03
ENSG00000151790	TDO2	2.6	2.58E-02
ENSG00000167858	TEKT1	2.8	9.94E-03
ENSG00000138336	TET1	2.2	2.87E-02
ENSG00000087510	TFAP2C	2.2	3.22E-02
ENSG00000120708	TGFBI	3.0	5.10E-03
ENSG00000198959	TGM2	3.5	2.01E-03
ENSG00000137801	THBS1	2.2	3.26E-02
ENSG00000186340	THBS2	2.1	3.82E-02
ENSG00000065717	TLE2	-2.2	2.87E-02
ENSG00000174130	TLR6	2.5	3.05E-02
ENSG00000107807	TLX1	-3.6	1.79E-03
ENSG00000236311	TLX1NB	-3.0	1.20E-02
ENSG00000169908	TM4SF1	2.6	1.90E-02
ENSG00000135926	TMBIM1	2.0	4.25E-02
ENSG00000166448	TMEM130	-2.0	4.14E-02
ENSG00000181234	TMEM132C	3.0	6.04E-03
ENSG00000167619	TMEM145	-2.6	1.45E-02
ENSG00000179292	TMEM151A	-2.8	7.64E-03
ENSG00000258986	TMEM179	-2.4	1.87E-02
ENSG00000226287	TMEM191A	-3.2	5.08E-03

ENSG00000206140	TMEM191C	-2.4	3.33E-02
ENSG00000135048	TMEM2	2.0	4.45E-02
ENSG00000187824	TMEM220	2.5	2.23E-02
ENSG00000198133	TMEM229B	-2.2	3.30E-02
ENSG00000214597	TMEM249	-2.4	3.38E-02
ENSG00000105696	TMEM59L	-2.3	2.63E-02
ENSG00000125895	TMEM74B	-3.1	4.49E-03
ENSG00000176040	TMPRSS7	2.1	4.85E-02
ENSG00000187653	TMSB4XP8	-2.0	4.39E-02
ENSG00000173535	TNFRSF10C	-2.2	4.25E-02
ENSG00000028137	TNFRSF1B	3.2	5.67E-03
ENSG00000000005	TNMD	-2.3	2.84E-02
ENSG00000159173	TNNI1	-2.4	3.22E-02
ENSG00000118194	TNNT2	-2.8	1.40E-02
ENSG00000130595	TNNT3	-2.6	2.46E-02
ENSG00000131747	TOP2A	2.3	2.37E-02
ENSG00000261594	TPBGL	-2.3	3.63E-02
ENSG00000159713	TPPP3	2.6	1.40E-02
ENSG00000132481	TRIM47	2.2	2.77E-02
ENSG00000162722	TRIM58	2.9	8.55E-03
ENSG00000213186	TRIM59	2.2	2.99E-02
ENSG00000146054	TRIM7	-2.6	1.92E-02
ENSG00000187688	TRPV2	-3.1	6.52E-03
ENSG00000175513	TSGA10IP	-2.3	4.83E-02
ENSG00000156298	TSPAN7	-2.6	1.14E-02
ENSG00000235890	TSPEAR-AS1	-2.2	4.97E-02
ENSG00000184205	TSPYL2	-2.1	3.85E-02
ENSG00000180543	TSPYL5	3.8	1.25E-03
ENSG00000174521	TTC9B	-2.7	9.29E-03
ENSG00000112742	TTK	2.4	2.22E-02
ENSG00000104833	TUBB4A	-2.4	2.07E-02
ENSG00000117289	TXNIP	2.3	2.65E-02
ENSG00000197355	UAP1L1	2.0	4.51E-02
ENSG00000130477	UNC13A	-2.0	4.66E-02
ENSG00000113763	UNC5A	-2.7	1.20E-02
ENSG00000049247	UTS2	-2.4	3.02E-02
ENSG00000171724	VAT1L	-2.2	2.85E-02
ENSG00000148704	VAX1	3.6	1.75E-03
ENSG00000128564	VGF	-2.4	2.01E-02
ENSG00000106018	VIPR2	-3.0	8.51E-03
ENSG00000163032	VSNL1	-2.7	1.11E-02
ENSG00000187135	VSTM2B	-2.6	1.56E-02
ENSG00000168658	VWA3B	2.1	4.68E-02
ENSG00000145198	VWA5B2	-3.0	5.84E-03
ENSG00000225373	WASH5P	2.4	3.68E-02

ENSG00000166596	WDR16	2.4	2.32E-02
ENSG00000136918	WDR38	2.8	9.14E-03
ENSG00000174776	WDR49	2.0	4.82E-02
ENSG00000197748	WDR96	2.3	2.28E-02
ENSG00000156076	WIF1	-2.7	1.91E-02
ENSG00000169884	WNT10B	-2.2	3.65E-02
ENSG00000162552	WNT4	-2.5	1.50E-02
ENSG00000143184	XCL1	-3.3	3.83E-03
ENSG00000229807	XIST	3.6	1.76E-03
ENSG00000047597	XK	-2.2	3.07E-02
ENSG00000272501	XXbac-BPG299F13.17	-2.1	3.80E-02
ENSG00000137693	YAP1	2.1	3.76E-02
ENSG00000006047	YBX2	-2.4	2.45E-02
ENSG00000257315	ZBED6	2.3	2.79E-02
ENSG00000188707	ZBED6CL	-2.0	4.90E-02
ENSG00000181722	ZBTB20	2.3	3.23E-02
ENSG00000174460	ZCCHC12	-2.8	7.47E-03
ENSG00000166707	ZCCHC18	-2.2	3.18E-02
ENSG00000180787	ZFP3	2.8	7.94E-03
ENSG00000152518	ZFP36L2	2.0	4.26E-02
ENSG00000105278	ZFR2	-2.5	1.82E-02
ENSG00000004838	ZMYND10	2.1	3.73E-02
ENSG00000196247	ZNF107	2.0	4.29E-02
ENSG00000167383	ZNF229	3.9	8.07E-04
ENSG00000256771	ZNF253	3.5	1.75E-03
ENSG00000197935	ZNF311	3.1	6.57E-03
ENSG00000177932	ZNF354C	2.6	1.45E-02
ENSG00000187595	ZNF385C	-2.1	4.05E-02
ENSG00000197714	ZNF460	2.2	3.83E-02
ENSG00000196263	ZNF471	3.5	2.80E-03
ENSG00000164185	ZNF474	2.2	3.38E-02
ENSG00000256229	ZNF486	3.7	1.28E-03
ENSG00000196268	ZNF493	2.5	1.67E-02
ENSG00000081665	ZNF506	3.8	9.14E-04
ENSG00000198028	ZNF560	2.4	2.55E-02
ENSG00000258405	ZNF578	3.7	1.52E-03
ENSG00000245680	ZNF585B	2.6	1.42E-02
ENSG00000188171	ZNF626	3.8	9.36E-04
ENSG00000160229	ZNF66	2.4	3.25E-02
ENSG00000198046	ZNF667	3.7	1.20E-03
ENSG00000166770	ZNF667-AS1	3.5	2.98E-03
ENSG00000197928	ZNF677	3.8	1.15E-03
ENSG00000173041	ZNF680	2.5	1.77E-02
ENSG00000197124	ZNF682	2.3	2.56E-02
ENSG00000213967	ZNF726	3.1	6.49E-03

ENSG00000186777	ZNF732	2.8	1.51E-02
ENSG00000237440	ZNF737	3.3	3.02E-03
ENSG00000231205	ZNF826P	2.9	1.20E-02
ENSG00000185869	ZNF829	3.4	2.44E-03
ENSG00000257446	ZNF878	2.6	2.60E-02
ENSG00000213988	ZNF90	3.0	1.11E-02
ENSG00000184635	ZNF93	3.6	1.60E-03
ENSG00000188372	ZP3	-2.7	1.47E-02

6. REFERENCES

1. Sullivan, P.F., K.S. Kendler, and M.C. Neale, *Schizophrenia as a complex trait: evidence from a meta-analysis of twin studies.* Arch Gen Psychiatry, 2003. 60(12): p. 1187-92.
2. van Os, J., B.P. Rutten, and R. Poulton, *Gene-environment interactions in schizophrenia: review of epidemiological findings and future directions.* Schizophr Bull, 2008. 34(6): p. 1066-82.
3. Organization, W.H., *The Global Burden of Disease: 2004 Update*. 2008, WHO Press.
4. Knapp, M., R. Mangalore, and J. Simon, *The global costs of schizophrenia.* Schizophr Bull, 2004. 30(2): p. 279-93.
5. Saha, S., D. Chant, and J. McGrath, *A systematic review of mortality in schizophrenia: is the differential mortality gap worsening over time?* Arch Gen Psychiatry, 2007. 64(10): p. 1123-31.
6. Schultz, S.H., S.W. North, and C.G. Shields, *Schizophrenia: a review.* Am Fam Physician, 2007. 75(12): p. 1821-9.
7. Hafner, H., *Gender differences in schizophrenia.* Psychoneuroendocrinology, 2003. 28 Suppl 2: p. 17-54.
8. Dean, L., *Schizophrenia*, in *Medical Genetics Summaries*, V. Pratt, et al., Editors. 2012, National Center for Biotechnology Information (US): Bethesda (MD).
9. Barch, D.M. and A. Ceaser, *Cognition in Schizophrenia: Core Psychological and Neural Mechanisms.* Trends Cogn Sci, 2012. 16(1).
10. Smieskova, R., et al., *Do Subjects at Clinical High Risk for Psychosis Differ from those with a Genetic High Risk? – A Systematic Review of Structural and Functional Brain Abnormalities.* Curr Med Chem, 2013. 20(3): p. 467-81.
11. Bleuler, E., *Dementia Praecox oder Gruppe der Schizophrenien*. 1911, Leipzig, Germany: Deuticke.
12. Arieti, S., *Interpretation of Schizophrenia*. 1974: Basic Books.
13. Carlsson, A., *The current status of the dopamine hypothesis of schizophrenia.* Neuropsychopharmacology, 1988. 1(3): p. 179-86.
14. Bjorklund, A. and S.B. Dunnett, *Dopamine neuron systems in the brain: an update.* Trends Neurosci, 2007. 30(5): p. 194-202.
15. Shen, L.H., M.H. Liao, and Y.C. Tseng, *Recent advances in imaging of dopaminergic neurons for evaluation of neuropsychiatric disorders.* J Biomed Biotechnol, 2012. 2012: p. 259349.
16. Goldman-Rakic, P.S., et al., *Targeting the dopamine D1 receptor in schizophrenia: insights for cognitive dysfunction.* Psychopharmacology (Berl), 2004. 174(1): p. 3-16.
17. Takahashi, H., *PET neuroimaging of extrastriatal dopamine receptors and prefrontal cortex functions.* J Physiol Paris, 2013. 107(6): p. 503-9.
18. Coyle, J.T., *Glutamate and schizophrenia: beyond the dopamine hypothesis.* Cell Mol Neurobiol, 2006. 26(4-6): p. 365-84.
19. Javitt, D.C., *Negative schizophrenic symptomatology and the PCP (phencyclidine) model of schizophrenia.* Hillside J Clin Psychiatry, 1987. 9(1): p. 12-35.
20. Javitt, D.C. and S.R. Zukin, *Recent advances in the phencyclidine model of schizophrenia.* Am J Psychiatry, 1991. 148(10): p. 1301-8.
21. Lewis, D.A. and B. Moghaddam, *Cognitive dysfunction in schizophrenia: convergence of gamma-aminobutyric acid and glutamate alterations.* Arch Neurol, 2006. 63(10): p. 1372-6.
22. Yoon, J.H., et al., *GABA concentration is reduced in visual cortex in schizophrenia and correlates with orientation-specific surround suppression.* J Neurosci, 2010. 30(10): p. 3777-81.
23. Nakazawa, K., et al., *GABAergic interneuron origin of schizophrenia pathophysiology.* Neuropharmacology, 2012. 62(3): p. 1574-1583.
24. Insel, T.R., *Rethinking schizophrenia.* Nature, 2010. 468(7321): p. 187-93.

25. Susser, E.S. and S.P. Lin, *Schizophrenia after prenatal exposure to the Dutch Hunger Winter of 1944-1945.* Arch Gen Psychiatry, 1992. 49(12): p. 983-8.
26. St Clair, D., et al., *Rates of adult schizophrenia following prenatal exposure to the Chinese famine of 1959-1961.* Jama, 2005. 294(5): p. 557-62.
27. Brown, A.S. and E.J. Derkits, *Prenatal infection and schizophrenia: a review of epidemiologic and translational studies.* Am J Psychiatry, 2010. 167(3): p. 261-80.
28. Cannon, M., P.B. Jones, and R.M. Murray, *Obstetric complications and schizophrenia: historical and meta-analytic review.* Am J Psychiatry, 2002. 159(7): p. 1080-92.
29. Khashan, A.S., et al., *Higher risk of offspring schizophrenia following antenatal maternal exposure to severe adverse life events.* Arch Gen Psychiatry, 2008. 65(2): p. 146-52.
30. Mednick, S.A., M.O. Huttunen, and R.A. Machon, *Prenatal influenza infections and adult schizophrenia.* Schizophr Bull, 1994. 20(2): p. 263-7.
31. Boin, F., et al., *Association between -G308A tumor necrosis factor alpha gene polymorphism and schizophrenia.* Mol Psychiatry, 2001. 6(1): p. 79-82.
32. Ashdown, H., et al., *The role of cytokines in mediating effects of prenatal infection on the fetus: implications for schizophrenia.* Mol Psychiatry, 2006. 11(1): p. 47-55.
33. Deverman, B.E. and P.H. Patterson, *Cytokines and CNS development.* Neuron, 2009. 64(1): p. 61-78.
34. Byrne, M., et al., *Obstetric conditions and risk of first admission with schizophrenia: a Danish national register based study.* Schizophr Res, 2007. 97(1-3): p. 51-9.
35. Henquet, C., et al., *The environment and schizophrenia: the role of cannabis use.* Schizophr Bull, 2005. 31(3): p. 608-12.
36. Moore, T.H., et al., *Cannabis use and risk of psychotic or affective mental health outcomes: a systematic review.* Lancet, 2007. 370(9584): p. 319-28.
37. Sorensen, H.J., et al., *Early developmental milestones and risk of schizophrenia: a 45-year follow-up of the Copenhagen Perinatal Cohort.* Schizophr Res, 2010. 118(1-3): p. 41-7.
38. Jones, P., et al., *Child development risk factors for adult schizophrenia in the British 1946 birth cohort.* Lancet, 1994. 344(8934): p. 1398-402.
39. Mortensen, P.B., et al., *Effects of family history and place and season of birth on the risk of schizophrenia.* N Engl J Med, 1999. 340(8): p. 603-8.
40. March, D., et al., *Psychosis and place.* Epidemiol Rev, 2008. 30: p. 84-100.
41. Boydell, J., et al., *Incidence of schizophrenia in ethnic minorities in London: ecological study into interactions with environment.* Bmj, 2001. 323(7325): p. 1336-8.
42. Selemon, L.D. and N. Zecevic, *Schizophrenia: a tale of two critical periods for prefrontal cortical development.* Translational Psychiatry, 2015. 5(8): p. e623.
43. Johnstone, E.C., et al., *Cerebral ventricular size and cognitive impairment in chronic schizophrenia.* Lancet, 1976. 2(7992): p. 924-6.
44. Wright, I.C., et al., *Meta-analysis of regional brain volumes in schizophrenia.* Am J Psychiatry, 2000. 157(1): p. 16-25.
45. Olabi, B., et al., *Are there progressive brain changes in schizophrenia? A meta-analysis of structural magnetic resonance imaging studies.* Biol Psychiatry, 2011. 70(1): p. 88-96.
46. Harrison, P.J., N. Freemantle, and J.R. Geddes, *Meta-analysis of brain weight in schizophrenia.* Schizophr Res, 2003. 64(1): p. 25-34.
47. Gogtay, N., et al., *Comparison of progressive cortical gray matter loss in childhood-onset schizophrenia with that in childhood-onset atypical psychoses.* Arch Gen Psychiatry, 2004. 61(1): p. 17-22.
48. Arnold, S.J.M., et al., *Hippocampal Volume Is Reduced in Schizophrenia and Schizoaffective Disorder But Not in Psychotic Bipolar I Disorder Demonstrated by Both Manual Tracing and Automated Parcellation (FreeSurfer).* Schizophrenia Bulletin, 2015. 41(1): p. 233-249.

49. Crow, T.J., et al., *Schizophrenia as an anomaly of development of cerebral asymmetry. A postmortem study and a proposal concerning the genetic basis of the disease.* Arch Gen Psychiatry, 1989. 46(12): p. 1145-50.
50. Palaniyappan, L., et al., *Abnormalities in structural covariance of cortical gyrification in schizophrenia.* Brain Struct Funct, 2015. 220(4): p. 2059-71.
51. Faludi, G. and K. Mirnics, *Synaptic changes in the brain of subjects with schizophrenia.* Int J Dev Neurosci, 2011. 29(3): p. 305-9.
52. Arnold s, E., et al., *Some cytoarchitectural abnormalities of the entorhinal cortex in schizophrenia.* Archives of General Psychiatry, 1991. 48(7): p. 625-632.
53. Akbarian, S., et al., *Maldistribution of interstitial neurons in prefrontal white matter of the brains of schizophrenic patients.* Arch Gen Psychiatry, 1996. 53(5): p. 425-36.
54. Stolp, H.B., et al., *Reduced ventricular proliferation in the foetal cortex following maternal inflammation in the mouse.* Brain, 2011. 134(Pt 11): p. 3236-48.
55. Brennand, K., et al., *Phenotypic differences in hiPSC NPCs derived from patients with schizophrenia.* Mol Psychiatry, 2015. 20(3): p. 361-8.
56. Yoon, K.J., et al., *Modeling a genetic risk for schizophrenia in iPSCs and mice reveals neural stem cell deficits associated with adherens junctions and polarity.* Cell Stem Cell, 2014. 15(1): p. 79-91.
57. Pedrosa, E., et al., *Development of patient-specific neurons in schizophrenia using induced pluripotent stem cells.* J Neurogenet, 2011. 25(3): p. 88-103.
58. Robicsek, O., et al., *Abnormal neuronal differentiation and mitochondrial dysfunction in hair follicle-derived induced pluripotent stem cells of schizophrenia patients.* Mol Psychiatry, 2013. 18(10): p. 1067-76.
59. Eastwood, S.L. and P.J. Harrison, *Decreased synaptophysin in the medial temporal lobe in schizophrenia demonstrated using immunoautoradiography.* Neuroscience, 1995. 69(2): p. 339-343.
60. Perrone-Bizzozero N , I., *Levels of the growth-associated protein GAP-43 are.* 1996. 93(24): p. 14182-7.
61. Fatemi, S.H., et al., *Altered levels of the synaptosomal associated protein SNAP-25 in hippocampus of subjects with mood disorders and schizophrenia.* Neuroreport, 2001. 12(15): p. 3257-62.
62. Selemon, L.D. and P.S. Goldman-Rakic, *The reduced neuropil hypothesis: a circuit based model of schizophrenia.* Biol Psychiatry, 1999. 45(1): p. 17-25.
63. Black, J.E., et al., *Pathology of layer V pyramidal neurons in the prefrontal cortex of patients with schizophrenia.* Am J Psychiatry, 2004. 161(4): p. 742-4.
64. Broadbelt, K., W. Byne, and L.B. Jones, *Evidence for a decrease in basilar dendrites of pyramidal cells in schizophrenic medial prefrontal cortex.* Schizophr Res, 2002. 58(1): p. 75-81.
65. Kalus, P., et al., *The dendritic architecture of prefrontal pyramidal neurons in schizophrenic patients.* Neuroreport, 2000. 11(16): p. 3621-5.
66. Glantz, L.A. and D.A. Lewis, *Decreased dendritic spine density on prefrontal cortical pyramidal neurons in schizophrenia.* Arch Gen Psychiatry, 2000. 57(1): p. 65-73.
67. Rajkowska, G., L.D. Selemon, and P.S. Goldman-Rakic, *Neuronal and glial somal size in the prefrontal cortex: A postmortem morphometric study of schizophrenia and huntington disease.* Archives of General Psychiatry, 1998. 55(3): p. 215-224.
68. Brennand, K.J., et al., *Modelling schizophrenia using human induced pluripotent stem cells.* Nature, 2011. 473(7346): p. 221-5.
69. Feinberg, I., *Schizophrenia: caused by a fault in programmed synaptic elimination during adolescence?* J Psychiatr Res, 1982. 17(4): p. 319-34.
70. Mirnics, K., et al., *Analysis of complex brain disorders with gene expression microarrays: schizophrenia as a disease of the synapse.* Trends Neurosci, 2001. 24(8): p. 479-86.
71. Das, D.K., et al., *Genetic and morphological features of human iPSC-derived neurons with chromosome 15q11.2 (BP1-BP2) deletions.* Mol Neuropsychiatry, 2015. 1(2): p. 116-123.

72. Frankle, W.G., J. Lerma, and M. Laruelle, *The Synaptic Hypothesis of Schizophrenia.* Neuron, 2003. 39(2): p. 205-216.
73. Fillman, S.G., et al., *Increased inflammatory markers identified in the dorsolateral prefrontal cortex of individuals with schizophrenia.* Mol Psychiatry, 2013. 18(2): p. 206-14.
74. Radewicz, K., et al., *Increase in HLA-DR immunoreactive microglia in frontal and temporal cortex of chronic schizophrenics.* J Neuropathol Exp Neurol, 2000. 59(2): p. 137-50.
75. Miller, B.J., et al., *Meta-analysis of cytokine alterations in schizophrenia: clinical status and antipsychotic effects.* Biol Psychiatry, 2011. 70(7): p. 663-71.
76. Kety, S.S., *The significance of genetic factors in the etiology of schizophrenia: results from the national study of adoptees in Denmark.* J Psychiatr Res, 1987. 21(4): p. 423-9.
77. McGuffin, P. and Gottesman, II, *Risk factors for schizophrenia.* N Engl J Med, 1999. 341(5): p. 370-1; author reply 372.
78. Cardno, A.G., et al., *Heritability estimates for psychotic disorders: the Maudsley twin psychosis series.* Arch Gen Psychiatry, 1999. 56(2): p. 162-8.
79. Gratten, J., et al., *Large-scale genomics unveils the genetic architecture of psychiatric disorders.* Nat Neurosci, 2014. 17(6): p. 782-790.
80. Schizophrenia Working Group of the Psychiatric Genomics, C., *Biological insights from 108 schizophrenia-associated genetic loci.* Nature, 2014. 511(7510): p. 421-7.
81. Walsh, T., et al., *Rare structural variants disrupt multiple genes in neurodevelopmental pathways in schizophrenia.* Science, 2008. 320(5875): p. 539-43.
82. Bayer, T.A., P. Falkai, and W. Maier, *Genetic and non-genetic vulnerability factors in schizophrenia: the basis of the "two hit hypothesis".* J Psychiatr Res, 1999. 33(6): p. 543-8.
83. Fatemi, S.H. and T.D. Folsom, *The Neurodevelopmental Hypothesis of Schizophrenia, Revisited.* Schizophr Bull, 2009. 35(3): p. 528-48.
84. Clinton, S.M. and J.H. Meador-Woodruff, *Abnormalities of the NMDA Receptor and Associated Intracellular Molecules in the Thalamus in Schizophrenia and Bipolar Disorder.* Neuropsychopharmacology, 2004. 29(7): p. 1353-62.
85. Clinton, S.M., V. Haroutunian, and J.H. Meador-Woodruff, *Up-regulation of NMDA receptor subunit and post-synaptic density protein expression in the thalamus of elderly patients with schizophrenia.* J Neurochem, 2006. 98(4): p. 1114-25.
86. Kristiansen, L.V., et al., *Expression of the NR2B-NMDA receptor subunit and its Tbr-1/CINAP regulatory proteins in postmortem brain suggest altered receptor processing in schizophrenia.* Synapse, 2010. 64(7): p. 495-502.
87. Kirov, G., et al., *Comparative genome hybridization suggests a role for NRXN1 and APBA2 in schizophrenia.* Hum Mol Genet, 2008. 17(3): p. 458-65.
88. Rees, E., et al., *Analysis of copy number variations at 15 schizophrenia-associated loci.* Br J Psychiatry, 2014. 204(2): p. 108-14.
89. Kirov, G., et al., *De novo CNV analysis implicates specific abnormalities of postsynaptic signalling complexes in the pathogenesis of schizophrenia.* Mol Psychiatry, 2012. 17(2): p. 142-53.
90. Gulsuner, S. and J.M. McClellan, *Copy Number Variation in Schizophrenia.* Neuropsychopharmacology, 2015. 40(1): p. 252-254.
91. Purcell, S.M., et al., *Common polygenic variation contributes to risk of schizophrenia and bipolar disorder.* Nature, 2009. 460(7256): p. 748-52.
92. Arion, D., et al., *Molecular evidence for increased expression of genes related to immune and chaperone function in the prefrontal cortex in schizophrenia.* Biol Psychiatry, 2007. 62(7): p. 711-21.
93. Kano, S., et al., *Altered MHC class I expression in dorsolateral prefrontal cortex of nonsmoker patients with schizophrenia.* Neurosci Res, 2011. 71(3): p. 289-93.

94. Eaton, W.W., et al., *Association of schizophrenia and autoimmune diseases: linkage of Danish national registers.* Am J Psychiatry, 2006. 163(3): p. 521-8.
95. Holley, S.M., et al., *Frontal cortical synaptic communication is abnormal in Disc1 genetic mouse models of schizophrenia.* Schizophr Res, 2013. 146(1-3): p. 264-72.
96. Mao, Y., et al., *Disrupted in schizophrenia 1 regulates neuronal progenitor proliferation via modulation of GSK3beta/beta-catenin signaling.* Cell, 2009. 136(6): p. 1017-31.
97. Cochran, S.M., et al., *Acute and delayed effects of phencyclidine upon mRNA levels of markers of glutamatergic and GABAergic neurotransmitter function in the rat brain.* Synapse, 2002. 46(3): p. 206-14.
98. Wen, Z., et al., *Synaptic dysregulation in a human iPS cell model of mental disorders.* Nature, 2014. 515(7527): p. 414-8.
99. Hogarty, G.E., *Prevention of relapse in chronic schizophrenic patients.* J Clin Psychiatry, 1993. 54 Suppl: p. 18-23.
100. Kapur, S. and P. Seeman, *Antipsychotic agents differ in how fast they come off the dopamine D2 receptors. Implications for atypical antipsychotic action.* Journal of Psychiatry and Neuroscience, 2000. 25(2): p. 161-166.
101. Brenner, H.D., et al., *Defining treatment refractoriness in schizophrenia.* Schizophr Bull, 1990. 16(4): p. 551-61.
102. Dimitrelis, K. and R. Shankar, *Pharmacological treatment of schizophrenia – a review of progress.* Progress in Neurology and Psychiatry, 2016. 20(3): p. 28-35.
103. Remington, G., *Understanding antipsychotic "atypicality": a clinical and pharmacological moving target.* Journal of Psychiatry and Neuroscience, 2003. 28(4): p. 275-284.
104. Miyamoto, S., et al., *Treatments for schizophrenia: a critical review of pharmacology and mechanisms of action of antipsychotic drugs.* Mol Psychiatry, 2005. 10(1): p. 79-104.
105. Chue, P. and J.K. Lalonde, *Addressing the unmet needs of patients with persistent negative symptoms of schizophrenia: emerging pharmacological treatment options.* Neuropsychiatr Dis Treat, 2014. 10: p. 777-89.
106. Duncan, G.E., B.B. Sheitman, and J.A. Lieberman, *An integrated view of pathophysiological models of schizophrenia.* Brain Res Brain Res Rev, 1999. 29(2-3): p. 250-64.
107. Stone, J.M., *Glutamatergic Antipsychotic Drugs: A New Dawn in the Treatment of Schizophrenia?* Ther Adv Psychopharmacol, 2011. 1(1): p. 5-18.
108. Zhao, W.N., et al., *A high-throughput screen for Wnt/beta-catenin signaling pathway modulators in human iPSC-derived neural progenitors.* J Biomol Screen, 2012. 17(9): p. 1252-63.
109. Lai, M.C., M.V. Lombardo, and S. Baron-Cohen, *Autism.* Lancet, 2014. 383(9920): p. 896-910.
110. Kolvin, I., *Studies in the childhood psychoses. I. Diagnostic criteria and classification.* Br J Psychiatry, 1971. 118(545): p. 381-4.
111. Kolvin, I., et al., *Studies in the childhood psychoses. II. The phenomenology of childhood psychoses.* Br J Psychiatry, 1971. 118(545): p. 385-95.
112. Ozonoff, S., et al., *A Prospective Study of the Emergence of Early Behavioral Signs of Autism.* Journal of the American Academy of Child and Adolescent Psychiatry, 2010. 49(3): p. 256-66.e1-2.
113. Cheung, C., et al., *Autistic disorders and schizophrenia: related or remote? An anatomical likelihood estimation.* PLoS One, 2010. 5(8): p. e12233.
114. Toal, F., et al., *Psychosis and autism: magnetic resonance imaging study of brain anatomy.* Br J Psychiatry, 2009. 194(5): p. 418-25.
115. Carper, R.A. and E. Courchesne, *Localized enlargement of the frontal cortex in early autism.* Biol Psychiatry, 2005. 57(2): p. 126-33.
116. Just, M.A., et al., *Autism as a neural systems disorder: a theory of frontal-posterior underconnectivity.* Neurosci Biobehav Rev, 2012. 36(4): p. 1292-313.

117. Hutsler, J.J. and H. Zhang, *Increased dendritic spine densities on cortical projection neurons in autism spectrum disorders.* Brain Res, 2010. 1309: p. 83-94.
118. Belichenko, P.V., et al., *Rett syndrome: 3-D confocal microscopy of cortical pyramidal dendrites and afferents.* Neuroreport, 1994. 5(12): p. 1509-13.
119. Bhakar, A.L., G. Dölen, and M.F. Bear, *The Pathophysiology of Fragile X (and What It Teaches Us about Synapses).* Annual review of neuroscience, 2012. 35: p. 417-443.
120. Sandin, S., et al., *THE FAMILIAL RISK OF AUTISM.* JAMA, 2014. 311(17): p. 1770-1777.
121. De Rubeis, S., et al., *Synaptic, transcriptional and chromatin genes disrupted in autism.* Nature, 2014. 515(7526): p. 209-15.
122. Fromer, M., et al., *De novo mutations in schizophrenia implicate synaptic networks.* Nature, 2014. 506(7487): p. 179-84.
123. Takahashi, K., et al., *Induction of pluripotent stem cells from adult human fibroblasts by defined factors.* Cell, 2007. 131(5): p. 861-72.
124. Takahashi, K. and S. Yamanaka, *Induction of pluripotent stem cells from mouse embryonic and adult fibroblast cultures by defined factors.* Cell, 2006. 126(4): p. 663-76.
125. Aasen, T., et al., *Efficient and rapid generation of induced pluripotent stem cells from human keratinocytes.* Nat Biotechnol, 2008. 26(11): p. 1276-84.
126. Petit, I., et al., *Induced pluripotent stem cells from hair follicles as a cellular model for neurodevelopmental disorders.* Stem Cell Res, 2012. 8(1): p. 134-40.
127. Tamaoki, N., et al., *Dental pulp cells for induced pluripotent stem cell banking.* J Dent Res, 2010. 89(8): p. 773-8.
128. Chou, B.K., et al., *A facile method to establish human induced pluripotent stem cells from adult blood cells under feeder-free and xeno-free culture conditions: a clinically compliant approach.* Stem Cells Transl Med, 2015. 4(4): p. 320-32.
129. Giorgetti, A., et al., *Generation of induced pluripotent stem cells from human cord blood using OCT4 and SOX2.* Cell stem cell, 2009. 5(4): p. 353-357.
130. Chailangkarn, T., A. Acab, and A.R. Muotri, *Modeling neurodevelopmental disorders using human neurons.* Curr Opin Neurobiol, 2012. 22(5): p. 785-90.
131. Marchetto, M.C., et al., *A model for neural development and treatment of Rett syndrome using human induced pluripotent stem cells.* Cell, 2010. 143(4): p. 527-39.
132. Chiang, C.H., et al., *Integration-free induced pluripotent stem cells derived from schizophrenia patients with a DISC1 mutation.* Molecular psychiatry, 2011. 16(4): p. 358-360.
133. Association, A.P., *Diagnostic and Statistical Manual of Mental Disorders, Fith Edition*. 2013.
134. Adewumi, O., et al., *Characterization of human embryonic stem cell lines by the International Stem Cell Initiative.* Nat Biotechnol, 2007. 25(7): p. 803-16.
135. Lavoinne, A. and B. Cauliez, *[Cardiac troponin I and T: specific biomarkers of cardiomyocyte].* Rev Med Interne, 2004. 25(2): p. 115-23.
136. Viotti, M., S. Nowotschin, and A.-K. Hadjantonakis, *SOX17 links gut endoderm morphogenesis and germ layer segregation.* Nat Cell Biol, 2014. 16(12): p. 1146-1156.
137. Elkabetz, Y., et al., *Human ES cell-derived neural rosettes reveal a functionally distinct early neural stem cell stage.* Genes Dev, 2008. 22(2): p. 152-65.
138. Koch, P., et al., *A rosette-type, self-renewing human ES cell-derived neural stem cell with potential for in vitro instruction and synaptic integration.* Proc Natl Acad Sci U S A, 2009. 106(9): p. 3225-30.
139. Lukovic, D., et al., *Highly Efficient Neural Conversion of Human Pluripotent Stem Cells in Adherent and Animal-Free Conditions.* Stem Cells Transl Med, 2017. 6(4): p. 1217-26.
140. Shi, Y., et al., *Human cerebral cortex development from pluripotent stem cells to functional excitatory synapses.* Nat Neurosci, 2012. 15(3): p. 477-86, s1.

141. Arlotta, P., et al., *Neuronal subtype-specific genes that control corticospinal motor neuron development in vivo.* Neuron, 2005. 45(2): p. 207-21.
142. Ganguli-Indra, G., et al., *CTIP2 Expression in Human Head and Neck Squamous Cell Carcinoma Is Linked to Poorly Differentiated Tumor Status.* PLoS ONE, 2009. 4(4): p. e5367.
143. Ahmed, Z., M. Berry, and A. Logan, *ROCK inhibition promotes adult retinal ganglion cell neurite outgrowth only in the presence of growth promoting factors.* Mol Cell Neurosci, 2009. 42(2): p. 128-33.
144. Causeret, F., et al., *Distinct roles of Rac1/Cdc42 and Rho/Rock for axon outgrowth and nucleokinesis of precerebellar neurons toward netrin 1.* Development, 2004. 131(12): p. 2841-52.
145. Roloff, F., et al., *Enhanced Neurite Outgrowth of Human Model (NT2) Neurons by Small-Molecule Inhibitors of Rho/ROCK Signaling.* PLoS One, 2015. 10(2).
146. Crespo-Facorro, B., C. Prieto, and J. Sainz, *Schizophrenia Gene Expression Profile Reverted to Normal Levels by Antipsychotics.* International Journal of Neuropsychopharmacology, 2015. 18(4): p. pyu066.
147. Glessner, J.T., et al., *Strong synaptic transmission impact by copy number variations in schizophrenia.* Proc Natl Acad Sci U S A, 2010. 107(23): p. 10584-9.
148. Hrckulak, D., et al., *TCF/LEF Transcription Factors: An Update from the Internet Resources.* Cancers (Basel), 2016. 8(7).
149. Peng, Y., Y. Xu, and D. Cui, *Wnt signaling pathway in schizophrenia.* CNS Neurol Disord Drug Targets, 2014. 13(5): p. 755-64.
150. Topol, A., et al., *Increased abundance of translation machinery in stem cell-derived neural progenitor cells from four schizophrenia patients.* Transl Psychiatry, 2015. 5: p. e662.
151. Calabrese, E.J., *Hormesis and medicine.* Br J Clin Pharmacol, 2008. 66(5): p. 594-617.
152. Ozeki, Y., et al., *Disrupted-in-Schizophrenia-1 (DISC-1): mutant truncation prevents binding to NudE-like (NUDEL) and inhibits neurite outgrowth.* Proc Natl Acad Sci U S A, 2003. 100(1): p. 289-94.
153. Gore, A., et al., *Somatic coding mutations in human induced pluripotent stem cells.* Nature, 2011. 471(7336): p. 63-7.
154. Hussein, S.M., et al., *Copy number variation and selection during reprogramming to pluripotency.* Nature, 2011. 471(7336): p. 58-62.
155. Kim, K., et al., *Donor cell type can influence the epigenome and differentiation potential of human induced pluripotent stem cells.* Nat Biotechnol, 2011. 29(12): p. 1117-9.
156. Laurent, L.C., et al., *Dynamic changes in the copy number of pluripotency and cell proliferation genes in human ESCs and iPSCs during reprogramming and time in culture.* Cell Stem Cell, 2011. 8(1): p. 106-18.
157. Ban, H., et al., *Efficient generation of transgene-free human induced pluripotent stem cells (iPSCs) by temperature-sensitive Sendai virus vectors.* Proc Natl Acad Sci U S A, 2011. 108(34): p. 14234-9.
158. Okita, K., et al., *A more efficient method to generate integration-free human iPS cells.* Nat Methods, 2011. 8(5): p. 409-12.
159. Warren, L., et al., *Highly efficient reprogramming to pluripotency and directed differentiation of human cells with synthetic modified mRNA.* Cell Stem Cell, 2010. 7(5): p. 618-30.
160. Kim, D., et al., *Generation of human induced pluripotent stem cells by direct delivery of reprogramming proteins.* Cell Stem Cell, 2009. 4(6): p. 472-6.
161. Graf, T. and T. Enver, *Forcing cells to change lineages.* Nature, 2009. 462(7273): p. 587-94.
162. Yang, N., et al., *Induced Neuronal (iN) Cells: How to Make and Define a Neuron.* Cell stem cell, 2011. 9(6): p. 517-525.

163. Mertens, J., et al., *Directly Reprogrammed Human Neurons Retain Aging-Associated Transcriptomic Signatures and Reveal Age-Related Nucleocytoplasmic Defects.* Cell Stem Cell, 2015. 17(6): p. 705-18.
164. Pang, Z.P., et al., *Induction of human neuronal cells by defined transcription factors.* Nature, 2011. 476(7359): p. 220-3.
165. Pfisterer, U., et al., *Efficient induction of functional neurons from adult human fibroblasts.* Cell Cycle, 2011. 10(19): p. 3311-6.
166. Kelaini, S., A. Cochrane, and A. Margariti, *Direct reprogramming of adult cells: avoiding the pluripotent state.* Stem Cells and Cloning : Advances and Applications, 2014. 7: p. 19-29.
167. Chambers, S.M., et al., *Highly efficient neural conversion of human ES and iPS cells by dual inhibition of SMAD signaling.* Nat Biotechnol, 2009. 27(3): p. 275-80.
168. Yu, P.B., et al., *Dorsomorphin inhibits BMP signals required for embryogenesis and iron metabolism.* Nat Chem Biol, 2008. 4(1): p. 33-41.
169. Handel, A.E., et al., *Assessing similarity to primary tissue and cortical layer identity in induced pluripotent stem cell-derived cortical neurons through single-cell transcriptomics.* Hum Mol Genet, 2016. 25(5): p. 989-1000.
170. Schwartz, P.H., et al., *Differentiation of Neural Lineage Cells from Human Pluripotent Stem Cells.* Methods (San Diego, Calif.), 2008. 45(2): p. 142-158.
171. Du, X. and J.M. Parent, *Using Patient-Derived Induced Pluripotent Stem Cells to Model and Treat Epilepsies.* Current neurology and neuroscience reports, 2015. 15(10): p. 71-71.
172. Studer, L., E. Vera, and D. Cornacchia, *PROGRAMMING AND REPROGRAMMING CELLULAR AGE IN THE ERA OF INDUCED PLURIPOTENCY.* Cell stem cell, 2015. 16(6): p. 591-600.
173. Zeng, H., et al., *Specification of region-specific neurons including forebrain glutamatergic neurons from human induced pluripotent stem cells.* PLoS One, 2010. 5(7): p. e11853.
174. W. Maxwell Cowan, T.M.J., and S. Lawrence Zipursky, *Molecular and Cellular Approaches to Neural Development*. 1998.
175. Rodier, P.M., *Vulnerable periods and processes during central nervous system development.* Environ Health Perspect, 1994. 102(Suppl 2): p. 121-4.
176. Rice, D. and S. Barone, Jr., *Critical periods of vulnerability for the developing nervous system: evidence from humans and animal models.* Environ Health Perspect, 2000. 108 Suppl 3: p. 511-33.
177. M, K.H., et al., *A Facile Method for Simultaneously Measuring Neuronal Cell Viability and Neurite Outgrowth.* Curr Chem Genom Transl Med, 2015. 9: p. 6-16.
178. Radio, N.M. and W.R. Mundy, *Developmental neurotoxicity testing in vitro: models for assessing chemical effects on neurite outgrowth.* Neurotoxicology, 2008. 29(3): p. 361-76.
179. Krug, A.K., et al., *Evaluation of a human neurite growth assay as specific screen for developmental neurotoxicants.* Arch Toxicol, 2013. 87(12): p. 2215-31.
180. Haggarty, S.J., et al., *Advancing drug discovery for neuropsychiatric disorders using patient-specific stem cell models.* Mol Cell Neurosci, 2016. 73: p. 104-15.
181. Luo, X., et al., *Association study of DISC1 genetic variants with the risk of schizophrenia.* Psychiatr Genet, 2016. 26(3): p. 132-5.
182. Carroll, D., *Genome editing: progress and challenges for medical applications.* Genome Medicine, 2016. 8: p. 120.
183. Bradshaw, N.J. and D.J. Porteous, *DISC1-binding proteins in neural development, signalling and schizophrenia.* Neuropharmacology, 2012. 62(3): p. 1230-1241.
184. Kvajo, M., et al., *A mutation in mouse Disc1 that models a schizophrenia risk allele leads to specific alterations in neuronal architecture and cognition.* Proc Natl Acad Sci U S A, 2008. 105(19): p. 7076-81.

185. Roberts, R.C., et al., *Decreased synaptic and mitochondrial density in the postmortem anterior cingulate cortex in schizophrenia.* Schizophr Res, 2015. 168(1-2): p. 543-53.
186. Hahn, C.G., et al., *Altered neuregulin 1-erbB4 signaling contributes to NMDA receptor hypofunction in schizophrenia.* Nat Med, 2006. 12(7): p. 824-8.
187. Simons, T.J.B., *Calcium and neuronal function.* Neurosurgical Review, 1988. 11(2): p. 119-129.
188. Brini, M., et al., *Neuronal calcium signaling: function and dysfunction.* Cell Mol Life Sci, 2014. 71(15): p. 2787-814.
189. Lidow, M.S., *Calcium signaling dysfunction in schizophrenia: a unifying approach.* Brain Research Reviews, 2003. 43(1): p. 70-84.
190. CAZZULLO, C.L., E. SMERALDI, and G. PENATI, *The Leucocyte Antigenic System HL-A as a possible Genetic Marker of Schizophrenia.* The British Journal of Psychiatry, 1974. 125(584): p. 25-27.
191. Neumann, J. and N. Koch, *Assembly of major histocompatibility complex class II subunits with invariant chain.* FEBS Lett, 2005. 579(27): p. 6055-9.
192. Torrey, E.F. and R.H. Yolken, *The schizophrenia-rheumatoid arthritis connection: infectious, immune, or both?* Brain Behav Immun, 2001. 15(4): p. 401-10.
193. Vinogradov, S., et al., *Negative association between schizophrenia and rheumatoid arthritis.* Schizophr Bull, 1991. 17(4): p. 669-78.
194. Shi, J., et al., *Common variants on chromosome 6p22.1 are associated with schizophrenia.* Nature, 2009. 460(7256): p. 753-7.
195. Stefansson, H., et al., *Common variants conferring risk of schizophrenia.* Nature, 2009. 460(7256): p. 744-7.
196. Reche, P.A. and E.L. Reinherz, *Sequence variability analysis of human class I and class II MHC molecules: functional and structural correlates of amino acid polymorphisms.* J Mol Biol, 2003. 331(3): p. 623-41.
197. Muller, N., et al., *The immune system and schizophrenia. An integrative view.* Ann N Y Acad Sci, 2000. 917: p. 456-67.
198. Rothermundt, M., V. Arolt, and T.A. Bayer, *Review of immunological and immunopathological findings in schizophrenia.* Brain Behav Immun, 2001. 15(4): p. 319-39.
199. Horvath, S. and K. Mirnics, *Immune system disturbances in schizophrenia.* Biol Psychiatry, 2014. 75(4): p. 316-23.
200. Benros, M.E., et al., *A nationwide study on the risk of autoimmune diseases in individuals with a personal or a family history of schizophrenia and related psychosis.* Am J Psychiatry, 2014. 171(2): p. 218-26.
201. Goddard, C.A., D.A. Butts, and C.J. Shatz, *Regulation of CNS synapses by neuronal MHC class I.* Proc Natl Acad Sci U S A, 2007. 104(16): p. 6828-33.
202. Shatz, C.J., *MHC Class I: an unexpected role in neuronal plasticity.* Neuron, 2009. 64(1): p. 40-45.
203. Glynn, M.W., et al., *MHCI negatively regulates synapse density during the establishment of cortical connections.* Nat Neurosci, 2011. 14(4): p. 442-51.
204. Sekar, A., et al., *Schizophrenia risk from complex variation of complement component 4.* Nature, 2016. 530(7589): p. 177-83.
205. Shayevitz, C., et al., *A re-review of the association between the NOTCH4 locus and schizophrenia.* Am J Med Genet B Neuropsychiatr Genet, 2012. 159b(5): p. 477-83.
206. Farrell, M.S., et al., *Evaluating historical candidate genes for schizophrenia.* Mol Psychiatry, 2015. 20(5): p. 555-62.
207. Siegel GJ, A.B., Albers RW, *Basic Neurochemistry: Molecular, Cellular and Medical Aspects*, ed. 6. 1999, Philadelphia: Lippincott-Raven.
208. Goldberg, J.L., *Intrinsic neuronal regulation of axon and dendrite growth.* Curr Opin Neurobiol, 2004. 14(5): p. 551-7.

209. Audesirk, T., et al., *Effects of inorganic lead on the differentiation and growth of cultured hippocampal and neuroblastoma cells.* Neurotoxicology, 1991. 12(3): p. 529-38.
210. Hall, H., et al., *Distribution of D1- and D2-dopamine receptors, and dopamine and its metabolites in the human brain.* Neuropsychopharmacology, 1994. 11(4): p. 245-56.
211. Sedvall, G.C. and P. Karlsson, *Pharmacological Manipulation of D1-Dopamine Receptor Function in Schizophrenia.* Neuropsychopharmacology, 1999. 21(6, Supplement 2): p. S181-S188.
212. Goldman-Rakic, P.S., *The Relevance of the Dopamine-D1 Receptor in the Cognitive Symptoms of Schizophrenia.* Neuropsychopharmacology, 1999. 21(6, Supplement 2): p. S170-S180.
213. Okubo, Y., et al., *Decreased prefrontal dopamine D1 receptors in schizophrenia revealed by PET.* Nature, 1997. 385(6617): p. 634-6.
214. Davis, K.L., et al., *Dopamine in schizophrenia: a review and reconceptualization.* Am J Psychiatry, 1991. 148(11): p. 1474-86.
215. Weinberger, D.R., *Implications of normal brain development for the pathogenesis of schizophrenia.* Arch Gen Psychiatry, 1987. 44(7): p. 660-9.
216. Sawaguchi, T. and P.S. Goldman-Rakic, *D1 dopamine receptors in prefrontal cortex: involvement in working memory.* Science, 1991. 251(4996): p. 947-50.
217. Williams, G.V. and P.S. Goldman-Rakic, *Modulation of memory fields by dopamine D1 receptors in prefrontal cortex.* Nature, 1995. 376(6541): p. 572-5.
218. Goldman-Rakic, P.S., *Working memory dysfunction in schizophrenia.* J Neuropsychiatry Clin Neurosci, 1994. 6(4): p. 348-57.
219. Stiles, T.L., M.S. Kapiloff, and J.L. Goldberg, *The role of soluble adenylyl cyclase in neurite outgrowth.* Biochim Biophys Acta, 2014. 1842(12 Pt B): p. 2561-8.
220. Song, H.J. and M.M. Poo, *Signal transduction underlying growth cone guidance by diffusible factors.* Curr Opin Neurobiol, 1999. 9(3): p. 355-63.
221. Liesi, P., L. Rechardt, and J. Wartiovaara, *Nerve growth factor induces adrenergic neuronal differentiation in F9 teratocarcinoma cells.* Nature, 1983. 306(5940): p. 265-7.
222. Rydel, R.E. and L.A. Greene, *cAMP analogs promote survival and neurite outgrowth in cultures of rat sympathetic and sensory neurons independently of nerve growth factor.* Proceedings of the National Academy of Sciences of the United States of America, 1988. 85(4): p. 1257-1261.
223. Tegenge, M.A., F. Roloff, and G. Bicker, *Rapid differentiation of human embryonal carcinoma stem cells (NT2) into neurons for neurite outgrowth analysis.* Cell Mol Neurobiol, 2011. 31(4): p. 635-43.
224. Bymaster, F.P., et al., *Antagonism by olanzapine of dopamine D1, serotonin2, muscarinic, histamine H1 and alpha 1-adrenergic receptors in vitro.* Schizophr Res, 1999. 37(1): p. 107-22.
225. Lidow, M.S. and P.S. Goldman-Rakic, *A common action of clozapine, haloperidol, and remoxipride on D1- and D2-dopaminergic receptors in the primate cerebral cortex.* Proceedings of the National Academy of Sciences of the United States of America, 1994. 91(10): p. 4353-4356.
226. Kebabian, J.W. and P. Greengard, *Dopamine-sensitive adenyl cyclase: possible role in synaptic transmission.* Science, 1971. 174(4016): p. 1346-9.
227. Singh, A.N., et al., *A neurochemical basis for the antipsychotic activity of loxapine: interactions with dopamine D1, D2, D4 and serotonin 5-HT2 receptor subtypes.* Journal of Psychiatry and Neuroscience, 1996. 21(1): p. 29-35.
228. Lieberman, J.A., et al., *ITI-007 for the Treatment of Schizophrenia: A 4-Week Randomized, Double-Blind, Controlled Trial.* Biol Psychiatry, 2016. 79(12): p. 952-61.
229. Li, P., et al., *Discovery of a tetracyclic quinoxaline derivative as a potent and orally active multifunctional drug candidate for the treatment of neuropsychiatric and neurological disorders.* J Med Chem, 2014. 57(6): p. 2670-82.

230. Lancaster, M.A., et al., *Cerebral organoids model human brain development and microcephaly.* Nature, 2013. 501(7467): p. 373-9.
231. Pasca, A.M., et al., *Functional cortical neurons and astrocytes from human pluripotent stem cells in 3D culture.* Nat Methods, 2015. 12(7): p. 671-8.

7. ANNEX

7.1 Publications

Greiner JF, **Grunwald LM**, Müller J, Sudhoff H, Widera D, Kaltschmidt C, Kaltschmidt B.(2013): Culture bag systems for clinical applications of adult human neural crest-derived stem cells, Stem Cell Res Ther. 2014 Mar 14;5(2):34

Greiner JF, Müller J, Zeuner MT, Hauser S, Seidel T, Klenke C, **Grunwald LM**, Schomann T, Widera D, Sudhoff H, Kaltschmidt B, Kaltschmidt C.(2014): 1,8-Cineol inhibits nuclear translocation of NF-κB p65 and NF-κB-dependent transcriptional activity, Biochim Biophys Acta. 2013 Dec;1833(12):2866-78

Manuscript in revision to publish parts of this thesis:
Grunwald LM, Haag K, Buckenmeier S, Eberle MC, Wildgruber D, Storchak H, Kriebel M, Weißgraeber S, Mathew L, Singh Y, Loos M, Kraushaar U, Fallgatter AJ, Volkmer H.: A stem cell-derived model of schizophrenia reflects the developmental phenotype of schizophrenia

7.2 Conferences

Poster:

Grunwald LM, Kriebel M, Eberle MC, Hess D, Kraushaar U, Fallgatter AJ, Volkmer H. (2015): Synaptic connectivity of iPSC - derived neurons from patients with schizophrenia, 8th International Meeting of the Stem Cell Network Northrhine Westphalia, Bonn

Grunwald LM, Kriebel M, Eberle MC, Hess D, Kraushaar U, Battke F, Singh Y, Fallgatter AJ, Volkmer H. (2015): Comparison of synaptic connectivity in iPSC - derived neurons from patients with schizophrenia and autism, 40th FEBS Congress, The Biochemical Basis of Life, Berlin

Grunwald LM, Kriebel M, Eberle MC, Kraushaar U, Battke F, Singh Y, Fallgatter AJ, Volkmer H. (2016): iPSC-derived neurons as a cellular model system for neuropsychiatric disorders, 46th annual meeting SFN, San Diego, USA

Grunwald LM, Kriebel M, Eberle MC, Kraushaar U, Buckenmeier S, Battke F, Singh Y, Fallgatter AJ, Volkmer H. (2017): iPSC-derived neurons from patient with schizophrenia as a cellular model system for neuropsychiatric disorders, 9th International Meeting of the Stem Cell Network Northrhine Westphalia, Münster

Presentation:

Grunwald LM, Kriebel M, Eberle MC, Hess D, Kraushaar U, Battke F, Singh Y, Fallgatter AJ, Volkmer H. (2015): Comparison of synaptic connectivity in iPSC - derived neurons from patients with schizophrenia and autism, 40th FEBS Congress, The Biochemical Basis of Life, Berlin

Grunwald LM, Kriebel M, Volkmer H. (2016): Development of an innovative testsystem based on iPSC-derived human neuronal cell types for drug development regarding neuropsychiatric diseases, Retreat Stem Cell Network Tübingen, Eglofs, Allgäu

7.3 Eidesstattliche Erklärung

Ich erkläre hiermit, dass ich die zur Promotion eingereichte Arbeit mit dem Titel: „iPSC-derived cortical neurons from patients with schizophrenia exhibit changes in early neuronal development“ selbständig verfasst, nur die angegebenen Quellen und Hilfsmittel benutzt und wörtlich oder inhaltlich übernommene Stellen als solche gekennzeichnet habe. Ich erkläre, dass die Richtlinien zur Sicherung guter wissenschaftlicher Praxis der Universität Tübingen (Beschluss des Senats vom 25.5.2000) beachtet wurden. Ich versichere an Eides statt, dass diese Angaben wahr sind und dass ich nichts verschwiegen habe. Mir ist bekannt, dass die falsche Abgabe einer Versicherung an Eides statt mit Freiheitsstrafe von bis zu drei Jahren oder mit Geldstrafe bestraft wird.

Tübingen den 17.01.2018

Lena-Marie Grunwald

7.4 Danksagung

Ganz besonders bedanken möchte ich mich bei Herrn Prof. Hansjürgen Volkmer für die Möglichkeit meine Doktorarbeit am Naturwissenschaflichen Medizinischen Institut an der Universität Tübingen zu erstellen. Vielen Dank für deinen wissenschaftlichen Input, die intensiven Diskussionen sowie die Chance des fachlichen Austausches bei internationalen Konferenzen und institutsübergreifenden Projekten.

Herrn Prof. Rammensee möchte ich für die Begutachtung dieser Arbeit, sein entgegengebrachtes Interesse und die schnelle Hilfe bei Fragen danken.

Dr. Martin Kriebel möchte ich für seine Unterstützung im Labor und bei der experimentellen Planung danken sowie für die Beantwortung meiner zahlreichen Fragen. Dr. Udo Kraushaar und Sandra Buckenmeier danke ich für die große Geduld bei der funktionellen Charakterisierung meiner generierten Zellen und ihre wissenschaftliche Unterstützung. Christine Dürr und Sybille Glock danke ich für ihre große Hilfe im Labor und die vielen Wochenendarbeiten. Außerdem danke ich Kathrina Haag für die bereichernde Zusammenarbeit und die zur Verfügungstellung ihrer Masterarbeit.

Für alle unterhaltsamen, kurzen und langen Mittagspausen sowie eure große Unterstützung möchte ich Mona Bodenhöfer, Dr. Julia Maier, Dr. Björn Tränkle, Florian Jetter, Simone Beuter und Martin Kriebel danken. Eure Freundschaft hat die Zeit am NMI und im Schwabenländle für mich sehr besonders gemacht und wird mir immer in positiver Erinnerung bleiben. Danke euch für den ganzen Spaß bei Ausflügen, gemeinsamen Grillfesten, Geburtstagsfeiern und den Wasen.

Ein ganz besonderer Dank geht an meine Familie, meine Eltern Maren und Michael Grunwald meine Schwester Anna Grunwald und meine Oma Helga Braatz. Danke, dass ihr mich jederzeit während meines Studiums und meiner Promotion, trotz großer räumlicher Entfernung, unterstützt habt und immer ein offenes Ohr in mancher schwierigen Situation hattet. Danke, für euren großen Rückhalt, eure Besuche und eure vielen Ratschläge.

Mein größtes Dankeschön ist an meinen Freund Sven Petrat gerichtet. Danke dir für deine große Geduld, dein großes Verständnis und deine aufbauenden und motivierenden Worte während der letzten Jahre.